Generation Of Cell-Penetrating Heme Oxygenase Proteins To Improve The Resistance Of Steatotic Livers To Reperfusion Injury Following Transplantation

by

Scott Michael Livingstone

Submitted in partial fulfilment of the requirements
for the degree of Master of Science

at

Dalhousie University
Halifax, Nova Scotia
January 2012

DALHOUSIE UNIVERSITY

DEPARTMENT OF MEDICAL SCIENCES

The undersigned hereby certify that they have read and recommend to the Faculty of Graduate Studies for acceptance a thesis entitled “Generation of Cell-penetrating Heme Oxygenase Proteins to Improve the Resistance of Steatotic Livers to Reperfusion Injury Following Transplantation” by Scott Michael Livingstone in partial fulfilment of the requirements for the degree of Master of Science.

Dated: January 30, 2012

Supervisor: _____

Readers: _____

_____

_____

_____

DALHOUSIE UNIVERSITY

DATE: January 30, 2012

AUTHOR: Scott Michael Livingstone

TITLE: Generation of Cell-penetrating Heme Oxygenase Proteins to Improve the Resistance of Steatotic Livers to Reperfusion Injury Following Transplantation

DEPARTMENT OR SCHOOL: Department of Medical Sciences

DEGREE: MSc CONVOCATION: May YEAR: 2012

_____

Signature of Author

Table Of Contents

List of Figures

Abstract

Liver transplantation is the only life-saving treatment for patients with end-stage liver disease; however, organ availability is insufficient to meet demands. Steatotic livers are extended criteria donor (ECD) organs that could be used for transplantation if not for an increased susceptibility ischemia reperfusion injury (IRI). Heme oxygenase-1 is a gene, that when upregulated has be shown to reduce IRI in animal models of transplantation. Increasing HO-1 activity in steatotic livers by delivery of a functional cell-penetrating HO-1 protein (through the use of cell-penetrating peptides) may provide protection against IRI, making these organs useful for transplantation. The purpose of this thesis was the generation and testing of a cell-penetrating HO-1 protein. HO-1 and EGFP gene sequences were cloned into the pET-28B(+) vector in frame with a CPP or TAT sequence. Resulting plasmids were cloned into *E. coli*, and protein expression was induced using IPTG. Proteins were purified using Ni-NTA affinity chromatography under denaturing and non-denaturing conditions. Non-denatured proteins were tested for HO-1 activity and the ability of both denatured and non-denatured proteins to transduce cells *in vitro* was tested by fluorescence microscopy. The cell-penetrating ability of non-denatured proteins was further tested in J774, HepG2 and HUVEC cells using immunofluorescence. Five HO-1 and two EGFP cell-penetrating proteins were generated expressed and purified successfully. Purified non-denatured HO-1 retains its enzymatic activity. Non-denatured CPP-EGFP and CPP-HO1 penetrated cells more effectively than their denatured counterparts. CPP-EGFP and CPP-HO1 proteins are able to penetrate multiple cell types *in vitro*. Successful generation and testing of a cell-penetrating HO-1 protein, for use in an animal model of steatotic liver transplantation. This protein demonstrates promise for use as a potential therapeutic agent in the field of liver transplantation.

List of Abbreviations and Symbols Used

a.a. – amino acid

ALF – acute liver failure

ATP – adenosine triphosphate

Bag-1 – bcl-2-associated athanogene-1

Bax – bcl-2-asociated x protein

Bcl-2 – b cell lymphoma 2

Bcl-X_L – b cell lymphoma extra large

BR – bilirubin

BSA – bovine serum albumin

BV- biliverdin

BVR – biliverdin reductase

CD4+ T cells – cluster of differentiation 4+ T cells

cDMEM – complete Dulbecco's modified eagle medium

cDNA – complementary deoxyribose nucleic acid

cGMP – cyclic guanine monophosphate

CMV - cytomegalovirus

CO – carbon monoxide

CoA – coenzyme A

CoPP – cobalt protoporphyrin

CPP – cell-penetrating peptide

DAMP – danger-associated molecular patterns

DGF – delayed graft function

DMSO – dimethyl sulfoxide

DNA- deoxyribonucleic acid

EBM – endothelial basal medium

dNTP – deoxynucleotide triphosphate

ECD – extended criteria donor

EDTA – ethylenediaminetetracetic acid

ER – endoplasmic reticulum

ERK1/2 – extracellular signal regulated kinases 1/2

ESLD – end stage liver disease

FBS – fetal bovine serum

FFA – free fatty acids

G6P – glucose-6-phosphate

G6PD – glucose-6-phosphate dehydrogenase

GT – guanine thymine

HCC – hepatocellular carcinoma

hEGF – human epidermal growth factor

His – histidine

HIV – human immunodeficiency virus

HO – heme oxygenase

HO-1 – heme oxygenase-1

HO-2 – heme oxygenase-2

HUVEC – human umbilical vein endothelial cells

HTK – histidine tryptophan ketoglutarate

ICAM-1 – intercellular adhesion molecule-1

IFN-γ – interferon-γ

II – ischemic injury

IL-1β – interleukin-1β

IL-6 – interleukin 6

IL-10 – interleukin 10

IL-12 – interleukin 12

IL-17 – interleukin 17

IL-18 – interleukin 18

IPTG – isopropyl β-D-1-thiogalactopyranoside

IR – ischemia reperfusion

IRI – ischemia reperfusion injury

IRS-1- insulin receptor substrate-1

IRS-2 – insulin receptor substrate-2

kDa – kiloDalton

LB – luria broth

LT – liver transplantation

MAPK – mitogen activated protein kinase

MCD – methionine choline deficient

mRNA – messenger ribonucleic acid

NADPH – nicotinamide adenine dinucleotide phosphate

Ni-NTA – nickel-nitrilotriacetic acid

NK cells – natural killer cells

NO – nitric oxide

NOS – nitric oxide synthase

iNOS – inducible nitric oxide synthase

PAI-1 – plasminogen activator inhibitor-1

PBS – phosphate buffered saline

PCR – polymerase chain reaction

PI3K – phosphatidyl-inositol-3-kinase

PKA – protein kinase A

PKC – protein kinase C

PNA – protein nucleic acids

PNF – primary non-function

PTD – protein transduction domain

PVDF – polyvinylidene fluoride

R3-IGF-1 – recombinant-insulin growth factor-1

RNA – ribonucleic acid

RNS – reactive nitrogen species

ROS – reactive oxygen species

SDS – sodium dodecyl sulfate

SDS-PAGE – sodium dodecyl suphate polyacrylamide gel electrophoresis

SEC – sinusoidal endothelial cell

sGC – soluble guanylate cyclase

sHO1 – soluble HO-1

siRNA – small interfering ribonucleic acid

SnPP – tin protoporphyrin

SOC – super optimal culture

TAT – trans-activator of transcription

TBS – tris buffered saline

TG – triglycerides

TLR-4 – toll-like receptor 4

TNF-α – tumor necrosis factor-α

tRNA – transfer ribonucleic acid

VCAM-1 – vascular adhesion molecule-1

VLDL – very low density lipoprotein

Acknowledgments

Ian Alwayn

David Woodhall

Kimberly Savage

Lois Murray

Tim Lee

Craig McCormick

Nichole McMullen

Atlantic Centre for Transplantation Research

Tim Lee lab

J. F. Legare lab

Dalhousie University Department of Surgery

Clinical Investigator Program

Nova Scotia Health Research Foundation

Capital District Health Authority

Canadian Foundation for Innovation

Chapter 1: Introduction

1.1 Liver Transplantation

The first human liver transplants were performed by Thomas Starzl in 1963 [1]. Although technically successful, poor outcomes, and high rejection and mortality rates limited its application to that of a last-ditch effort for a select number of patients with end-stage liver disease until the 1980's [2, 3]. Since that time there have been steady advances in immunosuppression, surgical techniques, and post-operative care that have led to widespread acceptance and utilization of this therapy [4, 5]. In a 2009, there were 452 liver transplants performed in Canada. In the same year, the reported 1, 3, and 5 year survival rates for recipients transplanted in 2008, 2006, and 2004 were 93.3%, 82.7% and 80%, respectively [6]. The statistics from the United States are even more striking, where 6320 liver transplants were performed in 2009 [7]. Survival rates in the US are similar, with reported rates in 2004 of 87%, 79% and 73% at 1, 3 and 5 years, respectively [7]. This success has led to a greater willingness of physicians to refer patients for liver transplantation (LT). Until recently liver transplantation was only used to treat patients with end stage liver disease (ESLD) or acute liver failure (ALF). However, in recent years its use has been applied to include patients with a host of primary liver diseases as well as patients with certain malignancies such as hepatocellular- (HCC) and cholangiocarcinomas [8, 9].

The increased demand for liver transplantation has not been paralleled by a similar increase in the availability of donor organs, and, as such, wait lists have grown progressively over the past 20 years. In Canada, at the end of 2009, there were 551 patients listed and waiting for liver transplantation, and an additional 91 people died waiting for an organ, representing a mortality rate of 14% [6]. With the ability to provide such a successful treatment, many health care practitioners find these statistics unacceptable.

1.2 Extended Criteria Organs

In attempt to increase the number of donor organs and reduce wait times, one of the major strategies being employed by transplant surgeons is the use of extended criteria donor (ECD) organs [10]. Although there are no set criteria defining ECD organs, they are generally considered to be organs at increased risk of poor function or failure that may subject the recipient to greater risk of morbidity or mortality [11, 12]. ECD organs can be broadly categorized according to the primary risk associated with transplantation of the organ. Such risks include: impaired graft function; graft failure; and transmission of donor disease to the recipient (such as Hepatitis B or C or cytomegalovirus (CMV)). The former makes up the greatest component. Several donor-related factors can place an organ at risk for delayed function including: donor age; race; height; extent and type of hepatic steatosis; time in intensive care unit; hemodynamic instability or need for inotropic support (intravenous medications to augment blood pressure and cardiac function); donor hypernatremia (abnormally elevated serum sodium levels); prolonged ischemia; partial-liver allograft; and prolonged organ ischemia [13-38]. Aside from age, the presence of hepatic steatosis is the most frequent cause for an organ to be considered marginal [39] and, as such, much research has been directed towards the acceptable use of steatotic livers for transplantation.

1.3 Hepatic Steatosis

Fat accumulation within the liver is considered to be pathologic when the hepatic fat content is greater than 5% of the actual wet liver weight [40]. The development of hepatic steatosis is a result of the accumulation of ectopic lipids within hepatocytes, owing to an imbalance between supply, formation, consumption, and hepatic oxygenation of triglycerides (TG) [41, 42]. The liver controls fatty acid and triglyceride metabolism through multiple mechanisms including: 1) the uptake of dietary fats, and circulating free fatty acids (FFA), which are subsequently converted to TG's and exported via very-low density lipoproteins (VLDL); 2) de novo lipogenesis from precursors such as glucose, amino acids and ethanol; and 3) β-oxidation of free fatty acids for gluconeogenesis in the

fasting state [41, 42]. Derangements in these pathways result in two different patterns of hepatic steatosis: microvesicular and macrovesicular steatosis (see fig 1). Microvesicular steatosis, which is characterised by the presence of numerous tiny fat droplets within the hepatocyte cytoplasm that surround but do not displace the nucleus [35, 43] is the result of mitochondrial injury and defects in β-oxidation of FFA. It is most commonly seen in the setting of critical illness and/or acute hepatic dysfunction, toxins, or metabolic disorders [35, 43-45]. Microvesicular steatosis is reversible and frequently absent in functional allografts within one week after transplantation [46]. Although there has been some evidence suggesting that the presence of microsteatosis poses a risk for poor graft function [47, 48], the majority of studies have not found impaired hepatic function when these organs are used for transplantation [49-52].

1.3.1 Macrovesicular Steatosis

Macrovesicular steatosis is characterized by the presence of only one or a few well-demarcated fat droplets within the hepatocyte cytoplasm with displacement of the nucleus to the edge of the cell [35, 43]. This is due to the accumulation of triglycerides within the hepatocyte, as a result of de novo lipogenesis, and is frequently associated with insulin resistance [39, 53-60]. It is now known that the primary cause of insulin resistance is the action of exocrine substances released by adipocytes termed "adipokines" [61-66]. Adipokines mediate an inhibition of glucose metabolism via the inhibition of the insulin receptor substrate-1 (IRS-1) pathway [42], resulting in increased pancreatic insulin secretion. However, signalling via the insulin receptor substrate-2 (IRS-2) pathway - which is responsible for the activation of *de novo* lipogenesis - remains intact. This coupled with an increase in the delivery of FFA to the liver, results in markedly increased TG production [41, 67]. These exocrine functions of adipocytes explain why hepatic steatosis is commonly associated with metabolic syndrome and obesity [68]. The high prevalence of these conditions in Western societies suggests that macrovesicular steatosis itself is likely very common [23, 38]; in fact a recent survey has indicated that up to 30% of the population in Western societies has a certain degree of hepatic steatosis [69], and autopsy studies have reported steatosis rates ranging from 4-24% [70-72]. Although

there are other causes of macrovesicular steatosis, such as alcohol abuse, the most prevalent risk factors in Western society are diabetes and hyperlipidemia, both of which are strongly associated with obesity [73]. The role of obesity as a contributor to hepatic steatosis is illustrated by an Italian study using hepatic ultrasound which found steatosis in 76% of obese (non-alcoholic) individuals, compared to only 16% of lean (non-alcoholic) individuals [74]. In multiple studies from the early 1990's the prevalence of hepatic steatosis in donors was found to range from 9-26% [33, 50, 75-81]. However obesity rates have significantly increased over the past 20 years in western societies, therefore it is likely that the presence of hepatic steatosis potential donors is even more common today. The high prevalence of macrovesicular steatosis in the general population poses a major challenge to the field of liver transplantation since unlike microvesicular steatosis, the presence of macrovesicular steatosis has been found to be a major risk factor for poor graft function following transplantation [35].

1.4 Macrovesicular Steatosis And Transplantation

In 1987 Portman et al. [82] first suggested that there may be an association between severe steatosis and graft primary non-function (PNF). Since that time there has been the accumulation of a large body of evidence correlating the presence of macrovesicular fat with an increased incidence of post-operative complications including: prolonged intensive care unit and hospital stay; delayed graft function (DGF) and PNF (up to 60%); biliary complications; and increased overall cost [46, 83-86]. However, the risk varies with the degree of steatosis within the liver. Hepatic steatosis is categorized as mild (<30%), moderate (30-60%) and severe (60%) according to the percentage of hepatocytes containing fat vacuoles within the cytoplasm [35, 87, 88]. There is a large amount of evidence indicating that livers with mild steatosis can be transplanted with results similar to those for nonsteatotic livers [35, 38] and although some transplant centres report good results with severely steatotic livers in highly selected patients [89-92], the majority of centres avoid transplanting livers with severe steatosis because of the exceptionally high complication and reduced survival rates associated with their use [33, 34, 36, 39, 73, 75, 81, 93-97]. The most controversy arises in the use of livers with moderate steatosis.

While the use of these livers does not appear to have as significant an effect on graft function and survival as severely steatotic livers do [86, 90, 93, 98, 99], many studies still report moderate rates of early graft dysfunction [39, 52, 81, 95, 100, 101], especially in the setting of prolonged cold ischemia [95]. While many centres will use moderately steatotic organs, these organs are generally reserved for low-risk patients or those in urgent need of transplantation. Over the past 20 years, research has demonstrated that the reason for the high rates of graft dysfunction in livers with macrovesicular steatosis is a reduced tolerance for organ ischemia and reperfusion injury sustained during transplantation [40, 91, 93, 102-104].

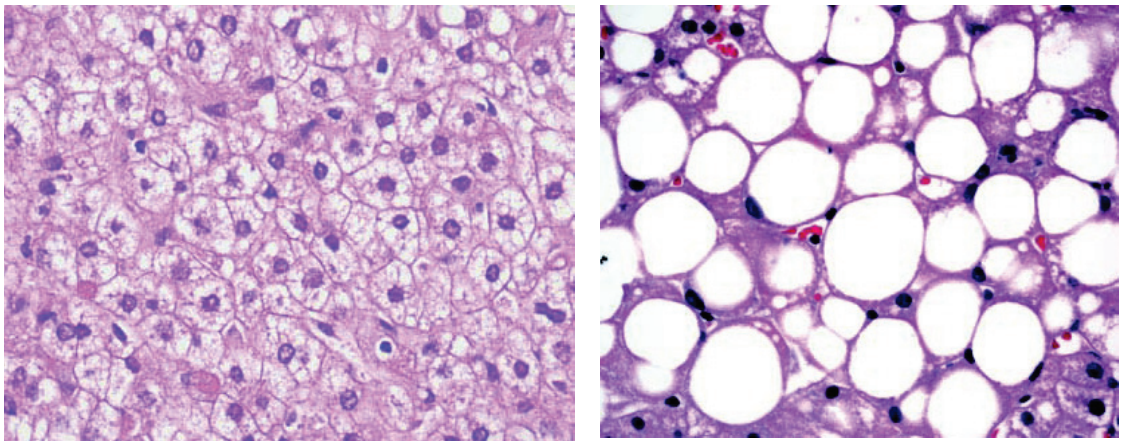

Figure 1. Microvesicular and macrovesicular steatosis. Hematoxalin and eosin staining of liver tissue demonstrating microvesicular and macrovesicular steatosis. In microvesicular steatosis (left) hepatocytes contain multiple small fat droplets in the cytoplasm without displacement of the nucleus. In macrovesicular steatosis (right) hepatocytes typically contain one or a small number of large fat droplets with displacement of the nucleus to the periphery of the cell. Used with permission from Yerian, 2011 [43].

1.5 Hepatic Steatosis And Ischemia Reperfusion Injury

1.5.1 Ischemia Reperfusion Injury And The Liver

Ischemia reperfusion injury (IRI) is the accumulated injury sustained by an organ as a result of direct cellular damage from ischemia and delayed damage from subsequent activation of the innate immune system following reperfusion. The specific sequence of events involved in IRI have not been determined precisely, as it is a complex interplay involving activation and recruitment of multiple cell types, and the production and release of cytotoxic compounds, inflammatory cytokines and complement. In the setting of liver transplantation there are two main types of ischemic injury: 1) cold ischemic injury (II) and 2) warm IRI [105]. Because all cadaveric donor transplants undergo a significant period of cold storage they are highly susceptible to cold II. Cold II in the liver is dominated by damage to sinusoidal endothelial cells (SEC's) and microcirculatory disruption [105-108]. Cold ischemia inhibits the Ca^{2+}-ATPase resulting in a slow increase in intracellular calcium with subsequent activation of calpains and disassembly of cell structural components [109, 110]. This leads to the release of matrix metalloproteinases, activation of the cell surface, platelet adhesion and reduced sinusoidal flow upon reperfusion [111-113]. The end result of cold storage injury is cellular death via a combination of apoptosis and cellular necrosis [105, 114]. In addition, during ischemia, there is a depletion of adenosine triphosphate (ATP) within SEC's, Kupffer cells and hepatocytes [115, 116], resulting in the impairment of the sodium/potassium ATPase, the accumulation of intracellular sodium, and cellular edema [117, 118]. This leads to sinusoidal narrowing and reduced microcirculatory flow on reperfusion [118].

Cellular damage and necrosis results in the release of danger-associated molecular pathogens (DAMP's), which are recognized by pattern recognition receptors (PRR's), such as toll-like receptor 4 (TLR-4), resulting in activation of cellular mediators of inflammation [118]. Following reperfusion kupffer cells are activated via TLR-4 signalling or by complement [113, 119] to produce and release reactive oxygen species (ROS) [120-122], and inflammatory cytokines including tumor necrosis factor-α (TNF-

α), interleukin-6 (IL-6), interleukin-12, (IL-12), interleukin-18 (IL-18) and interleukin-1β (IL-1β) [113, 118, 123-125]. This results in cellular damage and the recruitment of inflammatory cells. Reactive oxygen species are produced primarily by Kupffer cells and neutrophils via the xanthine oxidase system, as well as electron release from damaged mitochondria [126, 127]. ROS cause extracellular matrix breakdown, destroy cellular membranes through lipid peroxidation [105, 128], react with nitric oxide (NO) to create reactive nitrogen species (RNS) [113] and stimulate the release of inflammatory cytokines such as TNF-α and IL-10 from endothelial cells [129, 130]. Inflammatory cytokines recruit and activate neutrophils, monocytes and lymphocytes (primarily CD4+ T cells) to sites of injury [131-133]. Activated neutrophils release proteases and ROS resulting in extracellular matrix breakdown and cellular damage [106, 118]. CD4+ T cells perform multiple actions, including the stimulation of: neutrophils in response to IL-17 release [134]; hepatocytes to produce ROS; and endothelial cells and hepatocytes to express cellular adhesion molecules such as intercellular adhesion molecule-1 (ICAM-1) and vascular adhesion molecule-1 (VCAM-1) [113, 131, 135]. Selectins and integrins on the surface of activated neutrophils and platelets mediate adhesion to ICAM's and VCAM's resulting in congestion of sinusoids and a further reduction in circulatory flow [136-139]. CD4+ T cells release interferon-γ (IFN-γ) which further activates Kupffer cells to produce TNF-α, IL-1 and prostanoids [140], although the mechanism by which this is accomplished is not yet fully understood. The end result of these processes is cellular death via a combination of necrosis and apoptosis [105, 141], which if extensive enough can result in hepatic dysfunction or even non-function.

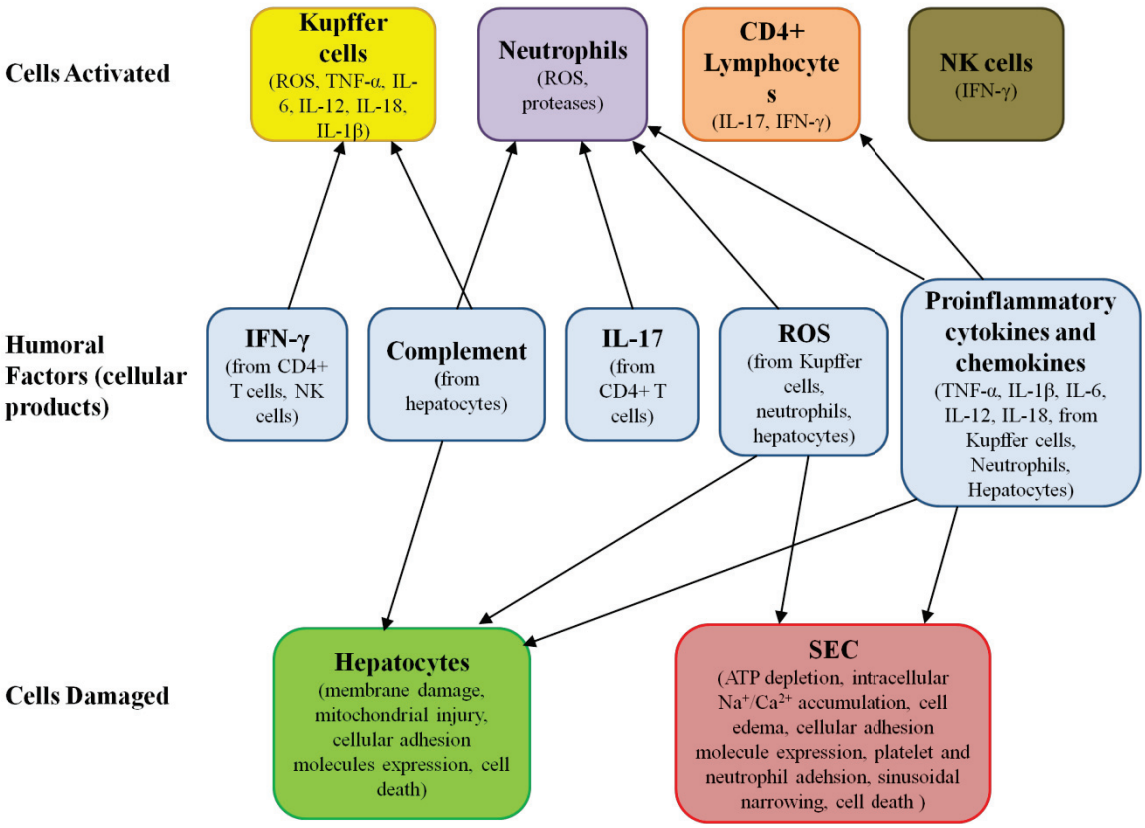

Figure 2. Cellular and humoral mediators of liver ischemia reperfusion injury. During cold storage, ATP depletion results in intracellular accumulation of Na^{+} and Ca^{2+} resulting in SEC swelling. Upon reperfusion Kupffer cells are activated by complement and release ROS and pro-inflammatory cytokines, resulting in hepatocyte and SEC damage and recruitment of neutrophils and lymphocytes. Neutrophils release ROS and proteases, furthering SEC and hepatocyte damage. IFN-γ from CD4+ T cells and NK cells further activates Kupffer cells. CD4+ T cells also release IL-17 resulting in recruitment of neutrophils and monocytes and further organ injury. Adapted with permission from Abu-amera et al., 2010 [118].

1.5.2 The Effects Of IRI On Steatotic Livers

There is a large body of evidence demonstrating that recipients of livers with moderate to severe macrovesicular steatosis suffer more postoperative complications, have increased rates of allograft dysfunction and non-function and even reduced survival. It is thought that the principal reason for this is an exaggerated IRI compared to non-steatotic livers [35, 103, 142]. Animal models of IRI and hepatic steatosis using a methionine and choline deficient (MCD) diet have found: increased transaminase levels [104]; increased leukocyte recruitment and adhesion [104]; increased sinusoidal stenosis and obstruction with reduced flow [143, 144]; greater mitochondrial injury with significantly lower ATP and ATPase levels [145]; massive necrosis [104]; and reduced survival in animals with steatotic livers [145]. Animal models using leptin receptor deficient Zucker rats similarly demonstrate: a predominance of necrosis vs. apoptosis in control animals [102]; increased lipid peroxidation [146]; higher transaminase levels [147]; lower ATP and ATPase levels [35]; increased free radical formation [148, 149]; reduced hepatic arterial and micocirculatory flow [150]; and reduced survival [147].

Several potential explanations for these findings have been hypothesized. It has been shown in animal models that the hepatic sinusoidal space is decreased by 50% in fatty livers [143, 151-153]. When combined with the cellular swelling and platelet and leukocyte adhesion seen in reperfusion injury there is an even greater reduction in sinusoidal flow [84]. The increased lipid content of steatotic livers provides more substrate for peroxidation resulting in the increased formation of free radicals that can cause further cellular damage [94, 148, 149]. There is also evidence of mitochondrial dysfunction in steatotic livers. Steatosis leads to an accumulation of non-esterified fatty acids which have an inhibitory effect on β-oxidation leading to a decrease in acetyl-coenzyme A (CoA) production and impaired gluconeogenesis [35]. The downstream effect is reduced intracellular energy levels and ATP depletion. Hepatic steatosis appears to alter Kupffer cell function and this may also play a role in reducing tolerance to IRI. In response to liver injury, Kupffer cells from steatotic mice demonstrate decreased phagocytic capability and increased release of ROS, IL-6, and IL-1β resulting in an

amplification of the inflammatory response and escalation of hepatocellular injury [39, 40, 144]. In addition, increased TNF-α levels have been demonstrated in animal models of hepatic steatosis, leading to increased expression of cellular adhesion molecules and increased leukocyte recruitment and adhesion [39]. Lastly, steatosis may result in derangements in the apoptotic pathway. Pro-apoptotic caspase levels are decreased in Zucker rat livers in response to IRI and this leads to massive necrosis, whereas in lean animals the degree of cellular death is much smaller and occurs predominantly via apoptosis [35]. This shift to necrosis results in exacerbation of the inflammatory response and more extensive organ injury. Because exacerbated IRI appears to be the major mechanism responsible for the increased rate of graft dysfunction observed in steatotic livers, research aimed at improving the utility of these organs has been aimed, primarily, at mechanisms that either inhibit IRI, or enhance hepatic resistance to this process. One such approach that has received intense interest is the upregulation of the heme oxygenase system.

Chapter 2: Heme Oxygenase

Heme oxygenase (HO) catalyzes the first and rate-limiting step in the breakdown of heme into biliverdin (BV), carbon monoxide (CO) and free divalent iron (Fe^{2+}) [154]. The enzyme was first identified in 1968 by Tenhunen et al. [155]. Three different isoforms of the enzyme have been identified. However only two (HO-1 and HO-2) are expressed in humans [156]. HO-2 is constitutively expressed under homeostatic conditions, HO-1 expression is highly inducible in response to cellular stress and a number of exogenous compounds [154, 157, 158]. Although both enzymes catalyze the same reaction, the significant induction of HO-1 expression under conditions of cellular stress has targeted it as a key gene for protection against inflammatory injury [154, 158]. The HO-1 gene is located on chromosome 22 at locus q12, and encodes a 32 kiloDalton (kDa) protein [159]. The gene is well conserved across species, with the human, mouse and rat genes sharing similar structural organization into five exons and four introns, and their cDNA's demonstrating 80% sequence homology [158]. Recombinant human HO-1 has also been used successfully in rodent models of disease [160]. The heme degrading function of the enzyme is mediated by a flexible bihelical structure surrounding the heme pockets, containing a conserved histidine residue (His-25) that serves as the heme ligand [161, 162]. Both isoforms contain similar hydrophobic regions at the extreme carboxy terminus, which serve to anchor them to cellular membranes [163-165]. Within the cell HO-1 is primarily localized to the endoplasmic reticulum (ER); but has also been found in the nucleus and associated with the plasma membrane [158]. HO-1 is most highly expressed in the spleen and specialized reticuloendothelial cells of the liver and bone marrow [166, 167]. In response to hemolysis, HO-1 activity is dramatically increased in the liver parenchyma, kidney, and circulating macrophages [167-169]. It is also highly expressed in activated monocyte/macrophages, dendritic cells [170]and consitutively expressed in CD4+CD25+ T cells [170-173]. Although the p38 mitogen activated protein kinase (MAPK) pathway appears to represent the major pathway responsible for HO-1 induction [158, 174], a number of other pathways including the extracellular signal-regulated kinases 1/2 (ERK1/2) [157, 174, 175], protein kinase C (PKC) [176, 177], protein kinase A (PKA) [178], and phosphatidyl-inositol-3-kinase (PI3K) pathways

[179, 180], are also known to play a role in the induction of HO-1 expression. A major inducer of HO-1 expression is oxidative stress [181]. HO-1 mRNA levels are increased in viable rat tissue within four hours of reperfusion [182]. It is likely that this is an adaptive mechanism for cellular protection from inflammatory injury. Indeed, there is a host of evidence supporting a key role for HO-1 in cellular protection against IRI.

2.1 HO-1 And IRI

HO-1 activity is important in the maintenance of oxidant/antioxidant homeostasis. Most HO-1 deficient (HO-1 -/-) mice do not survive to term, and those that do demonstrate growth retardation and normochromic, microcytic anemia and die within one year. On examination, these animals demonstrate iron deposition in their kidneys and livers, and evidence of chronic inflammation with hepatosplenomegaly, leukocytosis and hepatic periportal inflammation [154]. These mice also display increased mortality in a model of lung IRI [183]. A human case of HO-1 deficiency has been reported with findings of endothelial cell damage, iron accumulation in the liver and kidney and increased cell susceptibility to heme overloading in vitro [184].

Overexpression of HO-1improves resistance to oxygen hyperoxic cellular injury in pulmonary epithelial cells [185, 186] and prevents TNF-α-mediated apoptosis in murine lung fibroblasts and endothelial cells through increased expression of the anti-apoptotic molecules B cell lymphoma-2 (Bcl-2), bcl-2-associated athanogene-1(Bag-1) and bcl-2-associated x protein (Bax) [187-190]. HO-1 expression has been found to be protective against IRI in animal models of lung, heart, kidney and liver transplantation [189-195]. There is also evidence to support the importance of HO-1 in protecting against IRI in human transplantation. A dinucleotide repeat polymorphism, containing a variable number of guanine thymine (GT) repeats within the HO-1 promoter, has been described [196]. Promoters with short GT repeat sequences are associated with high HO-1 expression, while those with long GT repeat sequences are associated with low expression [197]. Katana et al. examined the promoters of kidney transplant recipients

and donors, and found an association between recipients with high expression polymorphisms and improved graft function two years post transplant [159].

In the case of the liver, HO-1 upregulation has been shown to preserve microcirculatory function [198-202], inhibit leukocyte adhesion and accumulation within the sinusoids [203-205], reduce the production of inflammatory cytokines [204, 206, 207], prevent ATP depletion [208], and reduce apoptosis [202, 204, 205, 207, 209] in animal models of IRI. There is also evidence that HO-1 may confer protection by inducing a switch from a Th1 to a Th2 response. In a rat LT model Ke et al. found that HO-1 overexpression resulted in increased levels of the Th2 cytokines IL-4 and IL-10 and decreased levels of the Th1 cytokines IFN-γ and IL-2 [210]. The end result of these effects is reduced hepatocellular injury, preserved liver function, and improved graft and recipient survival [201, 211]. Conversely, inhibition of HO-1expression using small interfering ribonucleic acid (siRNA), or HO-1 knockout mice (HO-1+/-) results in increased levels of TNF-α, IL-6 and IFN-γ, enhanced leukocyte adhesion and recruitment, and increased apoptosis [204, 205]. In an animal model of transplantation following extended cold storage, inhibition of HO-1 activity using tin protoporhyrin (SnPP) ameliorated the beneficial effects seen from heat preconditioning or cobalt protoporphyrin (CoPP) treatment [202].

The benefits of increased HO-1 activity have been studied in animal models of hepatic steatosis. Using rats fed a methionine and choline deficient diet (MCD), Mokuno et al. demonstrated that HO-1 upregulation via heat shock preconditioning results in a reduction in TNF-α and IL-10 levels, reduced necrosis, and improved survival, following transplantation [211]. HO-1 overexpression using adenoviral gene transfer in Zucker rats results in reduced hepatocyte injury and improved liver function and survival following liver transplantation [198]. Similar effects have been seen with HO-1 upregulation by ischemic preconditioning [212-214]. These protective effects appear to be mediated through the end products of Heme breakdown by HO-1: BV/bilirubin (BR) and CO.

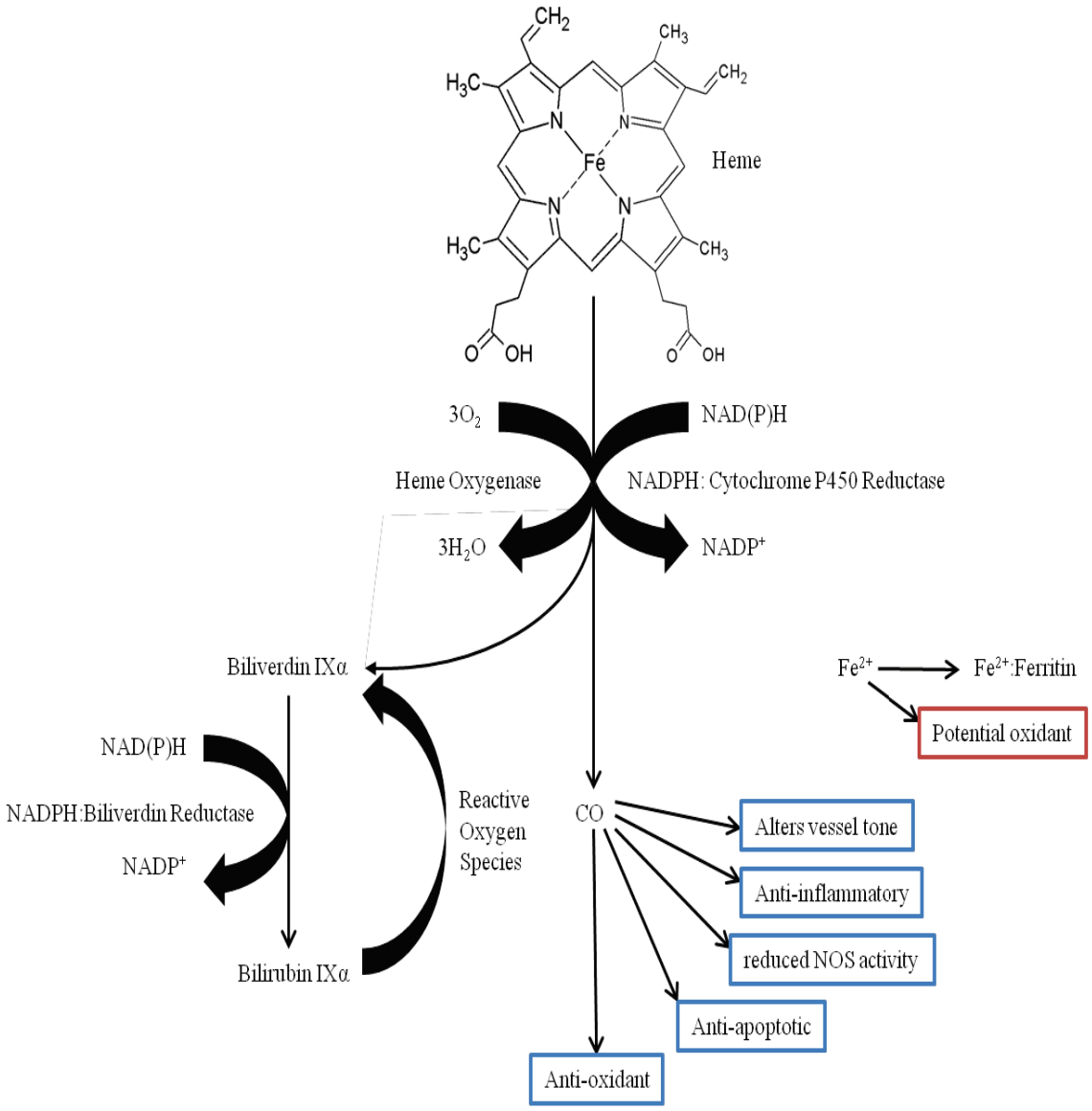

Figure 3. Heme Oxygenase-1 catalyzes the rate-limiting step in the conversion of heme to biliverdin, carbon monoxide and free iron. Biliverdin is converted to bilirubin which functions as a free radical scavenger and is recycled back to biliverdin. Free iron is bound by ferritin preventing its injurious effects. Carbon monoxide stimulates vascular relaxation, and has anti-inflammatory, anti-oxidant and anti-apoptotic effects.

2.1.1 Biliverdin/Bilirubin

The metabolism of heme by HO-1 leads to the production of BV. Within the cell BV is rapidly converted to BR by biliverdin reductase (BVR). Both BV and BR are important endogenous antioxidants whose activities have been demonstrated *in vitro* and *in vivo* [215, 216]. Biliverdin therapy was found to result in improved portal venous flow, increased bile production, reduced hepatocelullar damage and preservation of hepatic histologic structure in a rat model of liver transplantation [217]. BV given as an adjuvant during and after transplantation results in a decrease in endothelial expression of cellular adhesion molecules, reduced infiltration by neutrophils and inflammatory macrophages, reduced production of inducible nitric oxide synthase (iNOS) mRNA and pro-inflammatory cytokines (IL-1β, TNF-α, and IL-6), and increased expression of anti-apoptotic molecules (Bcl-2, Bag-1) in a rat model of LT [217]. BR has been shown to rescue cells from hydrogen peroxide induced damage [218] and to suppress oxidative stress in rats treated with copper sulphate or exposed to ultraviolet radiation [219, 220]. By scavenging oxygen radicals BR is, itself, oxidized to BV which is then recycled back to BR by BVR, resulting in an amplification of BR bioactivity that allows for small quantities of BR to effectively neutralize much larger amounts of oxygen radicals. This is supported by research demonstrating that BR is capable of protecting cells from a 10,000 fold increase in oxidative stress generated by hydrogen peroxide [218, 221]. These findings suggest that HO-1 produced BV and BR play a major role in cytoprotection against IRI through ROS scavenging and the suppression of inflammatory and apoptotic signalling.

2.1.2 Carbon Monoxide

Another major product of HO-1-mediated heme degradation is CO. Although previously thought of as a toxic substance, in small quantities, CO has been found to have significant anti-inflammatory and vasodilatory effects. CO administration provides protection against inflammatory injury in animal models of heart, lung, kidney, liver and small bowel IRI [222, 223]. In humans CO production, evaluated by measurement of

carboxyhemoglobin, is associated with improved survival in liver transplant patients [224]. CO inhalation improves survival after IRI in HO-1 deficient mice, although alone it is unable to fully compensate for the loss of HO-1 activity [183]. These beneficial effects are achieved through a number of different mechanisms. CO inhalation suppresses expression of early pro-inflammatory genes (TNF-α, IL-6, nitric oxide synthase (NOS)) via inhibition of ERK1/2 signalling [182], and causes vasorelaxation and inhibition of platelet activation and aggregation [225] - processes that requires both cyclic guanine monophosphate and p38MAPK signalling [187]. The p38 MAPK pathway also appears to be responsible for the anti-apoptotic effects of CO. CO inhalation in a mouse model reduced apoptosis through activation of the MKK3/p38MAPK pathway resulting in decreased expression of Fas and FasL, inhibition of the activity of caspases 3, 8 and 9, and increased expression of the anti-apoptotic molecules Bcl-2 and B cell lymphoma extra large (Bcl-X_L) [226]. The vasoactive properties of CO can be attributed to at least two separate mechanisms. CO stimulates soluble guanylate cyclase (sGC), resulting in the generation of cGMP and activation of calcium-dependent sodium channels [227, 228], with subsequent smooth muscle and hepatic stellate cell relaxation and a reduction in sinusoidal tone [229, 230]. In addition, CO inhibits cytochrome p450 mediated production of endothelin-1, a compound known to increase sinusoidal resistance [231]. CO generated by hepatocytes may also play a role in the regulation of bile excretion through alteration of the contractility of the bile canaliculus [232]. Other anti-inflammatory effects of CO include the down-regulation of iNOS and plasminogen activator inhibitor type 1 (PAI-1) expression in macrophages, endothelial cells, fibroblasts and hepatocytes [187, 225, 233]. Based on the wide body of research on the biologic functions of HO-1, it is apparent that it exerts its primary cytoprotective effects through the actions of its enzymatic products: biliverdin and carbon monoxide.

2.1.3 Fe^{2+} And Ferritin

Although much of the beneficial effects of HO-1 expression are mediated through the production of BV and CO, another key role is the regulation of free iron in conjunction with HO-1 expression. Fe^{2+} is the other product of heme degradation by HO-1. Fe^{2+} causes cytotoxicity through incorporation into phospholipid bilayers and the generation of hydroxyl radicals [234, 235] via the Fenton reaction [236]. However, HO-1 induction also results in a concomitant increase in the expression of ferritin [237-239] and the ATPase pump responsible for exporting iron from the cell [240]. Fe^{2+} is immediately bound by ferritin [241], and this combination of ferritin sequestration and export from the cell serves to protect cells from the potentially injurious effects of free iron.

2.2 Mechanisms Of HO-1 Upregulation

The data supporting the role for HO-1 as a major mediator of protection against IRI has made upregulation of its expression a major area of interest in the field of transplantation. Much work has gone into finding the best mechanism by which this can be accomplished and applied safely and ethically to the field of human solid organ transplantation.

As previously mentioned the HO-1 promoter is governed by multiple regulatory elements [159], and multiple different signalling pathways have been implicated in the induction of its expression [157]. The most well known inducers of HO-1 expression are heme and cobalt protoporphyin, and these compounds have been used in multiple animal studies. Heme is known to cause cytotoxic injury through the production of free radicals, and cytoskeletal and DNA damage [184, 189, 242, 243]. The administration of such a potentially injurious substance to donor or recipient would not likely receive ethical approval for clinical trials. Similarly, cobalt ions can stimulate the production of inflammatory cytokines and ROS [244-249]. Another one of the most studied mechanisms for HO-1 upregulation is ischemic preconditioning, which involves subjecting the organ to a short period of ischemia and reperfusion prior to the period of prolonged ischemia. This results in activation of cytoprotective mechanisms including

HO-1expression, and primes the organ for the greater stress to come [106, 250]. Despite promising results in animal studies trials of ischemic preconditioning in humans have reported disappointing results with no benefit to graft or patient survival [147], and a recent Cochrane database review concluded that there is currently no evidence to support the preconditioning of donor livers [251]. A variety of natural compounds have also been found to induce HO-1 expression [182, 252]. However, the potential for HO-1 upregulation with these compounds could be limited by dosing, and they require pre-treatment of the donor, which can be fraught with ethical issues.

Multiple studies have examined the effects of HO-1 overexpression using adenoviral gene transfer [198, 200, 207, 208, 253]. These delivery systems allow for efficient transduction of multiple cell types with high capacity vectors capable of achieving stable long-term overexpression of a gene of interest [254-256]. However, the cells most sensitive to liver IRI are sinusoidal endothelial cells, and adenoviruses poorly transduce endothelial cells [256]. In addition, HO-1 has been found to be highly expressed in many tumors of different tissue origin, and can induce cancer cell proliferation, angiogenesis, metastasis, and resistance to apoptosis and chemotherapy [170, 257-262]. These findings suggest that long term HO-1 overexpression may have detrimental effects. Cellular transduction by adenoviral vectors incites an innate and subsequent adaptive immune response towards the virus and the transgene [254, 255]. Recombination between the helper virus and host genome has also been reported in certain cell types [256]. An ideal therapy would be able to temporarily provide a large increase in HO-1 activity within the target tissues during the time when it is most required - during ischemia and immediately post-reperfusion. The ability to treat donor organs in an *ex vivo* situation would also alleviate many of the ethical concerns associated with systemic pretreatment of donors. A potential method to achieve this goal this would be the creation of an HO-1 protein that is able to transverse the cellular membrane independent drugs or viral particles. This could be accomplished by incorporation of a protein transduction domain sequence to generate a cell-penetrating recombinant HO-1 protein.

Chapter 3: Cell-Penetrating Peptides

Cell-penetrating peptides (CPPs) (also known as protein transduction domains (PTDs) are short cationic amino acid (a.a.) sequences (generally 9-20 a.a.) that are capable of crossing cellular membranes independent of normal receptor-ligand interactions. Cellular transduction by a polycationic peptide was first reported in 1965 [263], and this was confirmed in 1988 and 1991 when it was found that the trans-activator of transcription (TAT) protein of the human immunodeficiency virus (HIV) and the *Drosophila* Antennapedia homeodomain were able to transduce human cells [264, 265]. In 1994 Derossi et al. determined that the cell-penetrating ability of Antennapedia was due to a 16 a.a. sequence (RQIKIYFQNRRMKWKK), which they termed penetratin [266]. This was followed in 1997 by Vives et al. who identified the minimal peptide sequence of TAT required for cellular uptake [267]. Since that time a number of other transducible peptides have been discovered and synthesized [268]. These peptide sequences have garnered specific interest not only because they are able to cross cellular membranes, but also because they are able to transport linked cargo along with them into the cell [268]. As such, they are currently one of the most promising tools for the delivery of biologically active molecules into cells, and a potential keystone in the future of targeted therapeutics for many diseases [269-271].

CPPs have been shown to efficiently deliver a variety of biomolecules including: full length functional proteins; plasmid DNA; siRNA; peptide nucleic acids (PNA); liposomes; nanoparticles and even pharmaceuticals [268, 272]. They possess some key advantages over viral gene delivery methods in that they are free of infectious material, can be produced in large quantities and stably stored by lyophilisation, can be used to deliver active proteins rather than just nucleic acids, and their transduction capacity appears to be size-independent (proteins in excess of 100kDa have been delivered successfully into cultured cells [273]) [268, 274]. As researchers have begun to understand mechanisms by which CPP's transduce cells, and the sequence characteristics that convey these abilities, they have modified them or designed new sequences to

overcome limitations and enhance function leading to the development of chimeric and synthetic classes of CPP's in addition to the original protein-derived ones [272].

3.1 Mechanisms Of Transduction

Although a large amount of work has gone into elucidating the mechanisms of CPP transduction, it is still incompletely understood. It was originally thought that CPP's entered cells in an energy- and receptor-independent fashion; however research over the past 10 years has shown that this is not the case [273, 275, 276]. It is likely that not all CPP's are internalized by a single mechanism, and some appear to use more than one mechanism, although it is generally accepted that for most polycationic CPP's internalization occurs primarily via endocytosis [277-280]. The internalization process occurs through three primary steps: 1) electrostatic interactions with the plasma membrane 2) endocytosis and 3) release into the cytoplasm by retrograde transport [268, 274, 276]. The electrostatic interactions are believed to be mediated by interactions between the guanidium groups on arginine residues and proteoglycans associated with cellular membranes [276, 281, 282]. Following interaction with the cellular membrane the CPP is taken up by endocytosis. Endocytosis can occur through any of 3 major mechanisms: 1) clathrin-mediated 2) caveolin-mediated and 3) macropinocytosis, and there is evidence that CPP internalization occurs by each of these [283-287]. Relocation to the cytoplasm or nucleus occurs after endosomal escape via reverse transport [288]. Although the major pathway for CPP uptake appears to be via endocytosis, there is also evidence to support nonendosomal pathways which can occur in parallel with endosomal uptake [276, 281, 289]. The exact mechanism of uptake appears to vary, not only between individual CPPs, but is also dependent upon the specific cargo [272, 290-292].

Regardless of the mechanism through which a CPP enters the cell there is considerable evidence supporting the ability of these molecules to transport cargo into cells both *in vitro* and *in vivo*. This has led to the investigation of CPP-mediated delivery of therapeutic molecules in models of disease including stroke [293-296], cardioprotection

[297-300], neuropathic pain [301], and oncology [302-307], among others. A small number of studies have evaluated the therapeutic benefits of CPP-delivered HO-1. Ribeiro et al. showed that a TAT-HO-1 fusion protein was able to transduce pancreatic β-cells and protect them from TNF-α mediated cytotoxicity. These cells were then able to reverse chemically-induced diabetes upon islet cell transplantation [308]. Ma et al. demonstrated that a recombinant HO-1 protein containing an N-terminal modified TAT sequence was able to transduce and protect hearts from prolonged cold storage in an animal model of cardiac transplantation. Transduced hearts had less ischemic damage, reduced apoptosis, and there was improved graft and recipient survival following transplantation in comparison to untreated controls, or to organs treated with a cell-penetrating HO-1 lacking enzymatic activity, or cell-penetrating enhanced green fluorescent protein (EGFP) [160]. Most recently Li-hui et al. found that TAT-HO-1 is able to transduce rat liver cells and reduce SEC apoptosis in an *ex vivo* model of IR. These studies suggest that cell-penetrating peptides can be used as a vehicle for HO-1 delivery to organs *ex vivo*, and that a cell-penetrating HO-1 has therapeutic potential in the protection of solid organs from IRI after transplantation.

Chapter 4: Summary And Objective

Advances in the field of liver transplantation have led to it becoming the therapy of choice for those with end-stage liver disease or certain hepatic cancers not amenable to liver resection. The number of patients who are candidates for this life-saving therapy far outweighs the availability of donor organs. As wait lists have grown, and more patients die while waiting for an organ, transplant surgeons have become more aggressive in using organs previously thought too high-risk for transplantation. Livers with significant macrovesicular steatosis comprise a large proportion of these extended criteria organs. The use of steatotic livers for transplantation has been associated with increased rates of graft dysfunction, non-function, biliary complications, chronic rejection and decreased patient survival. This is because of their increased susceptibility to ischemia-reperfusion injury (IRI). Heme oxygenase 1 has emerged as a major therapeutic target in the protection of organs from IRI. Upregulation and overexpression of HO-1 has been shown to reduce IRI in animal models of liver transplantation, including models of hepatic steatosis. However, current methods for HO-1 therapeutics are limited by ethical concerns regarding the pre-treatment of donors (in the case of heme and CoPP); limitations in the ability to increase HO-1 expression and activity (natural products and anaesthetics); inconsistent results (ischemic preconditioning); or the generation of an aggressive innate immune response, DNA recombination between host and vector genomes and the potential for increased oncogenic activity with long term HO-1 overexpression (adenoviral gene transfer). Cell-penetrating peptides (CPP) have emerged over the past 10 years as major targets for the delivery of therapeutic bioactive molecules to cells. These peptides represent an ideal method for HO-1 therapeutics in the setting of transplantation. A CPP-HO1protein solution or lyophilized powder can be brought by the retrieval team and administered to the organ during cold storage. Such a protein allows for the delivery of active HO-1 and can be re-administered as necessary prior to implantation. The dose can be escalated as required and is potentially unlimited in its ability to increase HO-1 activity. There are no issues with long-term HO-1 overexpression and potential oncogenicity, as the protein is delivered and present during the time of ischemia and immediate post reperfusion period, and because the half-life of HO-1 is only 15 hours it will not persist within the organ long term [309].

CPP-HO1 molecules have already demonstrated efficacy in cytoproctection against IRI in *in vitro* and animal models; however, it has not been tested in an animal model of liver transplantation, or in steatotic livers. As steatotic livers are more susceptible to IRI than non-steatotic livers, it is hypothesized that treatment with a CPP-HO-1 will lead to a significant benefit in terms of reduced liver injury, improved graft function, and improved survival. The objective of this project is the creation of a functional CPP-HO-1 for use in an animal model of steatotic liver transplantation.

Chapter 5: Materials And Methods

5.1 Creation Of Expression Plasmids

5.1.1 Plasmids Used

Multiple plasmids were used in this study. The plasmid pINCY, containing the human HO-1 cDNA sequence was purchased from Open Biosystems (Huntsville, AL) and used as the template for HO1 PCR amplification. The cDNA template for EGFP was the plasmid pEGFP-C1 (Clontech, Mountain View, CA, USA) (generously donated by Dr. Kishore Pasumarthi). Two separate expression plasmids were used: 1) pET28B(+) (Novagen, Gibbstown, NJ, USA) containing a *lac I* coding sequence; a kanamycin resistance gene; a bacteriophage T7 promoter upstream of a lac operator sequence, a 6X histidine tag, and a multiple cloning site with restriction sites for, among others, NheI, EcoRI and HindIII. A second 6X histidine tag is located downstream from the multiple cloning site, which was incorporated into the CPP,EGFP, CPP-HO1-1 and CPP-SDMHO1 clones. 2) pTAT2.1 (generously donated by Dr. Steve Dowdy) is derived from pET28B and contains a kanamycin resistance gene; and a bacteriophage T7 promoter upstream of a 6X histidine tag, a TAT sequence (AGGAAGAAGCGGAGACAGCGACGAAGA) and a multiple cloning site that includes restriction sites for EcoRI and HindIIII.

5.1.2 Primers

All forward primers contained a 5' EcoRI restriction site just upstream from the gene coding sequence and all reverse primers contained a 5' HindIII restriction site just downstream from the gene coding sequence. Other primer-specific inclusions are listed as follows.

1. **pCPP-EGFP**:
   a) forward primer (**CPP-EGFP +**)
      5'AAGCTAGCGGCTATGCTCGCGCTGCTGCTCGCCAGGCTCGCG
      CTGGTGAATTCCGCCACCATGGTGAGCAAGGGCG-3' containing a

5’ NheI restriction site, a CPP sequence, and an internal EcoRI site upstream to the EGFP sequence

b) reverse primer (**EGFP -**)

5’-GGCAAGCTTCTTGTACAGCTCGTCCATGCC-3’

2. **pTAT-EGFP**:

a) forward primer (**EGFP +**)

5’-TAGAATTCCACCATGGTGAGCAAGG-3’

b) reverse primer (**EGFP -**)

5’-GGCAAGCTTCTTGTACAGCTCGTCCATGCC-3’

3. **pCPP-HO1-1**:

a) forward primer (**HO1 +**)

5’-TAGAATTCATGGAGCGTCCGCAACCCGAC-3’

b) reverse primer (**HO1-1 -**)

5’-CGAAGCTTCATGGCATAAAGCCCTACAGC-3’

4. **pCPP-HO1-2**:

a) forward primer (**HO1 +**)

5’-TAGAATTCATGGAGCGTCCGCAACCCGAC-3’

b) reverse primer (**HO1-2 -**)

5’-CGAAGCTTCACATGGCATAAAGCCCTACAGC-3’ containing a stop codon just upstream from the 5’ HindIII restriction site.

5. **pTAT-HO1**:

a) forward primer (**TATHO1 +**)

5’-TAGAATTCCATGGAGCGTCCGCAACCCGAC-3’

b) reverse primer (**HO1-1 -**)

5’-CGAAGCTTCATGGCATAAAGCCCTACAGC-3’

6. **pSoluble HO1 (sHO1)**:

a) forward primer (**HO1 +**)

5’-TAGAATTCATGGAGCGTCCGCAACCCGAC-3’;

b) reverse primer (**sHO1 -**)

5’-AAATAAGCTTTCAAGCCTGGGAGCGGGTGTTGAGTGG-3’ containing a stop codon starting at base 796 of the HO-1 gene sequence.

The forward and reverse primers for CPP-EGFP and CPP-HO1-1 were derived from those described by Ma et al. [160]. All primers were purchased from IDT (Coralville, IA, USA) with the exception of the forward primers for pTAT-EGFP and pTAT-HO1, which were purchased from Invitrogen (Carlsbad, CA, USA).

5.1.3 Polymerase Chain Reaction

PCR amplification was performed in 50µl reaction volumes containing ~50ng of template DNA (pEGFP-C1 or pINCY), 200µM final concentration of dNTP's (NEB, Ipswich, MA, USA) 0.5µM final concentrations of forward and reverse primers, 1.5µl of stock DMSO (Finnzymes), 10µl of 5X Phusion HF Buffer (Finnzymes, Finland) and 1 unit (U) of Phusion Hot Start Taq Polymerase (Finnzymes). Reactions were carried out using an icycler (Biorad, Hercules, CA, USA) under the following cycling conditions: a hot start at 98°C, 30 seconds at 98°C, 35 cycles of (10 seconds at 98°C, 15 seconds at 70°C, 30 seconds at 72°C), 10 minutes at 72°C and then held at 4°C. Amplified DNA samples were then purified from the reaction mixture and unused dNTP`s using a commercial purification kit (Qiagen, Germany) according to the manufacturer's instructions. Purified samples were analyzed by gel electrophoresis through a 1% agarose (Invitrogen) gel containing ethidium bromide and imaged using an Alphaimager (AlphaInnotech Corporation, San Leandro, CA, USA). DNA concentration was determined using a Nanodrop 2000 spectrophotometer (Thermo Scientific, Waltham, MA, USA).

5.1.4 Site-Directed Mutagenesis

Ma et al., 2009 [160] described the creation of a non-functional HO-1 mutant containing the point mutations H25A and H132A. I desired to create a similar mutant for use as a negative control, and to do so created primers as described by Ma et al. which encode for a change from hisitidine to alanine at amino acids 25 and 132 of the HO-1 protein sequence. The primers sequences are (all from IDT):

1. **HO1-SDMH25A forward primer:**

   5’-ACCAAGGAGGTGGCCACCCAGGCA-3’

2. **HO1-SDMH25A reverse primer**

   5’-CTGCCTGGGTGGCCACCTCCTTGGT-3’

3. **HO1-SDMH132A forward primer**

   5’-GCTGCTGGTGGCCGCCGCCTACACC-3’

4. **HO1-SDMH132A reverse primer**

   5’-GGTGTAGGCGGCGGCCACCAGCAGC-3’

By performing PCR with these primers, a construct of pINCY containing the H25A and H132A point mutations within the HO-1 gene sequence was engineered using a QuikChange Lightning Site-Directed Mutagenesis Kit (Agilent Technologies) according gene to the manufacturer’s instructions. Briefly, the point-mutations were introduced by PCR amplification of plasmid pINCY with primer sets, the methylated template DNA was removed by DpnI digestion and the remaining amplified plasmid DNA containing the mutations of interest was transformed into XL-10 Gold competent *E. coli* cells. Mutated plasmid DNA was then isolated from overnight cultures of transformed bacteria using a miniprep kit (Invitrogen, Carlsbad, CA) according to the manufacturer’s instructions. The isolated DNA was used as a template for PCR using forward and reverse primers for CPP-HO1-1 as described above to create the final CPP-SDMHO1 clone.

5.1.5 Vector And Insert Preparation

Vector and insert preparation for the creation of CPP-EGFP was as follows: purified PCR product and empty pET-28B(+) were digested with NheI and HindIII restriction endonucleases (Fermentas, Burlington, ON, Canada). Digestion reactions contained 1 unit of each enzyme/µg DNA, and 1/10 volume of 10X Fast digest Buffer (Fermentas) in

sterile water and were carried out for 15 minutes at 37°C. Digested pET-28B(+) was subsequently treated with Thermosensitive FastAP alkaline phosphatase (Fermentas) for 10 minutes at 37°C and heat-inactivated at 75°C for 5 minutes. DNA was isolated from the reaction mixture using a PCR purification kit (Qiagen).

For the creation of pCPP-HO1-1, pCPP-HO1-2 and pCPP-sHO1, purified PCR product and pCPP-EGFP DNA were digested with EcoRI and HindIII as described above. pCPP-EGFP digestion resulted in the excision of the EGFP sequence leaving the CPP sequence cloned into pET28b(+) in frame. Digested pCPP-EGFP was then alkaline phosphatase treated as described above, and the pET-28B(+)-CPP sequence was used in ligation reactions for the creation of pCPP-HO1-1 and pCPP-HO1-2. For the creation of pCPP-sHO1 and pCPP-SDMHO1 the generated sHO1 and SDMHO1 PCR products and the digested fragment of pCPP-EGFP containing pET28b(+)-CPP were gel purified using a 0.8% agarose gel as described below.

Vector and insert preparation for the creation of pTAT-EGFP and pTAT-HO1 was accomplished by the following steps: purified PCR product and empty pTAT2.1 were digested with EcoRI and HindIII. Digestion products were then subjected to electrophoresis using a 0.8% agarose gel without ethidium bromide (EtBr). Following migration of the dye front to the end of the gel, the gel was soaked in ~200ml of 1XTBE containing 5ul of Ethidium bromide (Biorad) for 15 minutes. DNA in the gel was then visualized using UV light on a gel imager and bands corresponding to pTAT2.1, EGFP and HO-1 were excised with a razor blade and purified using a gel purification kit (Qiagen) according to the manufacturer's instructions.

5.1.6 Ligations And Transformations

Ligations were performed by combining 250ng of digested PCR product with 50ng of digested vector (5:1 insert to vector ratio) in a reaction volume of 20µl containing 0.5-1

unit of T4 DNA ligase (Fermentas) and 1/10 volume of 10X T4 DNA ligase buffer. Reactions were carried out for 30 minutes at room temperature, and ligation products transformed into chemically-competent *E. coli* Top10 cells (Invitrogen). Competent cells were allowed to thaw on ice and 10µl of ligation reaction was incubated with 20µl of cells for 15 minutes on ice. Cells were then subjected to heat shock for 30 seconds in a 42°C water bath and immediately chilled on ice for 2 minutes. Following this 250µl of SOC medium (NEB) was added and the cells were incubated at 37°C, shaking at 250rpm for 1hr in an Innova 43 shaker incubator (New Brunswick Scientific, Edison, NJ, USA) to allow for expression of the antibiotic resistance gene. After incubation 50µl of the transformation reaction was spread on Luria Broth (LB) Agar medium containing 50µg/mL kanamycin (Sigma, St. Louis, MO) and incubated overnight at 37°C to select for kanamycin-resistance conferred by expression of the kanamycin resistance gene on the recircularized vector. Single colonies were selected and cultured overnight at 37°C in LB broth containing 50µg/mL kanamycin using a shaker incubator. Bacterial cells were pelleted by centrifugation at 18,000 x *g* using a Microfuge 18 centrifuge (Beckman Coulter, Brea, CA, USA), and plasmid DNA isolated using a PureLink quick plasmid mini prep kit (Invitrogen) according to the manufacturer's instructions. Glycerol stocks of positive transformants were made by adding glycerol to a final concentration of 25% and freezing at -80°C.

Plasmid DNA was digested using either NheI and HindIII (CPP-EGFP, CPP-HO1-1, CPP-HO1-2) or EcoRI and HindIII (pTAT-EGFP, pTAT-HO1) as described previously and samples analyzed by agarose gel electrophoresis to identify plasmids that had incorporated the desired sequence (CPP-EGFP, CPP-HO1, EGP, HO1). The identities of candidate clones were confirmed by DNA sequence analysis (London Regional Genomics Centre, London, ON, Canada).

5.2 Protein Expression

5.2.1 Transformation Into Host Organism

Plasmids were transformed into Rosetta2(DE3)pLysS (Novagen) chemically competent *E. coli* cells as described for Top10 cells, and plated on Luria Broth (LB) Agar (EMD, Gibbstown, NJ, USA) containing 50µg/mL kanamycin and 34µg/mL chloramphenicol (Sigma). Glycerol stocks were made for each clone by selecting five colonies isolated from a single sequence confirmed transformant. These colonies were used to inoculate LB containing 50µg/mL kanamycin and 34µg/mL chloramphenicol and incubated at 37°C, with shaking at 250rpm until the OD_{590} was approximately 0.6. Cultures were frozen down with 20% glycerol (Sigma) and 0.5% Glucose (Sigma) and stored at -80°C.

5.2.2 Identification Of Protein Expressing Isolates

Liquid LB containing 50µg/mL kanamycin and 34µg/mL chloramphenicol was inoculated with a single colony from each transformant and cultured overnight at 37°C. A total of 0.2mL of overnight culture was used to inoculate 1.8mL of LB or TB (EMD) containing 50µg/mL kanamycin and 100µM IPTG (Sigma) and cultured at 37°C, with shaking at 300rpm for 16 hours. Cells were pelleted by centrifugation at 3700 x *g* and washed once with 1XPBS pH 7.4, before being resuspended in 1X phosphate buffered saline (PBS) pH7.4, containing 5mg/mL lysozyme. The suspension was incubated at 4°C, 200rpm on a Lab Rotator (Barnstead Lab Line, part of Thermo scientific, Waltham, MA, USA) rotary shaker for 30 minutes, and then sonicated with a microson ultrasonic cell disruptor (model MS-25, CM-1 microtip converter) (Heat Systems Ultrasonics, Farmingdale, NY, USA) at 90% output for 5-10 X 20-second cycles with 10-second intervals between each cycle. The whole of the sonication procedure was performed with the samples on ice. After sonication samples were incubated with 10 units of benzonase nuclease on ice for 15 minutes. Lysed samples were subjected to centrifugation at 20,000 x *g*, 4°C using a microfuge 22R centrifuge (Beckman Coulter) for 20min. Supernates were removed and total protein concentrations were determined using a spectrophotometric assay. Samples were diluted 1/100 in Bio-rad protein assay reagent

(Biorad) and OD_{595} was measured using a DU800 spectrophotometer (Beckman Coulter). Protein concentrations were calculated by plotting OD_{595} against a standard curve generated using known concentrations of bovine serum albumin (Sigma). An equal volume of 2XSDS sample buffer was added to each sample and a total of 3µg of protein from each isolate was analyzed for the presence of the expressed protein of interest using SDS-PAGE. The isolate that expressed the highest amount of protein for each clone was selected for use for all further protein expression experiments.

To determine the optimal conditions for protein expression multiple conditions were tested. Single colonies from freshly-plated glycerol stocks were used to grow overnight cultures as described previously and 1/10 volume of overnight culture was inoculated into LB or TB containing 50µg/mL kanamycin and 0µM, 0.7µM, 10µM, 100µM, or 1mM IPTG. Cultures were incubated at 37°C or 30°C, with shaking at 200rpm for 16hrs. Bacteria were then pelleted by centrifugation at 3700 x *g*, washed once with 1XPBS pH 7.4 and lysed as previously described. Protein concentration of supernatants was determined as previously described and expression was analyzed by SDS-PAGE. The conditions that provided the best expression, as indicated by the strongest protein band of expected size observed on the SDS-PAGE gel, were used for all further protein expression experiments.

To express protein for purification overnight cultures were made from single colonies of freshly plated glycerol stocks. 10mL of overnight culture was inoculated into 240mL of TB containing 2mM $MgCl_2$, pH 7.4 and 50µg/mL kanamycin, and grown at 37°C, with shaking at 250rpm in 1L Erlenmeyer flasks. Once cultures reached an OD_{600} of 0.4–0.6 (~1.5 hours), IPTG was added to final concentrations of (100µM: CPP-HO1-1, pTAT-HO1-5, sHO1, pTAT-EGFP, CPP-EGFP; 1mM: CPP-HO1-2, SDM-HO1) and cultured at 30°C, 200rpm for 16 hours.

5.3 Protein Purification

Since it has been suggested that denatured TAT-fusion proteins have better cell-penetrating efficiency [310, 311] I decided to purify the expressed proteins under both native and denaturing conditions to determine which resulted in better cell-penetrating efficiency.

5.3.1 Non-Denaturing Purification Buffers

The buffers used for purification under native conditions are as follows: 1) Lysis/binding buffer: 50mM NaH_2PO_4, 300mM NaCl, EDTA-free complete protease inhibitors (Roche, Penzberg, Germany), 10mM imidazole, 5mg/mL lysozyme, pH8.0. 2) Wash buffer: 50mM NaH_2PO_4, 300mM NaCl, EDTA-free complete protease inhibitors, 30mM imidazole, pH 8.0. 3) Elution buffer: 50mM NaH_2PO_4, 300mM NaCl, complete protease inhibitors, 500mM imidazole, pH 8.0.

5.3.2 Denaturing Purification Buffers

The buffers used for purification under denaturing conditions are as follows: 1) Lysis/binding buffer: 1XPBS, 5mg/mL lysozyme, 6M urea, 10mM imidazole, EDTA-free complete protease inhibitors, pH 7.4. 2) Wash buffer: 1XPBS, 6M urea, 30mM imidazole, EDTA-free complete protease inhibitors, pH 7.4. 3) Elution buffer: 1XPBS, 6M urea, 500mM imidazole, EDTA-free complete protease inhibitors, pH 7.4.

5.3.3 Purification

Cells from overnight *E. coli* expression cultures were pelleted by centrifugation at 3700 x *g*, 4°C for 10 minutes using an Allegra X-15R centrifuge (Beckman Coulter), washed once with 1XPBS pH 7.4, and resuspended in either native or denaturing lysis buffer (6mL/ 250mL culture). Bacteria were using a French press (American Instruments

Company, Division of Travenol Labs Inc., Silver Springs, Maryland, USA) at 14,000 psi, ~1mL/min flow rate, or sonicated 6X30 seconds, with 10 second intervals at 90% power output. Lysates were then subjected to centrifugation at 18,000 x *g*, 4°C, for 20 min, and supernatants removed and incubated with lysis buffer pre-equilibrated Ni-NTA agarose beads (Qiagen) for 1hr at 4°C on a rotary shaker. The remainder of the procedure was performed at 4°C in a cold room. Supernatants and Ni-NTA agarose beads were loaded onto a 5mL polypropylene column (Qiagen) and once the beads had settled, the sample was allowed to flow under gravity. Alternatively supernatants following centrifugation were added directly to columns containing pre-equilibrated beads, without the 1 hour incubation step. Flowthroughs were initially collected and analyzed for retained protein of interest by SDS-PAGE and Western blot analysis. Beads were washed with 10 volumes of wash buffer, and eluted using 2.5-5mL of elution buffer. Samples of eluate were saved for SDS-PAGE and Western blot analysis, and the remainder was added to a PD-10 size exclusion chromatography column (GE Healthcare, Little Chalfont, UK) pre-equilibrated with 25mL of cold histidine-tryptophan-ketoglutarate (HTK) organ preservation solution. After the sample had completely entered the packed bed of the PD-10 column it was eluted from the column in 2mL fractions by the addition of multiple volumes of 2mL HTK. Protein concentrations were determined by Bradford assay, and glycerol was added to protein-containing fractions to a final concentration of 10%; prior to freezing liquid nitrogen and storage at -80°C.

5.4 SDS PAGE And Western Blot Analysis

5.4.1 SDS-PAGE

Protein samples received an equal volume of 2X SDS PAGE sample buffer (10% v/v of 1.5M Tris pH 6.8, 6% v/v of 20% w/v SDS, 30% v/v stock glycerol, 15mL v/v stock β-mercaptoethanol, 0.0018% w/v bromophenol blue) were boiled for 10 minutes, loaded on a SDS-PAGE gel made up of a 4% stacking gel and 10% resolving gel (stacking gel (for 5mL): 3.075mL distilled H_2O, 1.25mL of 0.5M Tris-HCl pH 6.8, 0.025mL of 20% w/v SDS, 0.67mL of Acrylamide/Bis-acrylamide (30%/0.8% w/v), 0.025mL of 10% w/v

ammonium persulfate, 0.005mL TEMED. Resolving gel (for 30mL): 12.3mL of distilled H_2O, 7.5mL of 1.5M Tris-HCl pH 8.8, 0.15mL of 20% w/v SDS, 9.9mL of Acrylamide/Bis-acrylamide (30%/0.8% w/v), 0.15mL of 10% w/v ammonium persulfate, 0.02 mL TEMED) and subjected to electrophoresis at 110V using a Bio-Rad powerpac basic until the dye front reached the bottom of the gel (~1 hour). Gels were fixed and stained in the following solutions on a rotary shaker: 1) fixation solution - 50% methanol, 10% glacial acetic acid and 50% distilled water for 30 minutes 2) stain - 50% methanol, 10% glacial acetic acid, 50% water and 0.25% w/v Coomassie blue R-250 (Bio-Rad) for 3 hours 3) destain - 20% Methanol, 7.5% glacial acetic acid, 72.5% distilled water for 4-16 hours. Crumpled kimwipes were placed in the container to help soak up the excess stain. Once the gels had been destained they were dried onto Whatman paper using a gel Dryer (Bio-Rad) for 3 hours.

5.4.2 Antibodies

Primary antibodies used in this study included: mouse monoclonal anti-HO1 (ADI-OSA-110), (Stressgen, division of Enzo Life Sciences, Farmingdale, NY, USA), rabbit polyclonal anti-HO1 (ADI-SPA-895) (Stressgen); mouse monoclonal anti-histidine (OB05) (Novagen); rabbit polyclonal anti-GFP (ab290) (Abcam, Cambridge, UK). Secondary antibodies used included: horse anti-mouse horse radish peroxidase, and goat anti-rabbit horse radish peroxidase (both from Vector labs Inc., Burlington, CA, USA); goat anti-rabbit Cy2, and goat anti-mouse Cy3 (both from Jackson Immunoresearch, West Grove, Pennsylvania, USA).

5.4.3 Western Blot

Protein samples were prepared and separated on a 10% SDS PAGE gel as described previously. Once the dye front reached the bottom of the gel it was removed and incubated briefly in 1X Western transfer buffer. The gel was then loaded on a Western transfer apparatus (Bio Rad) and transferred to PVDF (Millipore, Billerica, MA) at 110V

for 1hour. PVDF membranes were then removed and blocked with 5% BSA in TBS containing 0.05% sodium azide for 30 minutes at room temperature or overnight at 4°C, with gentle agitation on a Rocker II benchtop rocker (Boekel Scientific, Feasterville Pennsylvania, USA). Blots were rinsed with 1X Tris buffered saline (TBS) and incubated with primary antibody against: HO1- mouse anti-HO1 (1:3000 dilution) ; EGFP – Rabbit polyclonal anti-EGFP (1:7500 dilution); His-tagged CPP-proteins – mouse monoclonal anti-HIS (1:1000 dilution) in blocking solution (5% BSA in TBS with 0.05% sodium azide), overnight at 4°C with gentle rocking. Blots were then washed with 1XTBS with 0.1% Tween-20 (TBST) (Sigma) for 3x10 minutes, and incubated with secondary antibody [goat anti-mouse HRP (1:10000 dilution); horse anti-rabbit hrp (1:10000 dilution)] in TBST with 5% (w/v) skim milk powder for 1hour at room temperature with gentle rocking. Finally, blots were washed with 1XTBST 3x10 minutes, incubated with ECL Plus developing reagent (Amersham, Amersham, UK) for 60-90 seconds and visualized imaged on a Kodak Image Station 4000mm Pro (Carestream Molecular Imaging, Woodbridge, CT).

5.5 Cell Culture

5.5.1 Cell Lines

Four separate cell lines were used: 1) HepG2 human hepatocellular carcinoma cells (American Type Culture Collection (ATCC); Manassas, VA, USA); 2) Human umbilical vein endothelial cells (HUVEC) generously donated by Dr. J-F. Légaré (Dalhousie University, NS); 3) J774 mouse macrophage cells generously donated by Dr. Tim Lee (Dalhousie University, NS) and 4) 293T human kidney fibroblast cells generously donated by Dr. Craig McCormick (Dalhousie University, NS).

5.5.2 Culture Medium

HepG2, J774 and HEK293T cells were cultured in Dulbecco's Modified Eagle's Medium (DMEM) (ATCC, Manassas, VA, USA and Gibco, Grand Island, NY, USA)

supplemented with 10% heat-inactivated Fetal Bovine Serum (FBS) (HyClone, Logan, UT), 100 units/mL of penicillin (Gibco) and 100 µg/mL of streptomycin (Gibco) (cDMEM). HUVECs were cultured in Endothelial Basal Medium (EBM™) containing provided supplements (Lonza Inc., Walkersville, MD, USA) including hydrocortisone, human epidermal growth factor (hEGF), FBS, vascular endothelial growth factor (VEGF), human fibroblast growth factor-basic (hFGF-B), recombinant insulin-like growth factor-1 (R3-IGF-1), ascorbic acid, heparin and gentamicin/amphotericin-B (EGM™).

5.5.3 Maintenance Of Cell Lines

All cell lines were grown in 75cm^2 tissue culture flasks (Corning Incorporated, Corning, NY, USA) at 37°C in a 5% CO_2 humidified atmosphere. Once cells reached 70-90% confluency they were passaged by the following process: The medium was aspirated, and cells were washed once with 1X PBS, treated 2.5mL of 0.05 % trypsin with EDTA•4Na (Gibco) at 37°C until cells were loosened from the base of the flask with gentle agitation. An equal volume of fresh medium was added to the trypsinized cells, and 0.5-1mL of cell suspension was added to 13mL of fresh medium in a T75 tissue culture flask. If cells were to be plated for experimentation they were counted using a haemocytometer and plated at the appropriate density.

5.5.4 In Vitro Cell Penetration Assay

Cells (HepG2, J774 and HUVEC) were plated on glass coverslips in a 12 well plate (BD Falcon, Franklin, NJ, USA) at a density of 1.0X10^5 cells/coverslip and cultured overnight in 2mL of medium/well at 37°C in a 5% CO_2 humidified atmosphere. The following day medium was removed and replaced with 2mL of serum free medium and 500µg of protein (in HTK/10%glycerol) was added to each well. Cells were then incubated at 37°C, 5% humidified CO_2 for 2-5 hours. Negative controls were cells treated with serum free medium alone, and cells treated with HTK without protein. Following treatment the

medium was aspirated, cells were washed once with warm PBS and fixed with 4% paraformaldehyde (1mL/well) for 15 min. Coverslips bearing cells treated with CPP-EGFP and pTAT-EGFP were mounted on slides using fluorescent mounting medium (Fluoromount: Sigma), and examined using a Zeiss Axiovert 200M microscope (Carl Zeiss AG, Oberkochen, Germany) with a Hamamatsu Orca R2 Camera (Hamamatsu Photonics, Hamamatsu, Shizuoka, Japan) and Axiovision Rel. 4.8.1 software (Carl Zeiss, AG). CPP-HO1-1, CPP-HO1-2, pTAT-HO1, CPP-SDM-HO1, and CPP-sHO1 treated cells underwent immunofluorescence staining prior to microscopic analysis.

5.5.5 Immunofluorescence

Immunofluorescence staining was used to examine for cellular penetration by HO-1 and EGFP. Slides bearing samples that had been fixed with 4% paraformaldehyde were treated with 1mL of ice cold 100% methanol and incubated at -20°C for 1 hour, washed 2X with 1mL PBS and treated with primary antibodies [Rabbit polyclonal Anti-HO1 (diluted 1:1000) and Mouse monoclonal anti-His (diluted 1:1000)] diluted in 1%BSA in PBS for 1 hour at room temperature. Cells were then washed 3X 5 minutes with PBS and incubated with secondary antibodies [Goat anti-rabbit Cy2 and Goat anti-mouse Cy3 (both generously donated by Dr. J.F. Legare, Dalhousie University)] diluted in 1%BSA in PBS for 1 hour. Cells were then washed once with 1mL of PBS containing a 1:5000 dilution of Hoechst stain (Invitrogen) for 5 minutes, and received 2 further 5 minute washes with PBS. Coverslips were then mounted on slides using fluorescent mounting medium and cells were analyzed by fluorescence microscopy as described previously.

5.5.6 Live Cell Fluorescence

HepG2 cells were suspended in 1.5mL microcentrifuge tubes at a density of $1X10^5$ cells/tube. Cells were then pelleted by centrifugation at 1000 x *g* for 5 minutes at 4°C and then resuspended in serum free DMEM. CPP-EGFP and pTAT-EGFP proteins were added at a concentration of 7.5µM and samples were incubated for 1hr at 37°C with

intermittent mixing. A mock treatment sample received serum free DMEM to a volume of 1mL and a negative control received no additives. Cells were then washed twice with 1X PBS, plated in a chamber slide and examined for fluorescence as described previously.

5.7 Bilirubin Production Assay

HEK293T cells were seeded onto a 60mm culture dish (BD Falcon, Franklin, NJ, USA) and grown overnight, then washed with 1XPBS and homogenized in an ice cold buffer containing (20mM Tris-HCl, 0.5% Triton X-100, 0.1% sodium cholate and EDTA-free complete protease inhibitors). Total protein content of homogenates was determined by Bradford assay. A reaction mixture containing 4.4µg cellular protein (from lysates), 250µg BSA, 25µM Hemin (Sigma), 2mM glucose-6-phosphate (G6P), 0.25U glucose-6-phosphate dehydrogenase (G6PD) (Sigma), 2mM nicotinamide adenine dinucleotide phosphate (NADPH) (Sigma), 5.5U recombinant Biliverdin Reductase (Sigma), and 300µg purified protein, was incubated at 37°C in the dark for 1 hour. After incubation bilirubin concentration was determined by measuring the difference in absorbance between 464 and 530nm and multiplying by the extinction coefficient of $40mM^{-1}cm^{-1}$. Prior to measurements the spectrophotometer was blanked using a sample containing all of the reaction components except for purified protein and cellular extract. Control samples included reaction mixture treated with protein isolated from uninduced culture and a reaction mixture without the NADPH electron donor. Reactions were performed in triplicate, mean values and standard error of the mean were calculated for each group and plotted on a graph. Statistical analysis was performed using a one way ANOVA test to compare the variance between the means of the 3 sample groups, using a p-value of 0.01.

Chapter 6: Results

6.1 Cloning Scheme For pCPP-EGFP, pTAT-EGFP, pCPP-HO1-1, pCPP-HO1-2, pCPP-SDMHO1, pCPP-sHO1 And pTAT-HO1

To produce a recombinant cell-penetrating HO-1 protein required the generation of a plasmid containing the CPP DNA sequence in frame with the HO-1 gene sequence. For ease of testing the cell-penetrating capability of the CPP peptide, I also decided to produce a cell-penetrating enhanced green fluorescent protein that could be easily analysed using fluorescence microscopy. Such proteins had already been created, but were unavailable upon request; therefore the decision was made to produce these plasmids myself. Plasmids containing seven different clones (pCPP-HO1-1, pCPP-HO1-2, pCPP-SDMHO1, pCPP-EGFP, pCPP-sHO1, pTAT-HO1, and pTAT-EGFP) were created. The first step was to create a CPP-EGFP plasmid; primers (CPP-EGFP +, EGFP -) were sequences described in Ma et al., 2009 [160]. CPP-EGFP + consisted of the PTD-4 sequence described by Ho et al. [312] with a glycine linker and an incorporated EcoRI cut site followed by the N-terminal sequence for EGFP. This design allowed for PCR amplification of a CPP-EGFP sequence from pEGFP-C1 template DNA for cloning into the expression vector pET-28b(+). The EcoRI cut site allowed for excision of the EGFP sequence so that another sequence of choice (such as HO1, SDMHO1, or sHO1) could be cloned downstream from the CPP sequence (Figure 4). The glycine residue was inserted to increase the rotational flexibility of the CPP tag. The various CPP-HO1 clones were all created by amplification of the HO-1 sequence from the pINCY template using primers described in Ma et al. [313] (for pCPP-HO1-1 and pCPP-SDMHO1), or primers designed by me (for pCPP-HO1-2 and pCPP-sHO1). The product of pCPP-HO1-1 (created using primers HO1 + and HO1-1 -) correlates to the PTD-HO1 protein mentioned in Ma et al., containing a PTD-4:HO1 sequence flanked by 6XHIS-tag sequences at both the N- and C-termini. The pCPP-SDMHO1 clone was designed (using primers HO1-SDMH25A +, HO1-SDMH25A -, HO1-SDMH132A +, HO1-SDMH132A) to express a non-functional HO1 protein for use as a negative control with regards to the beneficial effects of HO1 activity. Concern over a potential inhibitory effect of the C-terminal 6XHIS tag on HO1 membrane binding led to the creation of pCPP-HO1-2

(using primers HO1 + and HO1-2 -), whose expression product lacks this tag. To try and overcome intial difficulties with protein expression and purification I also obtained the pTAT 2.1 plasmid from Dr. Steven Dowdy (University of California, San Diego), which contains a 6X histidine tag followed by a TAT sequence in frame with a downstream multiple cloning site. Gene sequences were amplified using primer sets TAT-HO1 + and HO1-1 – (for pTAT-HO1); and EGFP + and EGFP – (for pTAT-EGFP) and cloned into pTAT2.1 to generate the pTAT-HO1 and pTAT-EGFP. There were initial difficulties with purification of full length CPP-HO1 proteins, leading to poor yields of purified CPP-HO1 proteins. In an attempt simplify the purification and increase yields, I created a soluble CPP-HO1 (CPP-sHO1) construct (using the primers HO1 + and sHO1 -) lacking the final 23 amino acids at the C-terminus [313].

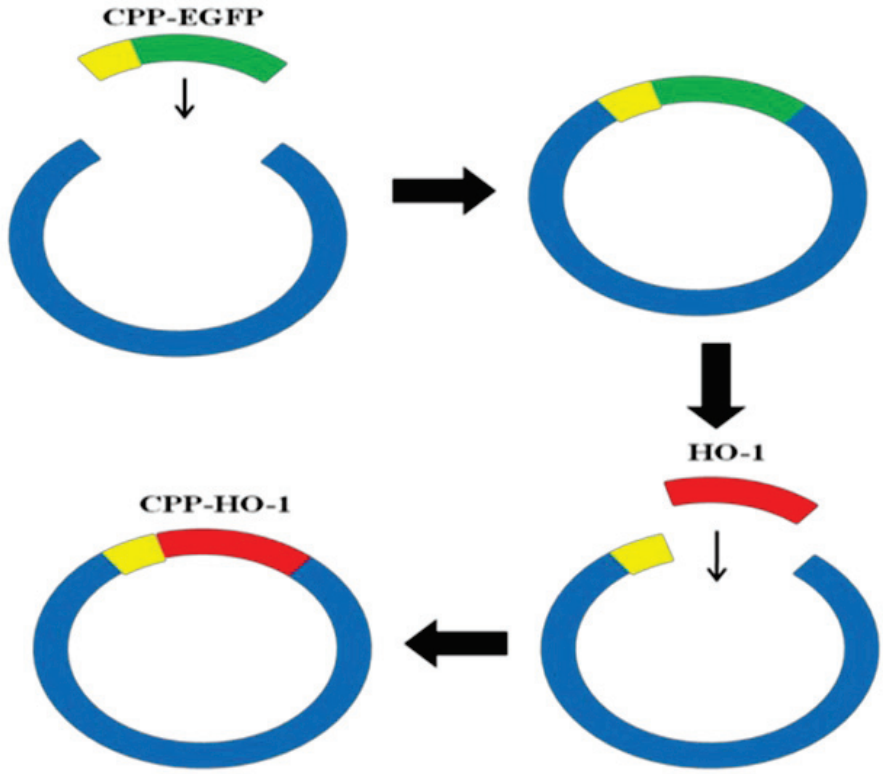

Figure 4. Schematic for cloning of CPP-EGFP and subsequent cloning of CPP-HO1-1, CPP-HO1-2, CPP-SDMHO1 and CPP-sHO1. The CPP-EGFP PCR product is cloned into pET-28b(+). The EGFP sequence is then excised and the HO-1 PCR product cloned into its place in the pET-28b(+)-CPP vector.

6.2 SDMHO-1, CPP-EGFP, TAT-HO1, TAT-EGFP

PCR using the appropriate template (either pEGFP-C1 of pINCY) and primer sets yielded DNA fragments of expected sizes for HO1-1, HO1-2, sHO1, EGFP (for pCPP-EGFP), HO1 (for pTAT-HO1) and EGFP (for pTAT-EGFP) (Fig. 5). These sequences were then cloned into the appropriate expression vectors (pET-28b(+) or pTAT2.1). NheI/HindIII restriction digests of the resultant clones yielded fragments of the expected sizes for CPP-HO1-1, CPP-HO1-2, CPP-sHO1, CPP-EGFP (Fig. 6A, C) indicating incorporation of the correct sequences into the expression vector. EcoRI/HindIII restriction digestion resulted in the excision of fragments consistent in size with the gene inserts for CPP-HO1-1, CPP-HO1-2, pTAT-HO1, CPP-EGFP, pTAT-EGFP (Fig.6B) and CPP-sHO1 (Fig. 6C). Digestion of the empty pET28b(+) vector with NheI/HindIII and EcoRI/HindIII yielded fragments of 5311bp and 5349bp, respectively, as well as a fragment of between 2 and 3kb that likely represents undigested supercoiled DNA. The identities for all clones were confirmed by DNA sequence analysis.

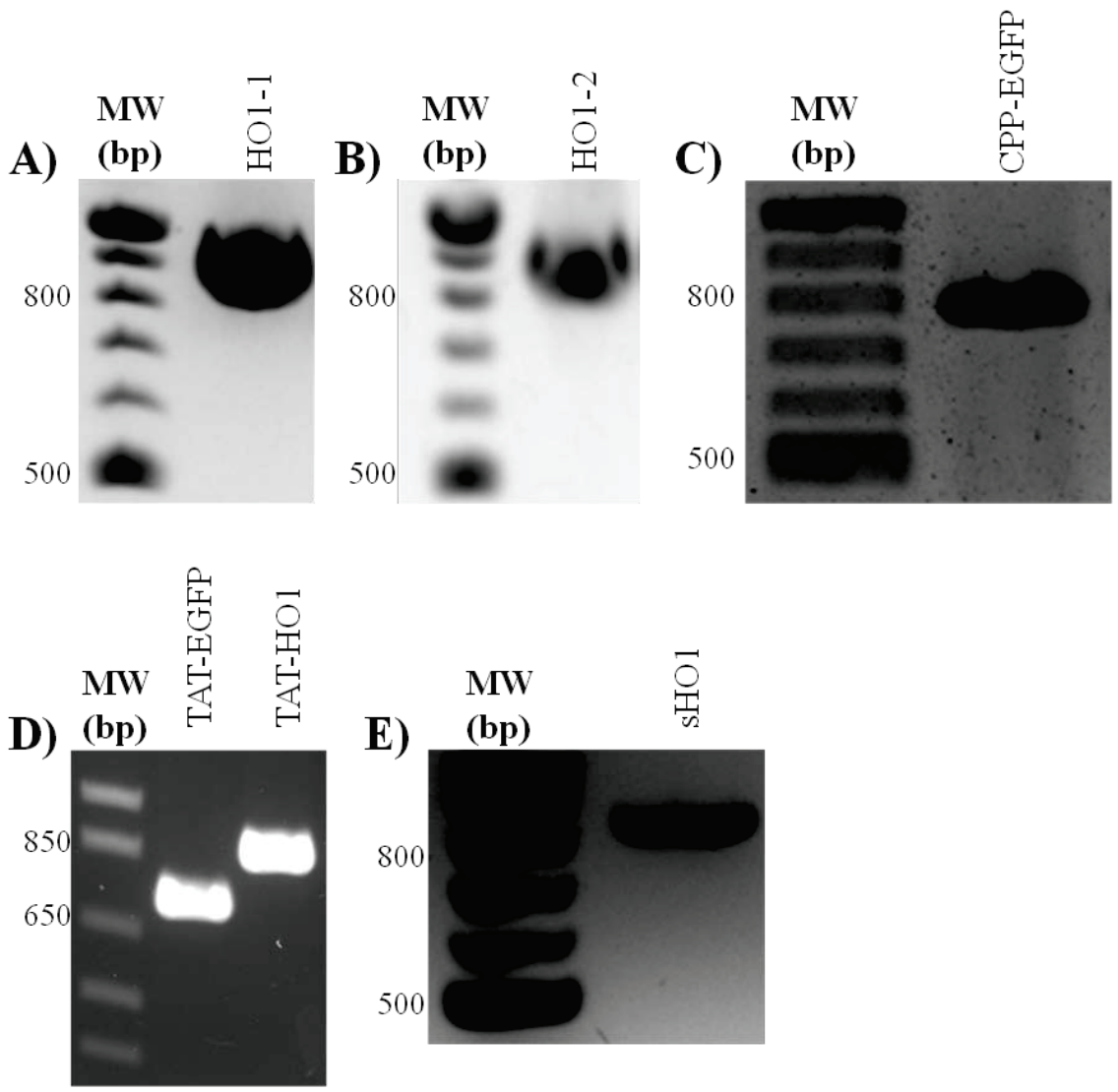

Figure 5. PCR products were generated for cloning. PCR was performed using the templates pEGFP-C1 and pINCY with appropriately selected primers. Final reaction products were analyzed by agarose gel electrophoresis. Products and sizes are : **A)** HO1-1, 880bp **B)** HO1-2 product, 882bp **C)** CPP-EGFP, 786bp **D)** Lane 1: TAT-EGFP, 738bp Lane 2: TAT-HO1, 881bp **E)** sHO1, 816bp

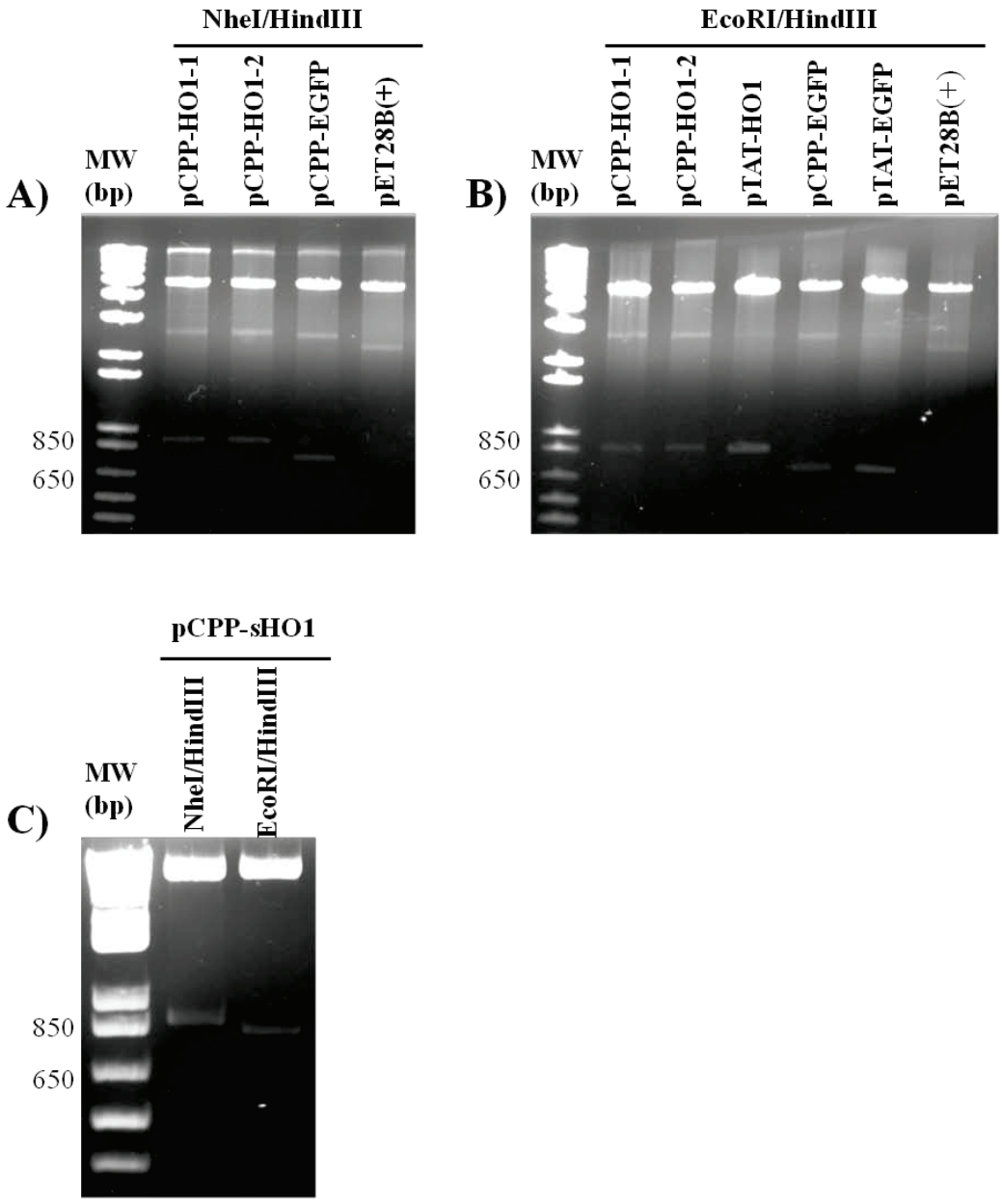

Figure 6. Restriction digestion confirmation of HO1 and EGFP clones. Clones were subjected to restriction digestion using either NheI/HindIII to excise the CPP-gene sequence or EcoRI/HindIII sequence alone. The resulted products were resolved using agarose gel electrophoresis. DNA bands of the expected size for the gene sequence of interest (HO1 or EGFP) indicated successful clone generation. Gene sizes in bp are listed in brackets. **A)** NheI/HindIII digests - Lane 1: pCPP-HO1-1(915bp); Lane 2: pCPP-HO1-2 (917bp); Lane 3: pCPP-EGFP (774bp); Lane 4: empty pET28b(+) vector (no insert). **B)** EcoRI/HindIII digests - Lane 1: pCPP-HO1-1 (870bp); Lane 2: pCPP-HO1-2 (872bp); Lane 3: pTAT-HO1 (871bp); Lane 4: pCPP-EGFP (729bp); Lane 5: pTAT-EGFP (727 bp); Lane 6: empty pET28B(+), (no insert). **C)** pCPP-sHO1 digests. Lane 1: NheI/HindIII (849bp); Lane 2: EcoRI/HindIII (804bp).

6.3 Isolate Screening

Following confirmation of clone sequences, the next step was to transform these clones into the *E. coli* strain Rosetta2(DE3)pLysS for protein expression. Because of the possibility of mutations or DNA damage during transformation, five transformants for each clone were screened for protein expression. Individual transformants, containing the sequences of interest confirmed by DNA sequence analysis, were induced to express the protein of interest with IPTG. Following induction, cultures were lysed and supernatants analyzed for protein production by SDS-PAGE analysis. For all CPP-HO1 transformants, IPTG treatment resulted in the production of protein bands consistent with the expected protein sizes (Fig 7): CPP-HO1-1 ~37 kDa (expected size 37.3 kDa); CPP-HO1-2 ~35 kDa and 32 kDa (expected size 35.8 kDa); TAT-HO1 ~37 kDa (expected size of 37.0 kDa); CPP-SDMHO1 ~37 kDa (expected size 37.3kDa); CPP-sHO1 ~ 32-33 kDa (expected size 33.3 kDa); CPP-EGFP ~32-33 kDa (expected size 32.1 kDa); TAT-EGFP ~ 32-33kDa (expected size 31.8 kDa). The observed bands were of greater intensity than bands of ~37 or 32 kDa observed in the control samples from cells transformed with empty pET28b(+) or pTAT2.1 vectors, respectively. In the cases of CPP-HO1-1, CPP-HO1-2, TAT-HO1 and CPP-sHO1 the presence of these induced proteins correlated with a green colouration of the bacterial pellet, indicative of biliverdin produced from the degredation of Heme by HO-1. For CPP-EGFP and TAT-EGFP the presence of the induced bands correlated with a yellow colouration of the bacterial pellet, which is presumed to be a result of EGFP production, as the pellet from uninduced cultures was beige. With the exception of clone 1 for CPP-HO1-1, TAT-HO1, CPP-EGFP and TAT-EGFP there was no significant difference in the degree of protein expression observed among the five clones tested. Clones 3, 4, 5, 4, 4, 3 and 2 were selected for future expression of CPP-HO1-1, CPP-HO1-2, TAT-HO1, CPP-SDMHO1, CPP-sHO1, CPP-EGFP and TAT-EGFP respectively.

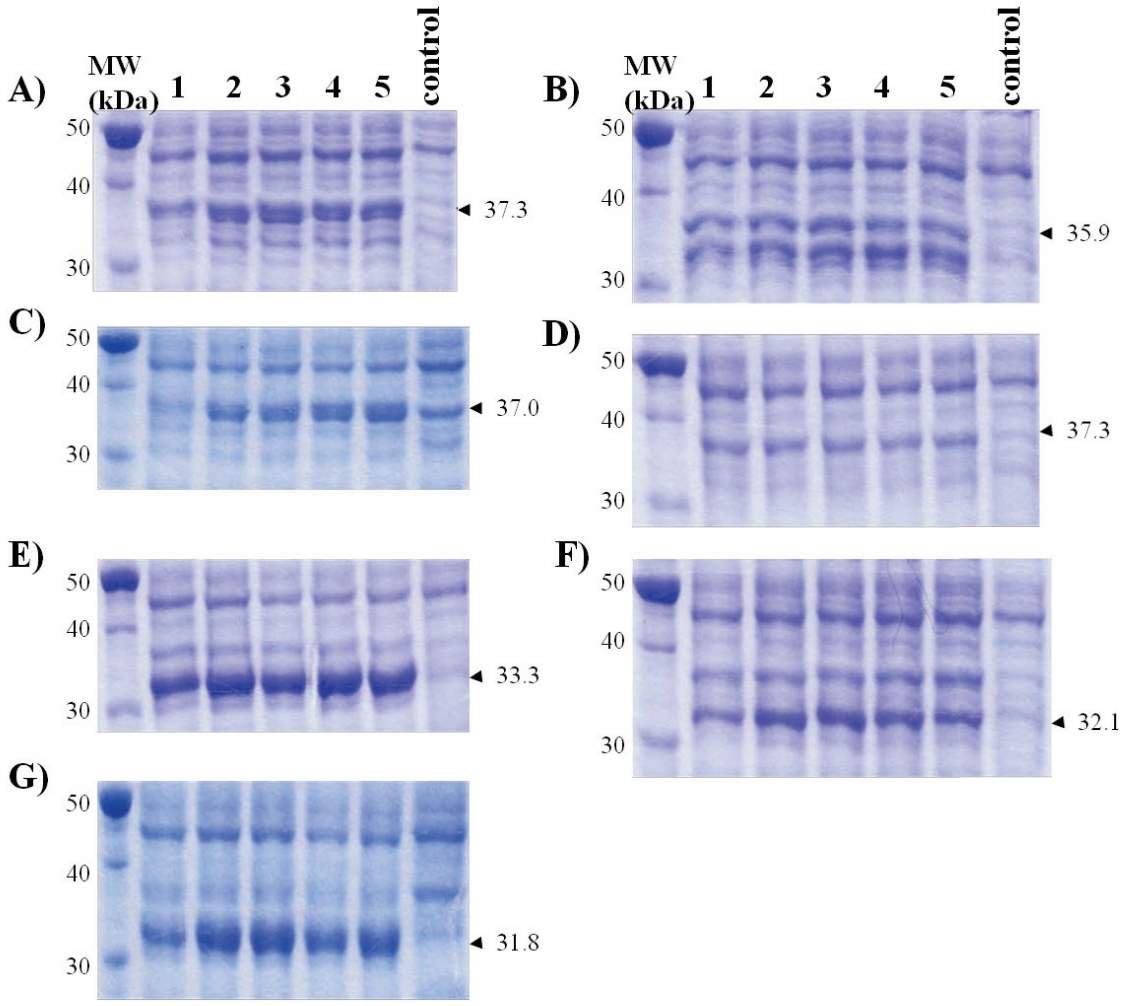

Figure 7. Protein expression *E. coli* bearing plasmids of interest. *E. coli.* Rosetta2(DE3)pLysS cells were transformed with the plasmids indicated below and five individual transformants for each clone were induced to express the protein of interest using 100µM IPTG, and cultured in LB at 37°C, 300rpm for 16 hours. Cells were then lysed and 10µg protein from each lysate was analyzed by electrophoresis through a 10% SDS-PAGE gel. For all gels (A-G) lanes 1-5 are individual transformants. *E. coli* transformed with empty pET28B(+) (A-B, D-F) or pTAT2.1 (C, G) was used as a negative control. **A)** CPP-HO1-1, protein size 37.3kDa. **B)** CPP-HO1-2, protein size 35.9kDa. **C)** TAT-HO1, protein size 37.0kDa. **D)** CPP-SDMHO1, protein size 37.3kDa. **E)** CPP-sHO1, protein size 33.3kDa. **F)** CPP-EGFP, protein size 32.1kDa. **G)** TAT-EGFP, protein size 31.8kDa. Arrows indicate the size of the protein of interest.

6.4 Protein Expression

Since the goal of this project was the production of proteins for potential therapeutic use, it was important to determine the optimal expression conditions in order to maximize protein yield. Individual *E. coli* Rosetta2(DE3)pLysS transformants of each clone were selected and grown in either LB or TB medium and expression of cloned genes was induced, using a range of IPTG concentrations at 37°C or 30°C for 16hr. Cells were lysed and proteins extracted from supernatants were analyzed by SDS-PAGE.

Following induction of protein expression with IPTG a change in colour of the bacterial culture from beige to green was observed for CPP-HO1-1 (Fig. 8A, Fig. 9), CPP-HO1-2, TAT-HO1, and CPP-sHO1 but not CPP-SDMHO1 (Fig. 9). This is believed to be due to the production of biliverdin from HO-1 metabolism of heme [160, 308], with a subsequent intracellular accumulation of biliverdin, resulting in a green change in colour of the bacterial cells, since upon centrifugation (Fig. 8B). Because LB is lighter in color than TB, the color change observed in LB cultures prior to pelleting the bacteria (Fig. 8A) is more dramatic than that seen with TB cultures (figure 9). Expression of CPP-EGFP and TAT-EGFP also resulted in a colour change of the culture and bacterial pellet from beige to yellow, which is presumed to be secondary to the production of EGFP (Fig. 8C, Fig. 9). These findings that bacterial colour change proved to be a reliable indicator of successful protein expression, was very useful, in that it allowed me to assess the success of protein expression visually, rather than subjecting each induction experiment to analysis by SDS-PAGE or Western blot, prior to undertaking a costly purification experiment.

6.4.1 Optimization Of Expression Conditions

The complexities protein folding and post-translational modifications, often result in significant variability in the efficiency of the expression of human proteins in *E. coli*. The optimal set of expression conditions was determined for each protein by culturing

transformed bacteria in either TB or LB and treating with multiple IPTG concentrations (0.7, 10, 100, 1000μM). The highest level of CPP-HO1-1 expression was found to occur when plasmid-bearing cells were grown in TB medium at 30°C (Fig. 10). When grown in LB at 37°C the presence of a band consistent in size with that expected for CPP-HO1-1 (37.3kDa) was observed in response to induction with 0.7, 10 and 1000μM IPTG (Fig. 10A); however, when grown at 30°C, expression was greatest in response to IPTG concentrations of 0.7, 100 and 1000μM (Fig. 10B). When grown in TB at 37°C only 1000μM IPTG resulted in any appreciable expression, as it was the only condition that resulted in the production of a protein band of expected size of greater intensity than seen in the uninduced control (Fig. 10C). Growth in TB at 30°C resulted in significant protein expression in response to 10, 100 and 1000μM IPTG (Fig. 10D); with 10μM giving the greatest protein expression of all conditions tested.

CPP-HO1-2 protein expression was greatest when plasmid-bearing cells were grown in TB and protein expression was induced at 30°C (Fig. 11). When grown in LB medium at 37°C the greatest amount of protein was seen when gene expression was induced with 1000μM IPTG (Fig. 11A), whereas at 30°C, similar protein levels were observed in response to IPTG concentrations of 0.7, 10 and 1000μM IPTG (Fig. 11B). When grown in TB at 37°C, expression increased with increasing concentrations of IPTG (Fig. 11C); however, even at 1000μM IPTG only a weak protein band was observed. Cultures grown in TB at 30°C demonstrated a doublet band in response to IPTG induction; the larger band is consistent with the expected size of CPP-HO1-2 (35.8kDa). Expression of a protein of this size was observed to the greatest degree at IPTG concentrations of 100 and 1000μM (Fig. 11D).

TAT-HO1 expression was greatest when plasmid-bearing cells were grown in TB and induced at 30°C (Fig. 12). When grown in LB medium at 37°C, only 10μM IPTG resulted in the production of a protein band of the predicted size of TAT-HO1 (37kDa) that was greater in intensity than that seen in the uninduced control (Fig. 12A). When

grown in LB at 30°C, a similar protein band was seen only in response to 100μM IPTG (Fig. 12B). When cultures were grown in TB medium at 37°C TAT-HO1 expression was observed to the greatest degree in response to 100μM IPTG (Fig. 12C). Cultures grown and induced at 30°C demonstrated significant TAT-HO1 expression with IPTG concentrations of 10, 100 and 1000μM (Fig. 12D).

CPP-SDMHO1 expression was greatest when plasmid-bearing cells were grown in TB and induced at 30°C (Fig 13). When grown in LB medium at 37°C, IPTG concentrations of 10, 100 and 1000μM resulted in the production of a protein band of the predicted size for CPP-SDMHO1 (37.3kDa) (Fig. 13A). When grown in LB at 30°C no appreciable expression was observed (Fig. 30B). Similarly, no expression was observed for cultures grown in TB and induced at 37°C Fig (Fig. 13C). However, when cultures were grown in TB at 30°C strong induction of CPP-SDMHO1 expression was observed in response to 10, 100 and 1000μM IPTG (Fig. 13D).

CPP-sHO1 protein expression was greatest when plasmid-bearing cells were grown in TB and protein expression was induced at 30°C (Fig. 14). When grown in LB medium at 37°C sHO1 expression, indicated by the presence of a 33.3kDa protein band, was greatest when induced with 1000μM IPTG (Fig. 14A). When grown in LB at 30°C all IPTG concentrations induced protein expression to a similar degree (Fig. 14B). When grown in TB medium at 37°C the greatest expression was observed with 100 and 1000μM IPTG (Fig. 14C). When grown in TB at 30°C strong expression was observed for IPTG concentrations of 10, 100 and 1000μM, with 100μM resulting in the greatest expression for all conditions tested (Fig. 14D).

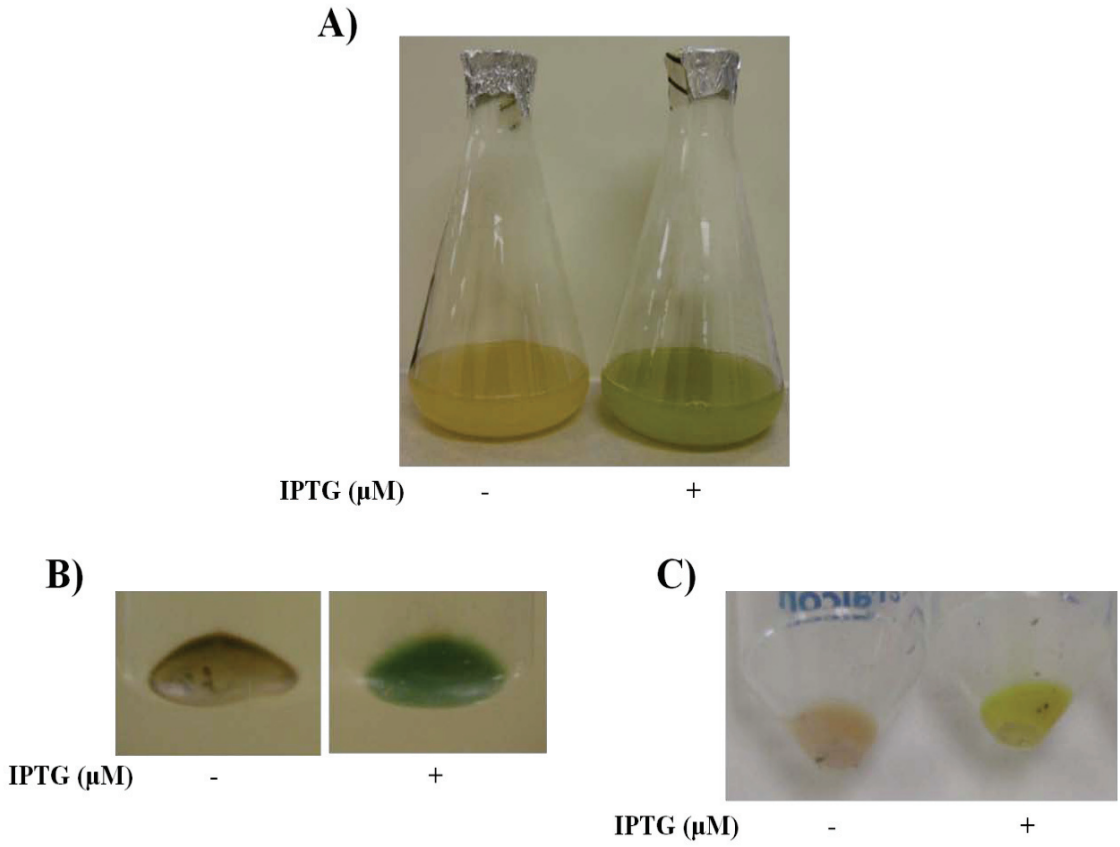

Figure 8. Protein expression is evidenced by colour change of the bacterial culture. Rosetta2(DE3)pLysS transformed with plasmids containing the sequence of interest were induced to express protein by the addition of 10µM IPTG to bacterial culture grown in LB medium and incubation at 37°C, 250rpm overnight. **A)** CPP-HO1-1 expression resulted in a change of the culture and **B)** bacterial pellet from beige to green, while **C)** CPP-EGFP expression resulted in a change of the bacterial pellet to yellow.

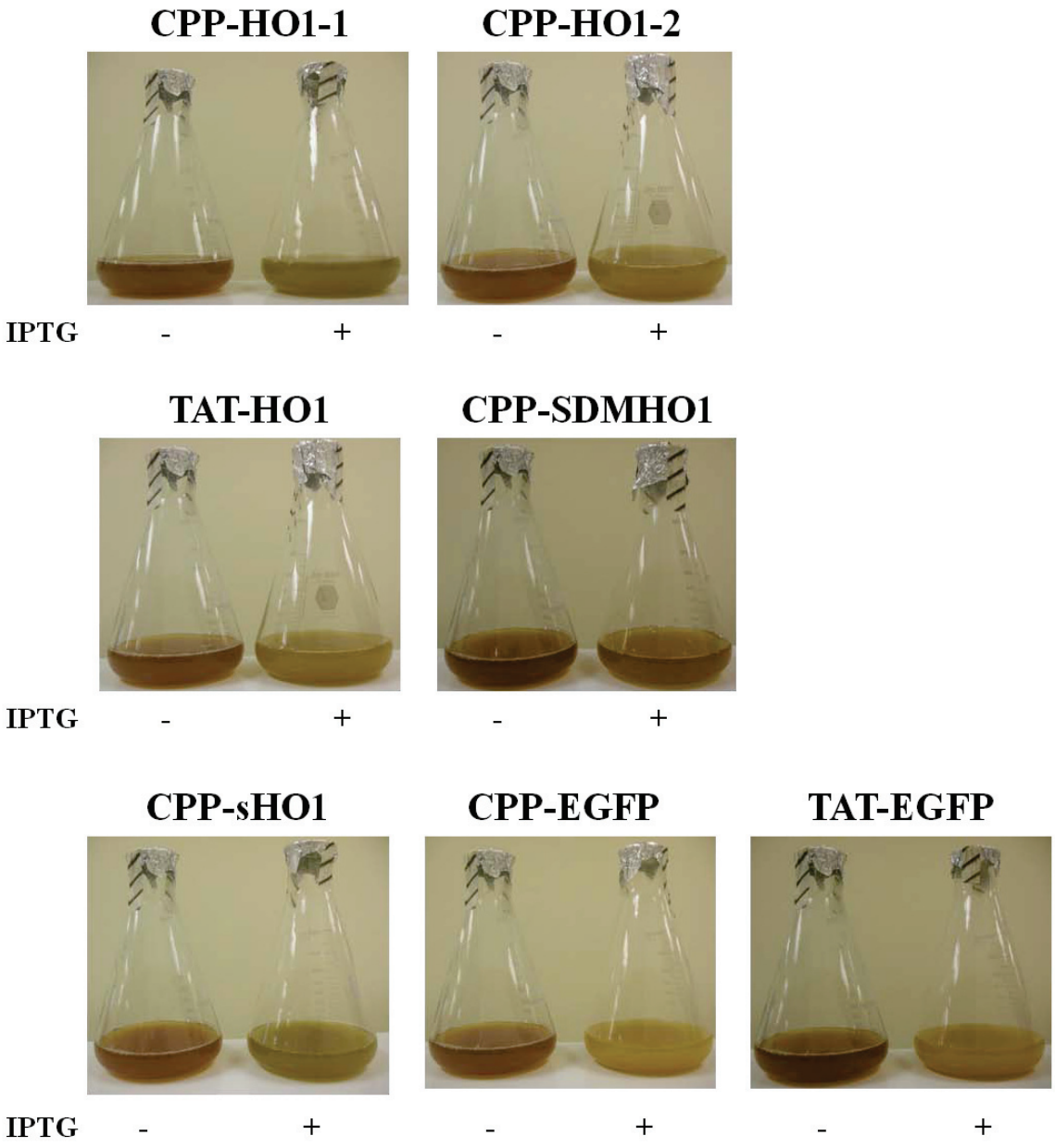

Figure 9. Bacterial culture colour change is indicative of HO1 activity and EGFP expression. Expression was induced by IPTG treatment of *E. coli* Rosetta2(DE3)pLysS containing the indicated plasmids, followed by overnight culture at 30°C, 250rpm. Protein expression resulted in a greenish colour change because of accumulated biliverdin in the case of CPP-HO1-1, CPP-HO1-2, TAT-HO1 and CPP-sHO1 but not the inactive mutant CPP-SDMHO1. Expression of CPP-EGFP and TAT-EGFP resulted in a colour change to yellow.

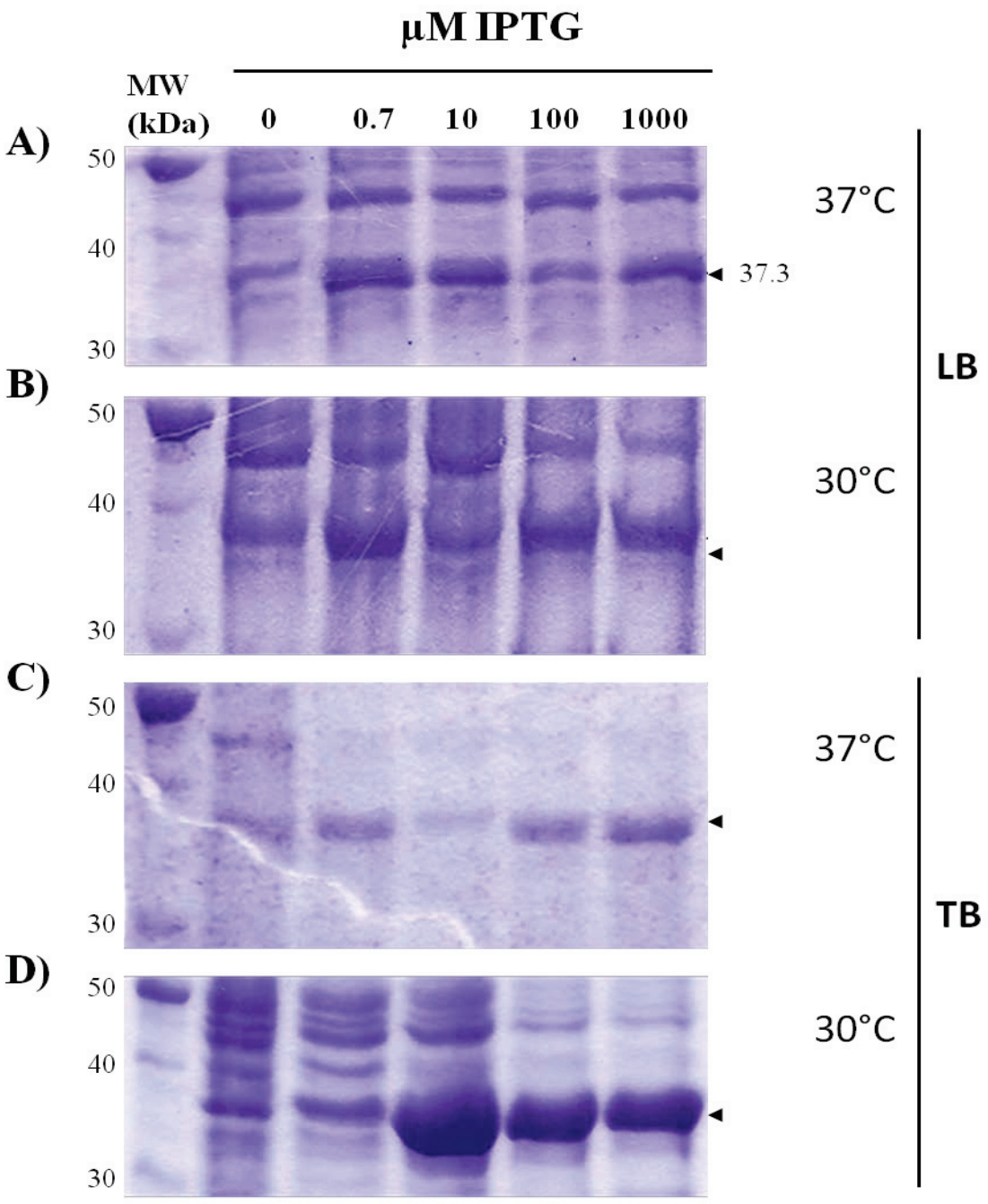

Figure 10. Optimization of CPP-HO1-1 protein expression. Single colonies from freshly plated cultures were inoculated into either LB or TB and grown to an OD_{600} of 0.6, induced with indicated concentrations of IPTG, and incubated at either 37°C or 30°C for 16hr. Total cellular protein was extracted by bacterial lysis using a french press. 20µg of protein from each lysate was resolved by 10% SDS-PAGE and stained with Coomassie blue. CPP-HO1-1 expression is indicated by a protein band of 37.3kDa. LB induction at A) 37°C or B) 30°C. TB induction at C) 37°C or D) 30°C. Arrowhead marks CPP-HO1-1 for all panels.

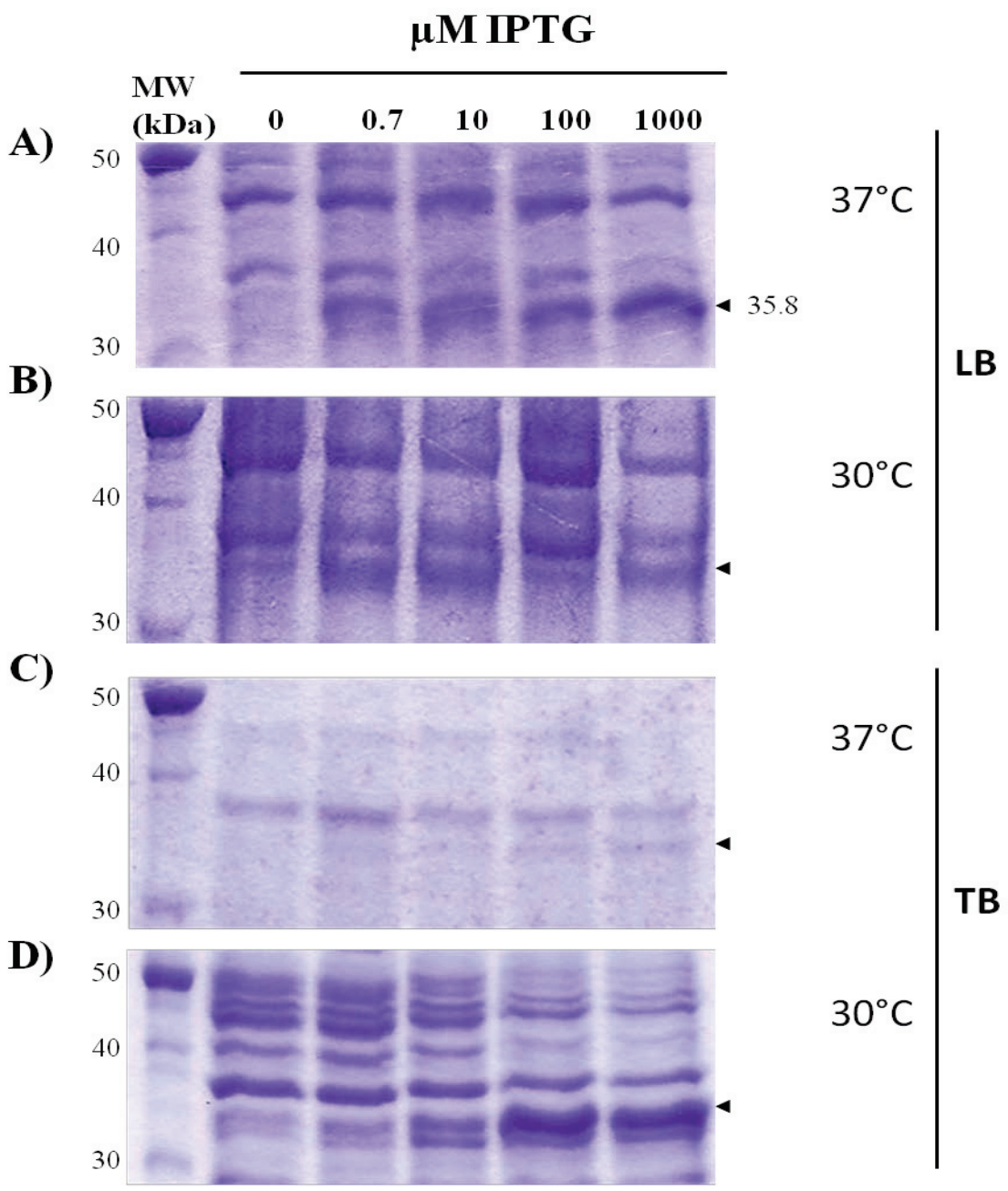

Figure 11. Optimization of CPP-HO1-2 protein expression. Single colonies from freshly plated cultures were inoculated into either LB or TB and grown to an OD_{600} of 0.6, induced with indicated concentrations of IPTG, and incubated at either 37°C or 30°C for 16hr. Total cellular protein was extracted by bacterial lysis using a french press. 20µg of protein from each lysate was resolved by 10% SDS-PAGE and stained with Coomassie blue. CPP-HO1-2 expression is indicated by a protein band of 35.8kDa. LB induction at A) 37°C or B) 30°C. TB induction at C) 37°C or D) 30°C. Arrowhead marks CPP-HO1-2 for all panels.

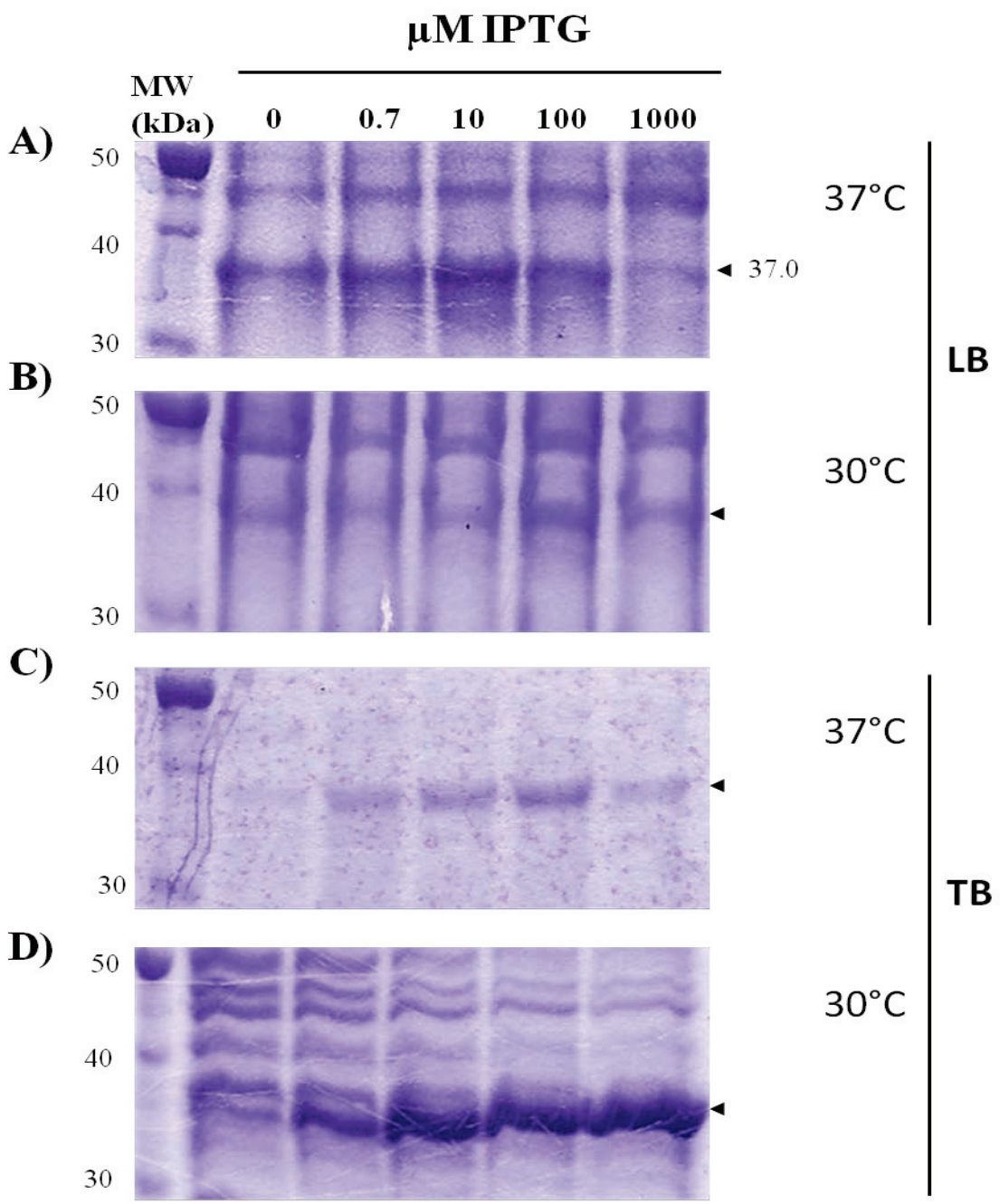

Figure 12. Optimization of TAT-HO1 protein expression. Single colonies from freshly plated cultures were inoculated into either LB or TB and grown to an OD_{600} of 0.6, induced with indicated concentrations of IPTG, and incubated at either 37°C or 30°C for 16hr. Total cellular protein was extracted by bacterial lysis using a french press. 20µg of protein from each lysate was resolved by 10% SDS-PAGE and stained with Coomassie blue. TAT-HO1 expression is indicated by a protein band of 37.0kDa. LB induction at A) 37°C or B) 30°C. TB induction at C) 37°C or D) 30°C. Arrowhead marks TAT-HO1 for all panels.

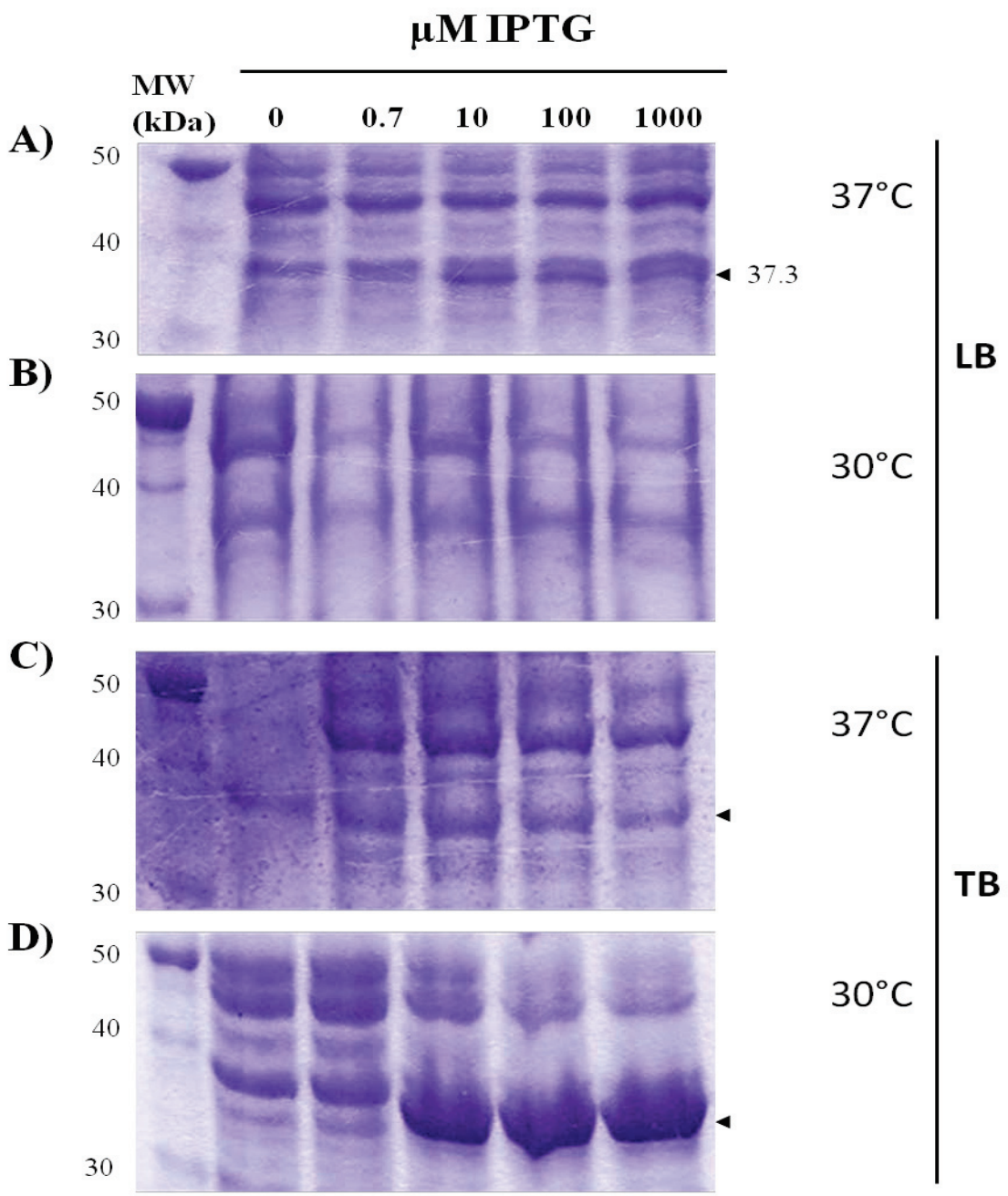

Figure 13. Optimization of CPP-SDMHO1 protein expression. Single colonies from freshly plated cultures were inoculated into either LB or TB and grown to an OD_{600} of 0.6, induced with indicated concentrations of IPTG, and incubated at either 37°C or 30°C for 16hr. Total cellular protein was extracted by bacterial lysis using a french press. 20µg of protein from each lysate was resolved by 10% SDS-PAGE and stained with Coomassie blue. CPP-SDMHO1 expression is indicated by a protein band of 37.3kDa. LB induction at A) 37°C or B) 30°C. TB induction at C) 37°C or D) 30°C. Arrowhead marks CPP-SDMHO1 for all panels.

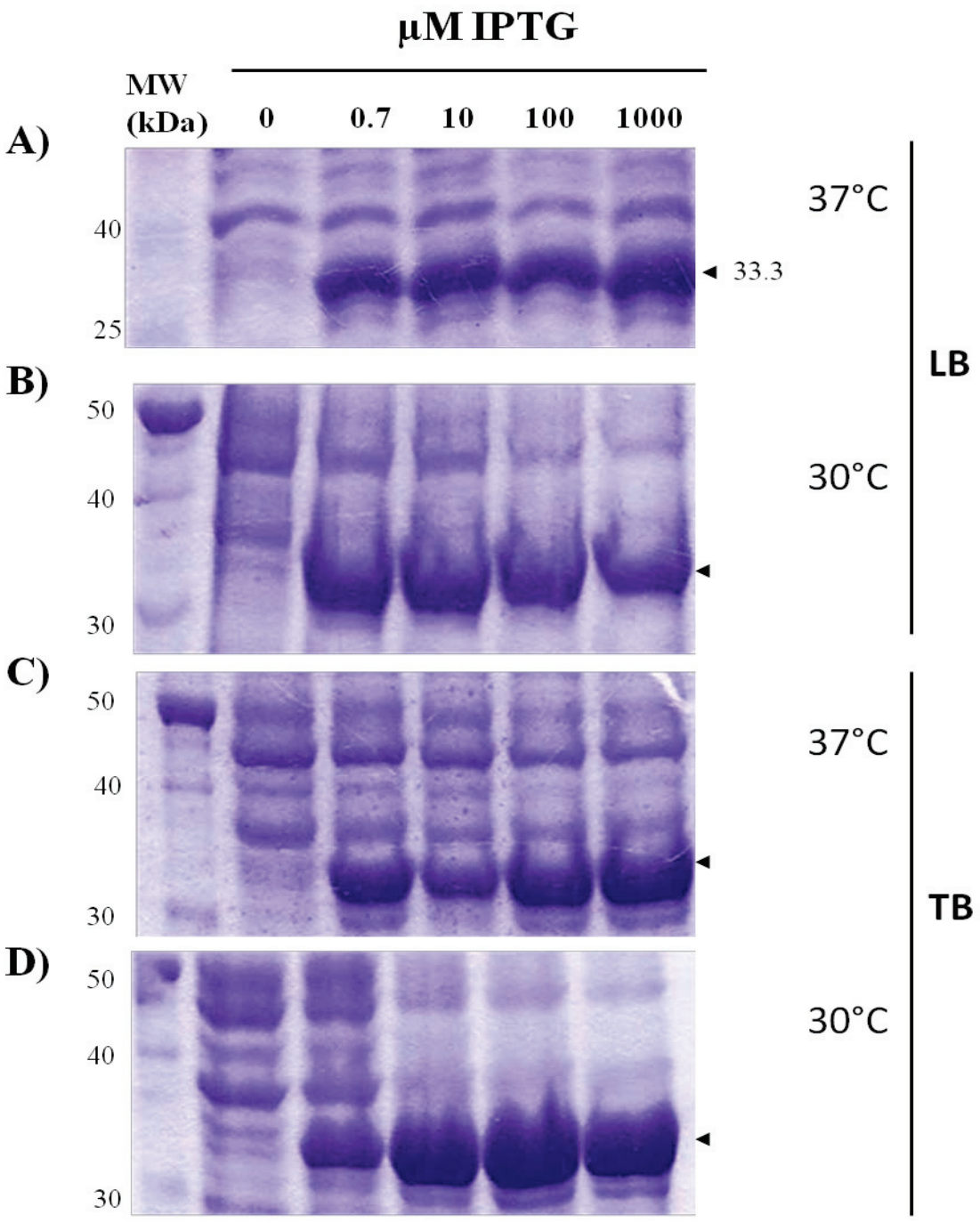

Figure 14. Optimization of CPP-sHO1 protein expression. Single colonies from freshly plated cultures were inoculated into either LB or TB and grown to an OD_{600} of 0.6, induced with indicated concentrations of IPTG, and incubated at either 37°C or 30°C for 16hr. Total cellular protein was extracted by bacterial lysis using a french press. 20µg of protein from each lysate was resolved by 10% SDS-PAGE and stained with Coomassie blue. CPP-sHO1 expression is indicated by a protein band of 33.3kDa. LB induction at A) 37°C or B) 30°C. TB induction at C) 37°C or D) 30°C. Arrowhead marks CPP-sHO1 for all panels.

CPP-EGFP protein expression resulted in the production of a 31.7 kDa band. Expression was greatest when plasmid-bearing cells were grown in LB medium and induced at 37°C with 10μM IPTG or 30°C with 0.7 or 100μM IPTG (Fig. 15). When cultures were grown in LB and induced at 37°C the greatest expression was observed with 10 and 100μM IPTG (Fig. 15A). When grown in LB at 30°C similar expression was observed with 0.7 and 100μM IPTG (Fig. 15B). When grown in TB medium and induced at 37°C similar expression was observed with 0.7, 10 and 100μM IPTG; however, expression in this growth media at these temperatures was less than for the other conditions (Fig. 15C). Cultures grown in TB and induced at 30°C showed similar expression with 10, 100 and 1000μM IPTG (Fig. 15D).

TAT-EGFP expression resulted in the production of a 32.1kDa band. Expression was greatest when plasmid-bearing cells were grown in LB medium and induced at 37°C (fig 16). When grown in LB at 37°C similar expression levels were observed with 0.7, 10, or 100μM IPTG (Fig. 16A). When grown in LB at 30°C significant expression was observed for all IPTG concentrations (Fig. 16B). When grown in TB and induced at 37°C the greatest expression was observed for IPTG concentrations of 0.7, 100 and 1000μM (Fig. 16C). When grown at 30°C greatest expression was observed in response to 10 and 100μM IPTG (Fig. 16D).

These experiments show that growth and induction in TB medium at 30°C provided the optimal conditions for all of the CPP- and TAT-HO1 proteins. CPP- and TAT-EGFP appeared to be optimally expressed by plasmid-containing cells grown in LB medium at 30°C. Therefore for future experiments it is recommended that growth in TB at 30°C be used for HO1 protein expression and EGFP protein expression be induced in LB medium at 30°C.

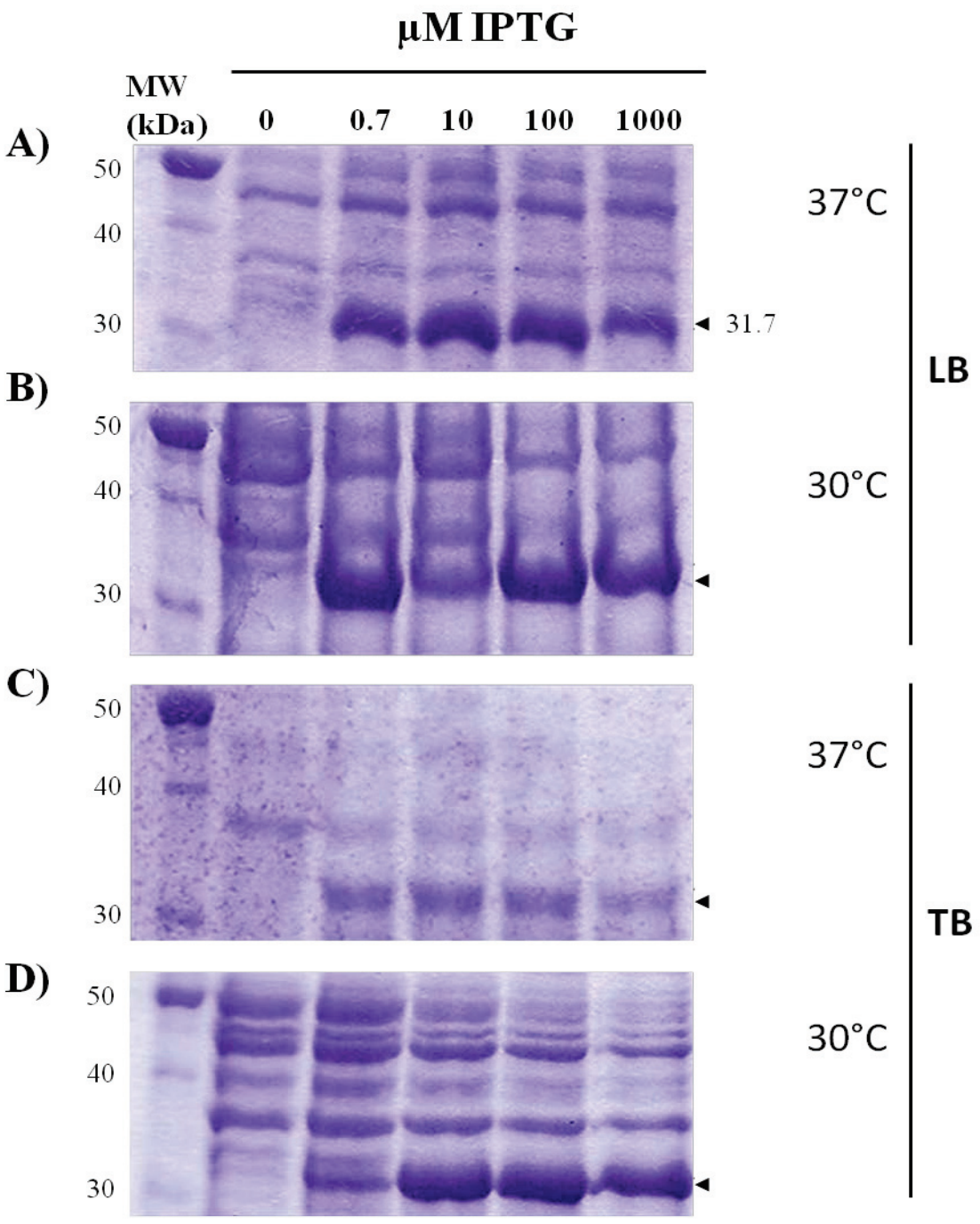

Figure 15. Optimization of CPP-EGFP protein expression. Single colonies from freshly plated cultures were inoculated into either LB or TB and grown to an OD_{600} of 0.6, induced with indicated concentrations of IPTG, and incubated at either 37°C or 30°C for 16hr. Total cellular protein was extracted by bacterial lysis using a french press. 20µg of protein from each lysate was resolved by 10% SDS-PAGE and stained with Coomassie blue. CPP-EGFP expression is indicated by a protein band of 31.7kDa. LB induction at A) 37°C or B) 30°C. TB induction at C) 37°C or D) 30°C. Arrowhead marks CPP-EGFP for all panels.

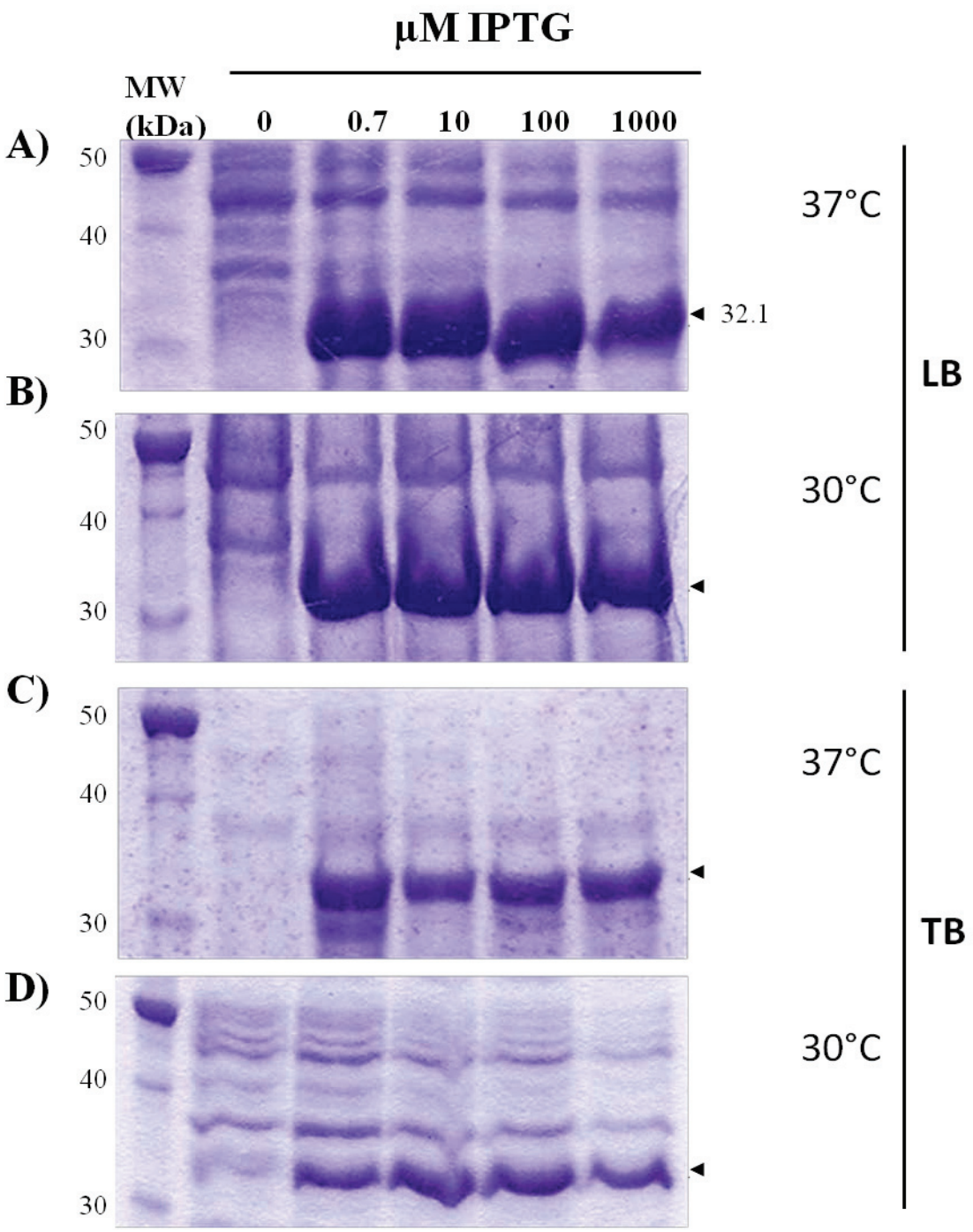

Figure 16. Optimization of TAT-EGFP protein expression. Single colonies from freshly plated cultures were inoculated into either LB or TB and grown to an OD_{600} of 0.6, induced with indicated concentrations of IPTG, and incubated at either 37°C or 30°C for 16hr. Total cellular protein was extracted by bacterial lysis using a french press. 20µg of protein from each lysate was resolved by 10% SDS-PAGE and stained with Coomassie blue. TAT-EGFP expression is indicated by a protein band of 32.1kDa. LB induction at A) 37°C or B) 30°C. TB induction at C) 37°C or D) 30°C. Arrowhead marks TAT-EGFP for all panels.

6.5 Protein Purification

Expressed proteins were extracted by bacterial lysis followed by gravity purification using Ni-NTA Agarose beads (Qiagen). SDS-PAGE analysis demonstrated partial purification of all expressed cell-penetrating proteins (Fig. 17A). All samples of full length HO1 proteins (CPP-HO1-1, CPP-HO1-2, TAT-HO1, CPP-SDMHO1) demonstrated the presence of a second band of ~33kDa in size (Fig. 17A). This may represent a truncated form of the protein secondary to degradation or incomplete translation. This doublet pattern has been observed by others when purifying recombinant HO-1 [163, 308]. Ribeiro et al. [308] suggested that this smaller sized band may represent a non-membrane binding form of the protein containing the most extreme C-terminal membrane binding region. This is a feasible explanation as the smaller sized protein bands are similar in size to the CPP-sHO1 protein (33.3kDa). CPP-sHO1, CPP-EGFP and TAT-EGFP were also present in the purified fraction, with purification of sHO1 being particularly efficient. The identity of these bands was confirmed by Western blot analysis using primary antibodies against HO1 (Fig. 17B), EGFP (Fig. 17C) and the histidine tag (Fig. 17D).

6,5,1 Purification Under Denaturing And Non-Denaturing Conditions

Previous studies have used cell-penetrating HO1 proteins purified using both denaturing (animal model of heart transplantation) [160] and non-denaturing (*in vitro* treatment of pancreatic β-cells) [308] methods. In this study I decided to compare the yield of CPP-EGFP and CPP-HO1-1 purified under both native and denaturing conditions. CPP-EGFP was efficiently purified by both methods although the yield was greater using denaturing conditions, as indicated by the presence of a stronger 31.7 kDa band on SDS-PAGE analysis (Fig. 18A, B). The identities of these bands were confirmed by Western blot analysis with primary antibodies against the GFP (Fig. 18C) or histidine tag (Fig. 18D). The yield of CPP-HO1-1 was greater when purified under native conditions (Fig. 19A, C), indicated by the presence of a stronger 37kDa band on SDS-PAGE compared to that seen under denaturing conditions. In addition, there was less evidence of truncated forms of the enzyme (indicated by doublet bands of ~35 and 33kDa (Fig. 19A)) when purified

under native conditions. The identity of the purified bands was confirmed by Western blot analysis using primary antibodies against HO1 and the histidine tag (Fig. 19C, D).

Initial problems with low yield resulted in attempting protein purification using a batch protocol, wherein Ni-NTA agarose beads were incubated with bacterial lysates for 1hr at 4°C prior to application to a column. This resulted in a mild increase in protein yield, but at the expense of purity when compared to a strictly gravity-purification method (wherein lysates were simply added to columns containing pre-equilibrated Ni-NTA agarose beads). A comparison of the profiles of proteins purified and observed by SDS-PAGE in Figures 17 (A) and 21 (A) vs. Figures 18 (A, B) and 19 (A, B) shows presence of multiple bands of various sizes with batch protocol purification (Fig. 17 (A), 21(A)) that were not seen with gravity purification (Fig. 18 (A, B), 19 (A, B)). The presence of multiple contaminating proteins in the batch protocol was felt to be unacceptable when purifying a protein for potential therapeutic use; therefore, the decision was made to carry out all further purifications using a gravity protocol.

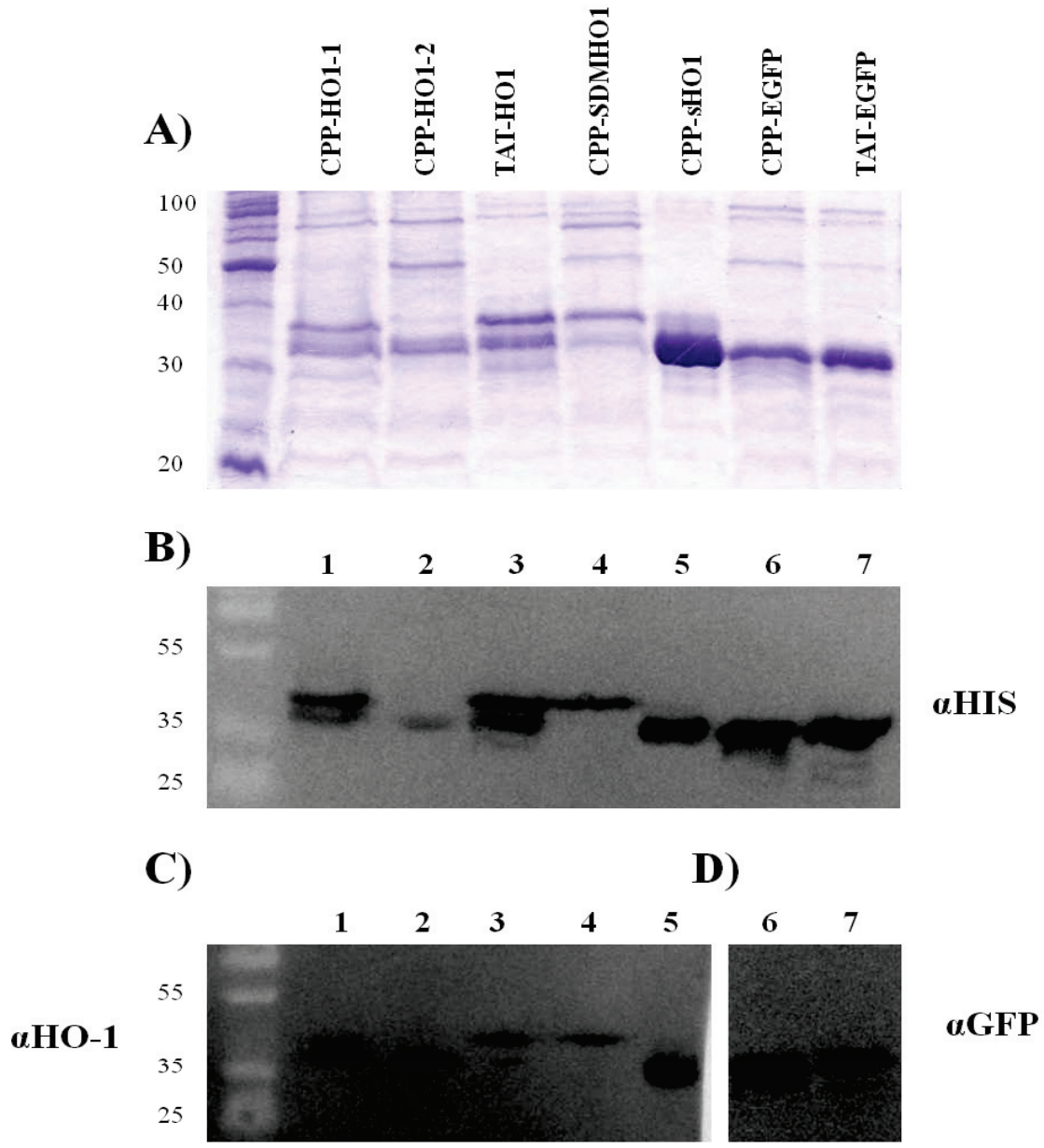

Figure 17. Purification of cell-penetrating proteins. Proteins were purified by Ni-NTA affinity chromatography, using a batch protocol under non-denaturing conditions. Purified proteins were separated by SDS-PAGE and stained with Coomassie blue or transferred to PVDF and examined by Western blot using anti-HO-1, anti-GFP and anti-HIS antibodies. **A)** Representative SDS-PAGE used for Western blot analysis; Western blots probed with **B)** anti-HO1 **C)** anti-GFP **D)** anti-His. Lanes 1-7 are the same for all panels. Lanes **1**: CPP-HO1-1; **2**: CPP-HO1-2; **3**: pTAT-HO1; **4**: CPP-SDM-HO1; **5**: CPP-sHO1; **6**: CPP-EGFP; **7**: pTAT-EGFP

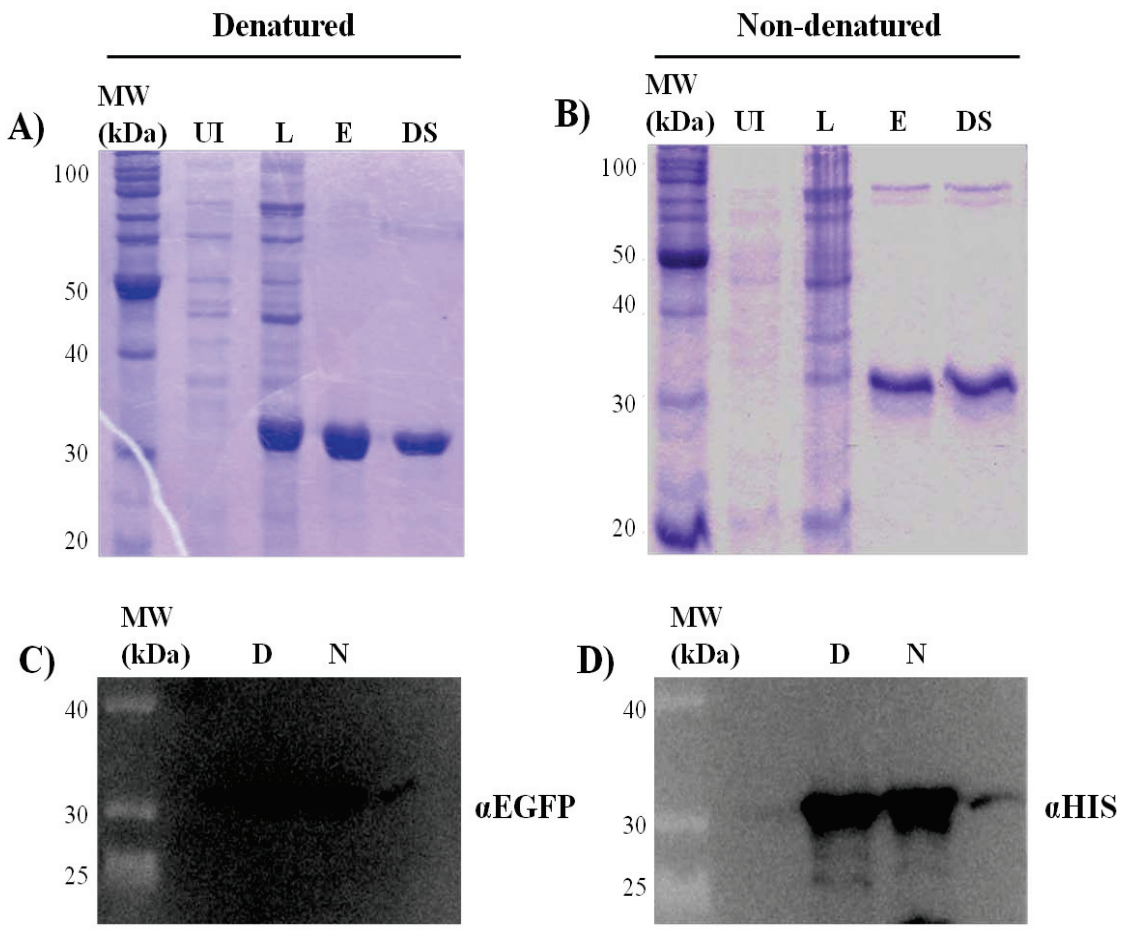

Figure 18. Gravity purification of CPP-EGFP using denaturing and non-denaturing conditions. Proteins were purified by Ni-NTA affinity chromatography, using denaturing (containing urea) or non-denaturing buffers. Purified proteins were separated by SDS-PAGE electrophoresis and stained with Coomassie blue or transferred to PVDF and examined by Western blot with anti-GFP or anti-HIS antibodies. **A)** Denatured and **B)** non-denatured CPP-EGFP. UI= supernates from whole cell lysates of uninduced culture, L = supernates from whole cell lysates of induced culture, E = Eluate from Ni-NTA column, DS = Desalted samples from PD-10 column. **C)** Anti-GFP and **D)** Anti-HIS blots of denatured and non-denatured CPP-EGFP D = proteins purified under denaturingconditions, N = proteins purified under non-denaturing conditions.

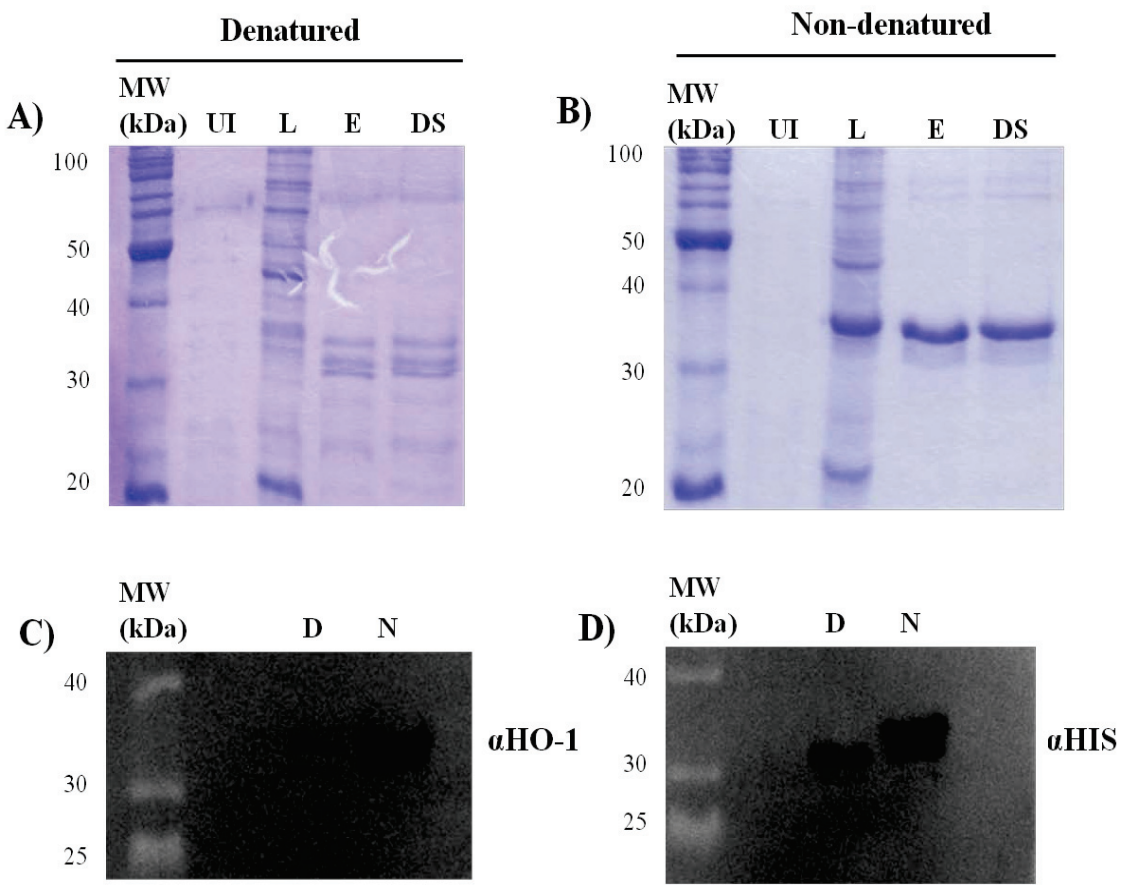

Figure 19. Gravity purification of CPP-HO1-1 using denaturing and non-denaturing conditions. Proteins were purified by Ni-NTA affinity chromatography, using denaturing (containing urea) or non-denaturing buffers. Purified proteins were separated by SDS-PAGE electrophoresis and stained with Coomassie blue or transferred to PVDF and examined by Western blot with anti-HO-1 or anti-HIS antibodies. **A)** Denatured and **B)** non-denatured CPP-HO1-1. UI= supernates from whole cell lysates of uninduced culture, L = supernates from whole cell lysates of induced culture, E = Eluate from Ni-NTA column, DS = Desalted samples from PD-10 column. **C)** Anti-HO-1 and **D)** Anti-HIS blots of denatured and non-denatured CPP-HO1-1 D = proteins purified under denaturingconditions, N = proteins purified under non-denaturing conditions.

Following purification the proteins needed to be separated from the salts, imidazole and urea (for denatured preparations) used during the purification process. To do this I opted to use desalting columns, because of their ease and speed of use compared to dialysis. Desalting of purified proteins was accomplished using PD-10 size exclusion chromatography columns pre-equilibrated with HTK medium. Purified protein samples were eluted in 2mL fractions to determine the fraction with the greatest yield in an attempt to obtain samples with the highest concentrations and greatest purity. This was performed for proteins purified using both denaturing and non-denaturing buffers. When purified under denaturing conditions the majority of HO-1 proteins were eluted from the columns in the first 2 fractions (Fig. 20 A-E). However, the yields for TAT-HO1 and CPP-SDMHO1 were poor, and it is difficult to determine exactly which fractions would have the highest yield (Fig. 20 C, D). CPP-EGFP and TAT-EGFP continued to elute through all 4 fractions, demonstrating the highest yields in fractions 1, 2 and 4 (Fig. 20 F, G). CPP-sHO1 also eluted through all fractions, although in its case, the highest yields were in fractions 1 and 2 (Fig. 20E). It is most likely that the elution patterns of CPP-EGFP and TAT-EGP in this case are due to artefact, possibly from an inadvertent mixing of samples. In the case of CPP-sHO1, however, it is possible that this pattern may be due to exceptionally high protein yield, to the point where a larger volume of HTK was required to completely elute the protein from the column. This is supported by the fact that after the first two lanes there is a sequential decrease in the intensity of the protein bands in lanes 3 and 4 Fig. 20E).

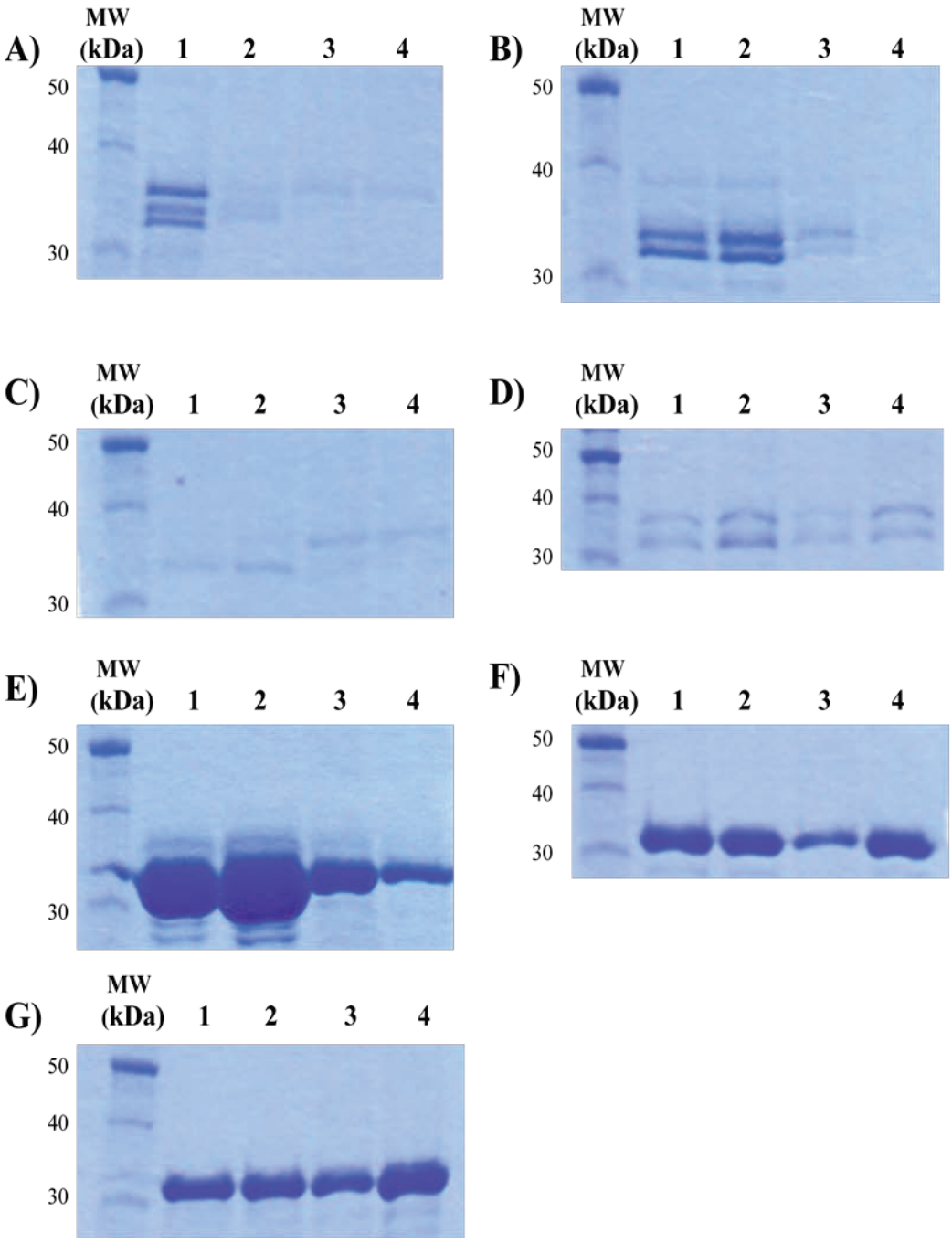

Figure 20. Denatured purified proteins elute early from desalting columns. Proteins were purified using denaturing conditions, desalted on a PD-10 column and eluted in 2mL fractions. Ten µL of each fraction, numbered 1-4 along with MW standards, was loaded onto an SDS-polyacrylamide gel, subjected to electrophoresis and stained with Coomassie blue. **A)** CPP-HO1-1 **B)** CPP-HO1-2 **C)** TAT-HO1 **D)** CPP-SDM-HO1 **E)** CPP-sHO1 **F)** CPP-EGFP **G)** TAT-EGFP.

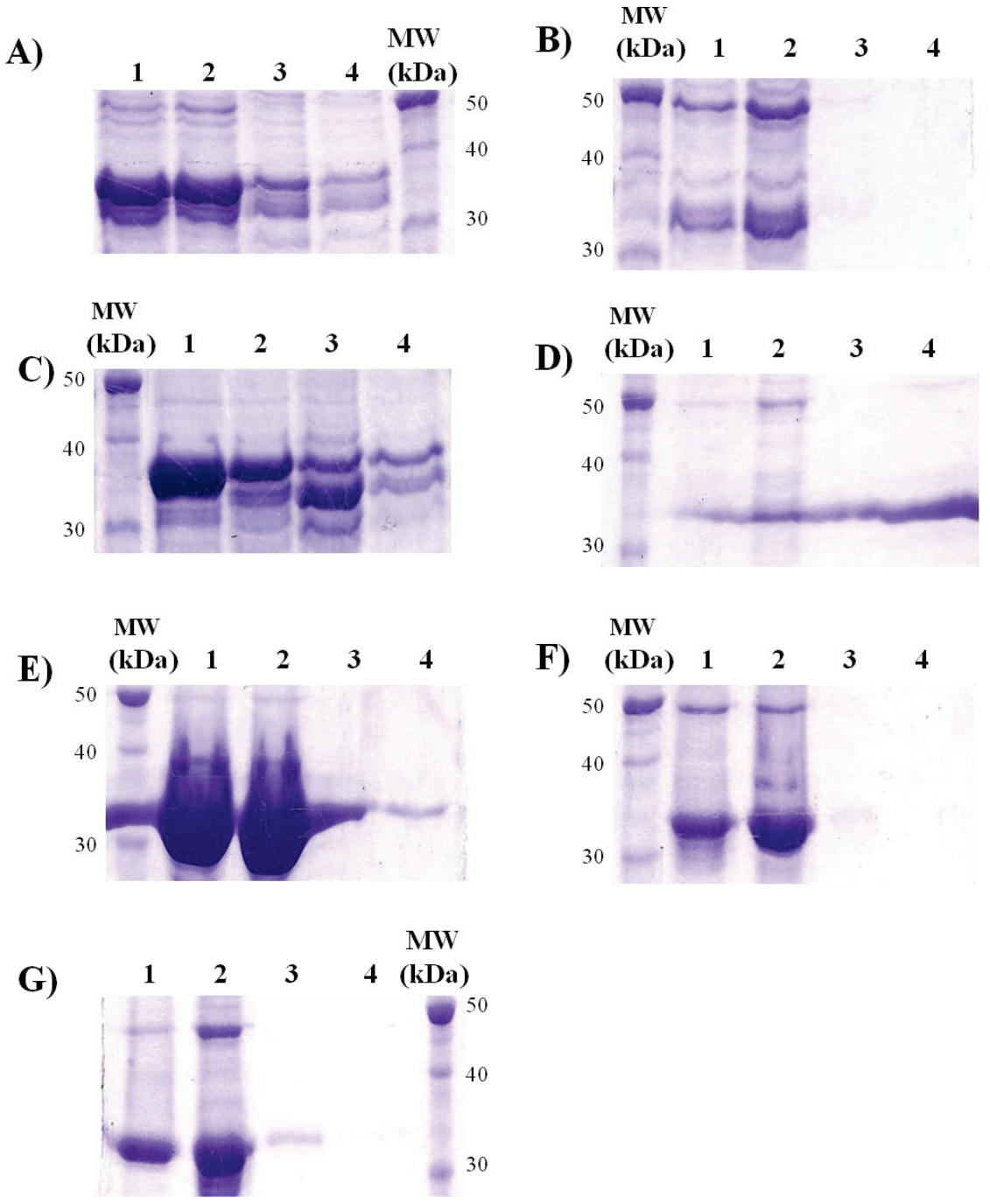

Figure 21. Non-denatured purified proteins elute early from desalting columns. Proteins were purified using denaturing conditions, desalted on a PD-10 column and eluted in 2mL fractions. Ten µL of each fraction, numbered 1-4 along with MW standards, was loaded onto an SDS-polyacrylamide gel, subjected to electrophoresis and stained with Coomassie blue. **A)** CPP-HO1-1 **B)** CPP-HO1-2 **C)** TAT-HO1 **D)** CPP-SDM-HO1 **E)** CPP-sHO1 **F)** CPP-EGFP **G)** TAT-EGFP.

Proteins purified under non-denaturing conditions demonstrated a similar pattern of elution as was seen with proteins purified under denaturing conditions (Fig. 21). Although CPP-HO1-1 and TAT-HO1 were present in greatest amount in fractions 1 and 2 there was still some protein identified in fractions 3 and 4, which is likely a result of the high yield for these two proteins in this purification run (Fig. 21 A, C). Of interest a strong protein band of ~32kDa in size was observed in lane 3 for TAT-EGFP (Fig. 21 C), suggestive of a possible truncated form of the protein. The protein bands seen in the CPP-HO1-2 gel (Fig. 21B) are of smaller size than the predicted full length protein and likely represent degradation products. CPP-SDMHO1 did not appear to be purified to any appreciable extent in this experiment, as demonstrated by the lack of any protein bands of corresponding size. This data suggests that the purification conditions do not significantly affect the way in which the proteins elute off the PD-10 column.

6.6 Natively Purified CPP-HO1-1 Retains HO-1 Enzymatic Activity

To determine if the presence of the CPP sequence or the purification process inhibited HO1 activity, a bilirubin production assay was performed using HEK-293T cell lysates treated with natively purified CPP-HO1-1. Bilirubin production was observed to be significantly higher in CPP-HO1-1 treated samples compared to control samples lacking the electron donor NADPH, or samples with protein isolated from uninduced cells containing the pCPP-HO1-1 plasmid (Fig. 22). The fact that CPP-HO1-1 is able to catalyze the degradation conversion of heme to bilirubin indicates that neither the CPP sequence or the non-denaturing purification process inhibits HO1 enzymatic activity.

6.7 Cellular Penetration Of Hepg2 And HUVEC Cells Is Improved With CPP-EGFP And CPP-HO1-1 Purified Under Non-Denaturing Conditions

To determine if there was any significant difference in the cell-penetrating ability of proteins purified under denaturing or non-denaturing conditions HepG2 cells were treated with CPP-EGFP. Following treatment with CPP-EGFP cells were washed, fixed and analyzed by fluorescence microscopy. Cells treated with CPP-EGFP purified under non-

denaturing conditions demonstrated substantially more fluorescence than cells treated with denatured CPP-EGFP, indicating a greater association of protein, particularly with the cellular membrane (Fig. 23). To determine if the same held true for CPP-HO1-1, HUVEC cells were treated with CPP-HO1-1 purified under denaturing and non-denaturing conditions, and subjected to immunofluorescence. After treatment with CPP-HO1-1 cells were washed, fixed, and probed with rabbit-anti-HO-1 and mouse-anti-HIS primary antibodies followed by goat anti-rabbit Cy2 (green) (Fig. 24 A and B panel 1) and goat anti-mouse Cy3 (red) (Fig. 24 A and B panel 2) secondary antibodies. Both denatured and non-denatured CPP-HO1-1 treated cells demonstrated fluorescence, indicating cellular penetration, although cellular fluorescence was greater with the non-denatured protein suggesting enhanced cellular penetration (Fig. 24). These results suggest that although CPP-EGFP and CPP-HO1 proteins purified under denaturing and non-denaturing conditions have cell-penetrating ability, this ability appears to be greater for proteins purified in their native configuration.

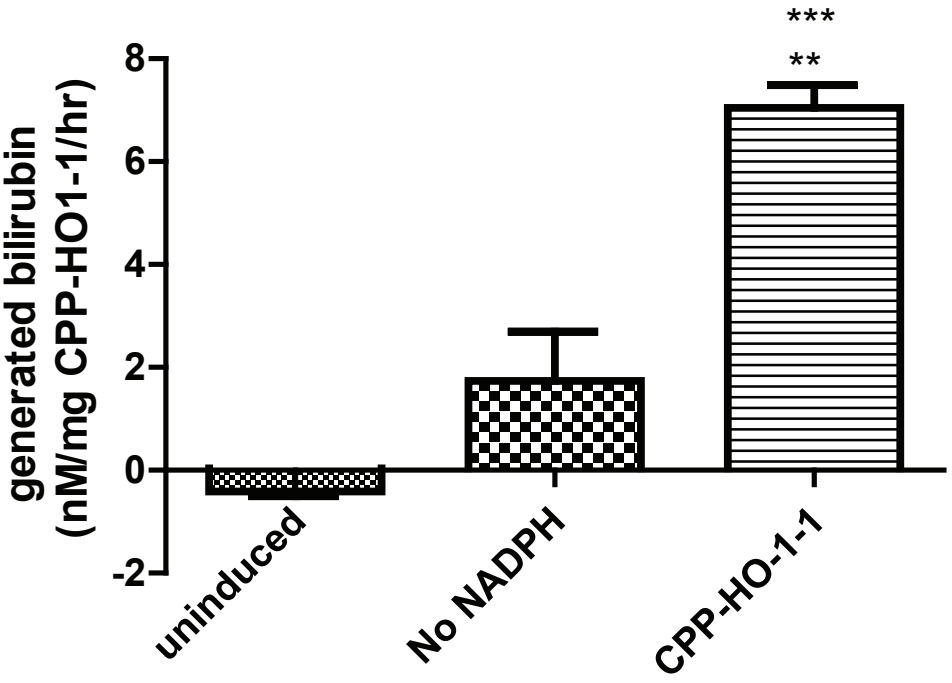

Figure 22. Natively purified CPP-HO1-1 retains HO-1 enzymatic activity. HEK-293T cell lysates were supplemented with G6PD, G6P, NADPH, Hemin, and BVR and treated with 300µg of purified CPP-HO1-1 for 1hr in the dark. Bilirubin concentration was quantified by measuring the difference in absorbance between 464 and 530nm and multiplying by an extinction coefficient of $40mM^{-1}cm^{-1}$. Measurentments for each group (treatment or control) were performed in triplicate. Mean values and standard error were calculated for each group and statistical analysis performed using a one way ANOVA test. Groups included a reaction mixture treated with protein purified from uninduced CPP-HO1-1 transformed cells (uninduced) and a reaction from which the electron donor NADPH was omitted – both controls, and a reaction mixture treated with CPP-HO1-1 purified under non-denaturing conditions. ** p of 0.01 to 0.001 (between CPP-HO1-1 and no NADPH) *** $p<0.001$ (between CPP-HO1-1 and uninduced).

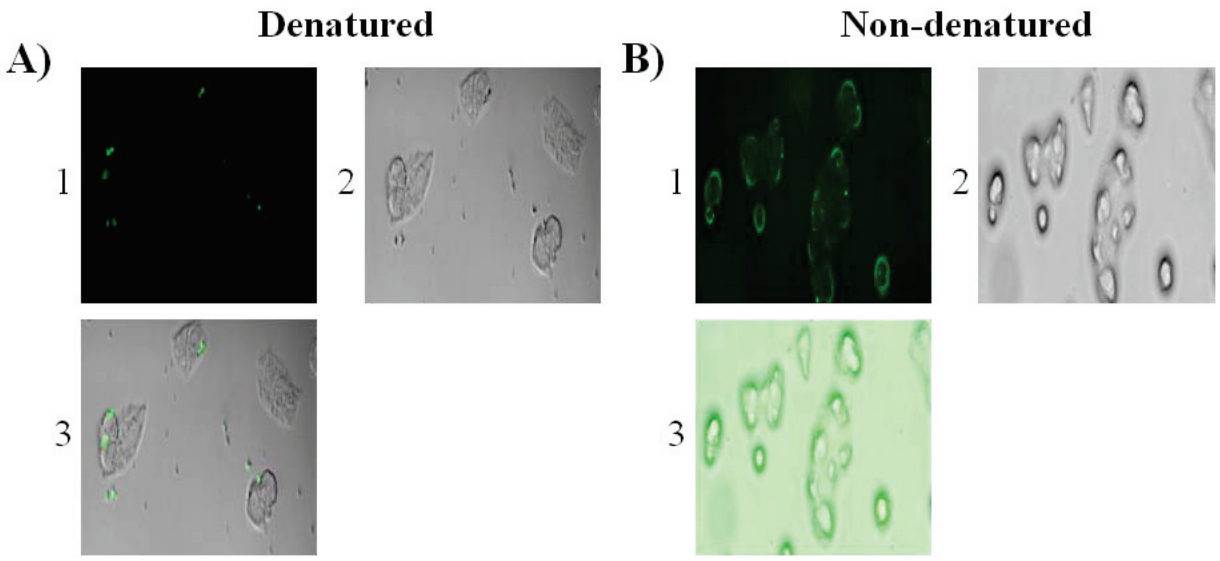

Figure 23. Non-denatured CPP-EGFP penetrates HepG2 cells more effectively than denatured CPP-EGFP. Cultured cells were treated with 500µg **A)** Denatured or **B)** non-denatured CPP-EGFP for 4 hours, washed, fixed and examined by fluorescence microscopy. For both panels **1:** EGFP **2:** brightfield **3:** merge.

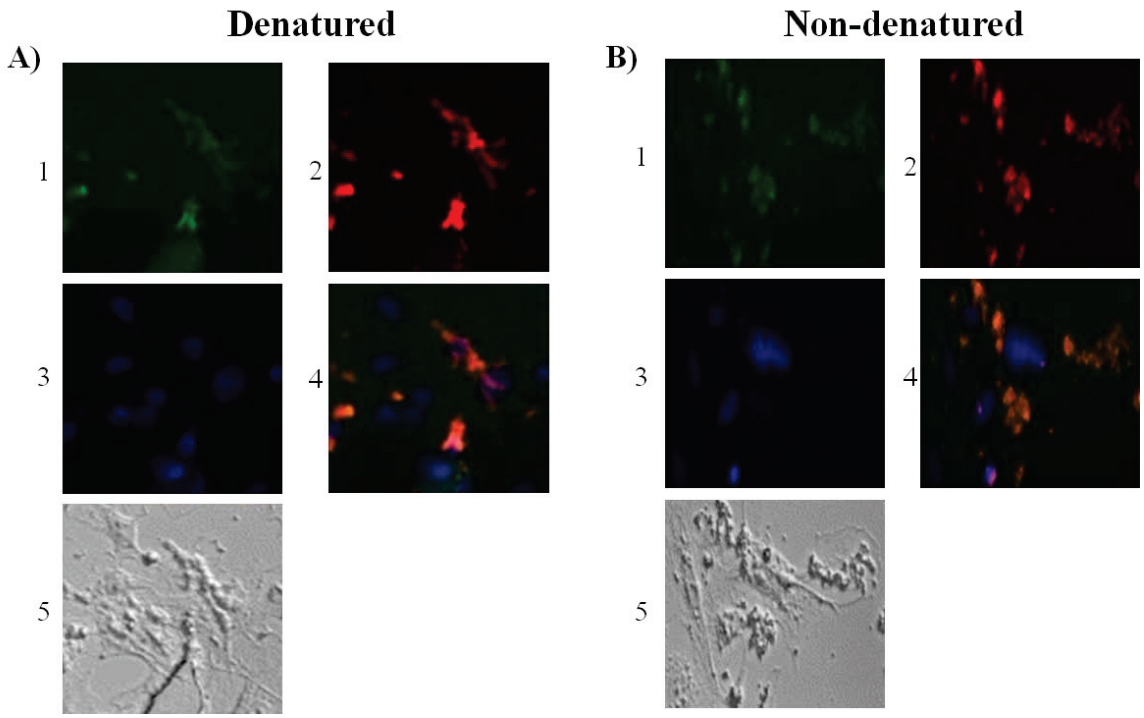

Figure 24. Non-denatured CPP-HO1-1 penetrates HUVEC cells more effectively than denatured CPP-HO1-1. Cells were treated with 500µg of denatured or non-denatured CPP-HO1-1 for 4 hours, washed, fixed, probed with primary rabbit anti-HO-1 and mouse anti-HIS, followed by anti-rabbit Cy2 (green) and anti-mouse Cy3 (red), DAPI stained (blue) and analyzed by fluorescence microscopy. **A)** HUVEC cells treated with denatured and **B)** non-denatured CPP-HO1-1. For both panels **1:** Mouse anti-HO1 **2:** Mouse anti-his **3:** DAPI nuclear staining **4:** merge **5:** brightfield.

6.8 Cellular Penetration Of J774, Hepg2 And HUVEC Cells By CPP-EGFP And TAT-EGFP

Hepatic IRI appears to involve three primary cell types: macrophages, hepatocytes and endothelial cells. I hypothesized that the potential beneficial effect of HO-1 activity in reducing IRI might be more pronounced if HO-1 activity could be increased in all three of these cell types. Therefore, I wanted to test the ability of the CPP- and TAT-sequences to mediate cellular transduction of a desired protein sequence in three representative tissue culture models (J774 murine macrophages, HepG2 human hepatoma cells, and HUVEC (human umbilical vein endothelial cells)). Because use of the CPP-EGFP and TAT-EGFP proteins allowed evaluation of the function of the CPP and TAT sequences without the need for immunofluorescence staining, I decided to treat cells with these proteins first. Cells were incubated with CPP-EGFP and TAT-EGFP, washed, fixed, and analyzed by fluorescence microscopy. With J774 cells minimal association was seen for CPP-EGFP (Fig. 25A), but TAT-EGFP demonstrated efficient cellular penetration (Fig. 25B). For HepG2 cells green fluorescence was observed following treatments with both CPP-EGFP and TAT-EGFP indicative of cellular penetration (Fig. 26). HUVEC cells demonstrated significant fluorescence following treatment with CPP-EGFP but only minimal fluorescence was observed with TAT-EGFP (Fig. 27). These results suggest that while the TAT sequence confers cell-penetrating ability to EGFP for both j774 and HepG2 cells, whereas the CPP sequence allows cellular penetration of HepG2 and HUVEC cells.

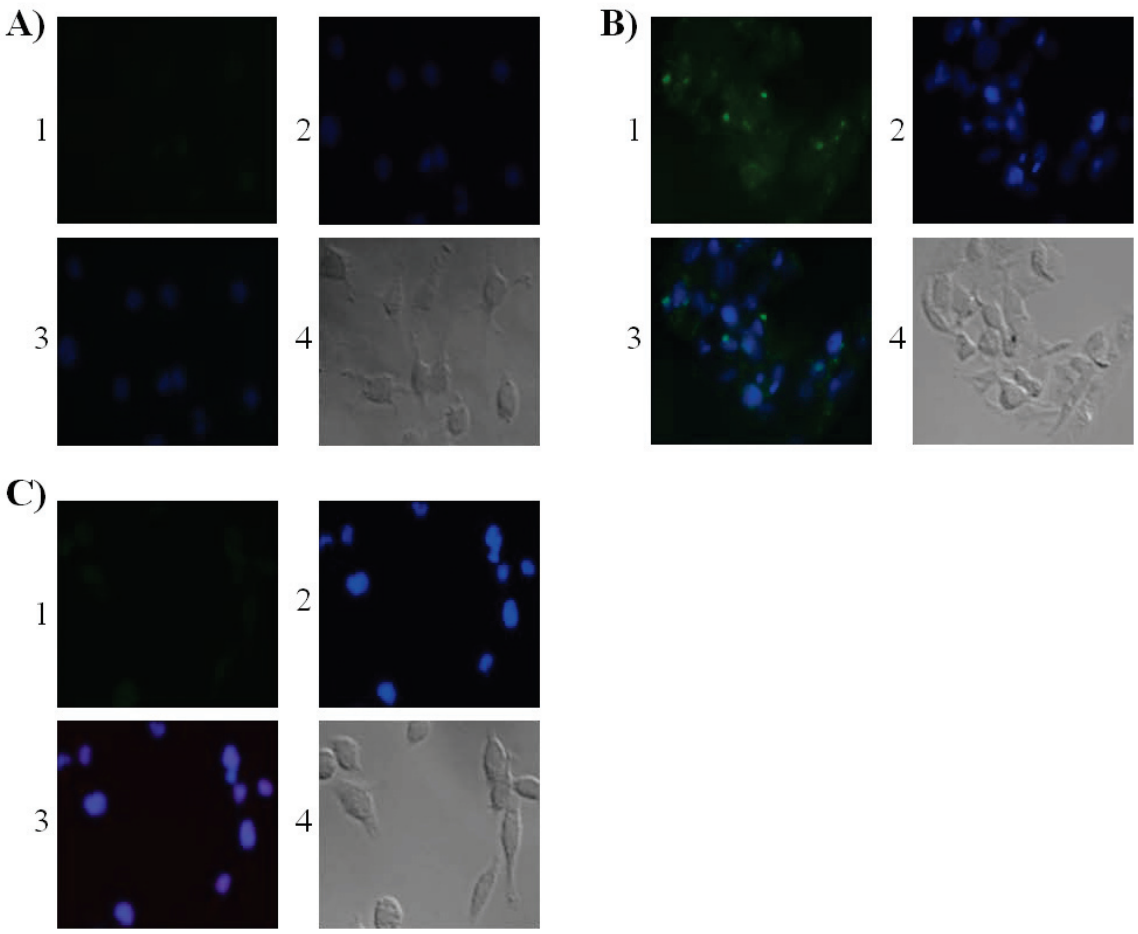

Figure 25. TAT-EGFP penetrates J774 cells. Cells were treated with 500µg of CPP-EGFP, TAT-EGFP, or HTK (mock treatment) for 4 hours. Cells were then washed, fixed, DAPI stained and analyzed by fluorescence microscopy. **A)** CPP-EGFP **B)** pTAT-EGFP **C)** Mock. For each panel, **1:** EGFP **2:** DAPI **3:** merge **4:** brightfield image.

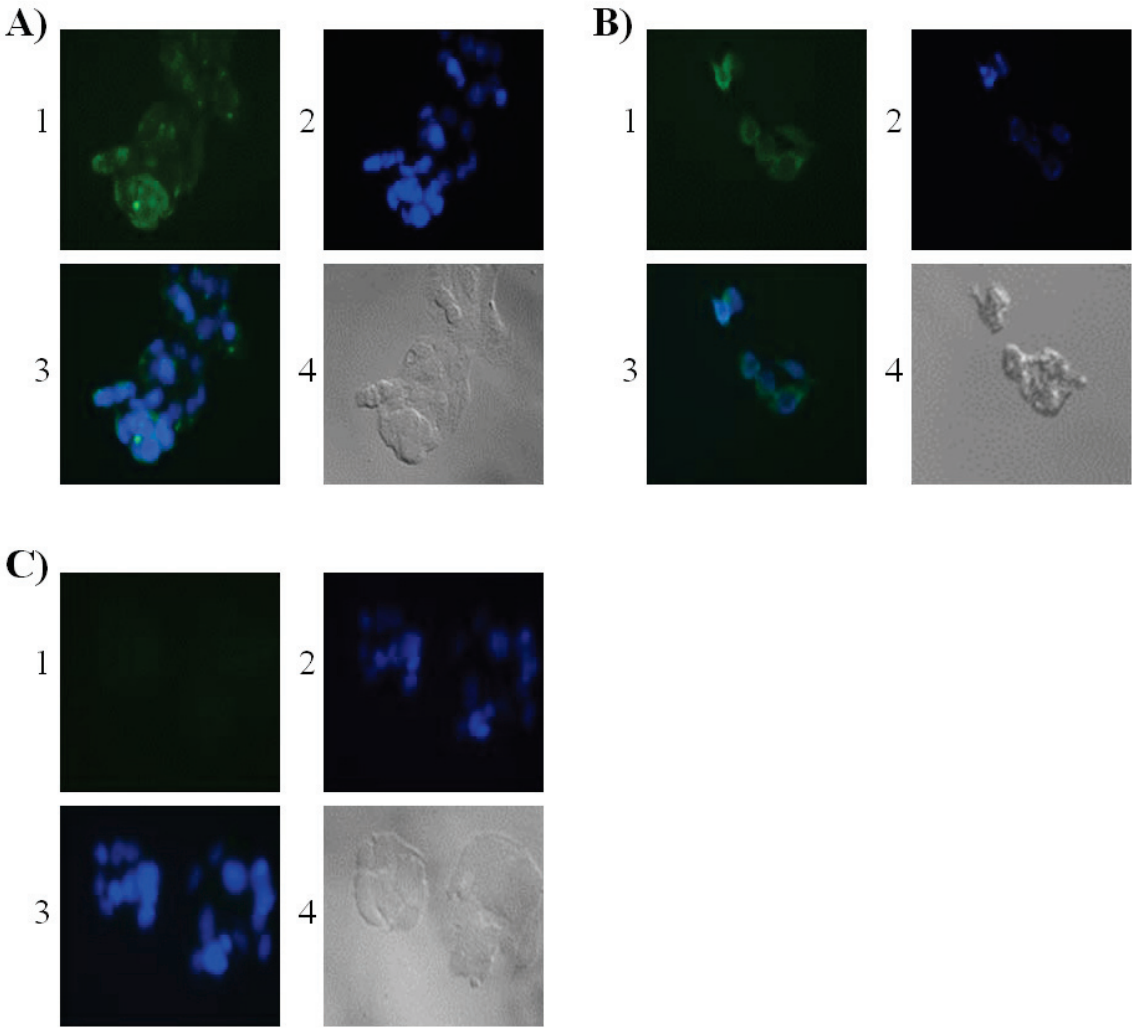

Figure 26. CPP-EGFP and TAT-EGFP penetrate HepG2 cells. Cells were treated with 500µg of CPP-EGFP, TAT-EGFP, or HTK (mock treatment) for 4 hours. Cells were then washed, fixed, DAPI stained and analyzed by fluorescence microscopy. **A)** CPP-EGFP **B)** pTAT-EGFP **C)** Mock. For each panel, **1:** EGFP **2:** DAPI **3:** merge **4:** brightfield image.

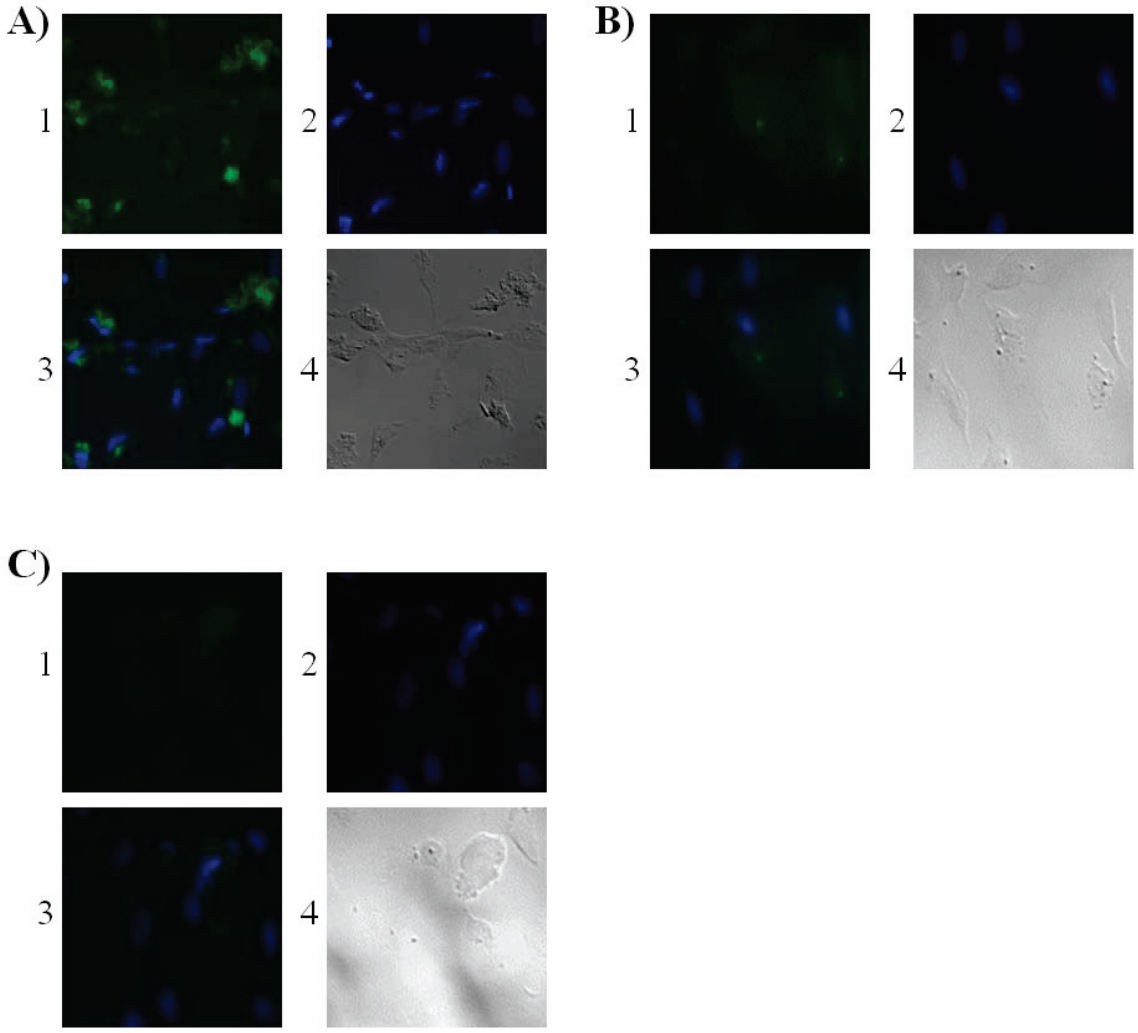

Figure 27. CPP-EGFP penetrates HUVEC cells. Cells were treated with 500µg of CPP-EGFP, TAT-EGFP, or HTK (mock treatment) for 4 hours. Cells were then washed, fixed, DAPI stained and analyzed by fluorescence microscopy. **A)** CPP-EGFP **B)** pTAT-EGFP **C)** Mock. For each panel, **1:** EGFP **2:** DAPI **3:** merge **4:** brightfield image.

6.9 The CPP- And TAT-Sequences Mediate Cellular Transduction Of Multiple Cell Types By HO-1

The data from the CPP-EGFP and TAT-EGFP experiments indicated that the CPP and TAT sequences mediate cellular penetration. The next step was to investigate if they are able to confer this capacity to HO-1 proteins. As previously mentioned I felt it important to evaluate the cell-penetrating ability of these proteins in representative models of three of the major cell types involved in IRI (J774 cells, HepG2 cells and HUVEC cells). To do this, cells were treated with the protein of interest or a mock treatment of HTK alone and subsequently examined by immunofluorescence microscopy using anti-HO-1 and anti-HIS antibodies.

All cell-penetrating HO1 proteins were found to associate with J774 cells *in vitro* (Fig. 28). This association was strongest for CPP-HO1-1, TAT-HO1 and CPP-sHO1 which stained strongly positive for both HO1 and his tag (Fig. 28 A,C,E). Only very weak staining was observed for CPP-HO1-2 and CPP-SDMHO1 (Fig. 28 B,D). In all cases his- tag staining correlated with that of HO1, confirming that the fluorescence observed with HO1 staining was due to the recombinant protein and not endogenous HO1. In addition, the membranes of cells treated with CPP-HO1-1, TAT-HO1 and CPP-sHO1 demonstrate a bubbling appearance on brightfield images that may represent endocytic vesicles through which the protein is taken up into the cell. These findings suggest that CPP-HO1-1, TAT-HO1 and CPP-sHO1 are able to transduce J774 cells *in vitro*.

All cell-penetrating HO1 proteins with the exception of CPP-HO1-2 were found to associate with HepG2 cells *in vitro* (Fig. 29). The strongest staining was observed for CPP-HO1-1, TAT-HO1 and CPP-sHO1 (Fig. 29 A,C,E). Some FITC and Cy5 fluorescence was observed in the mock treated sample (Fig. 28F). However, this can be attributed to background staining as it only surrounds the cells and does not highlight the cell membrane or any internal cellular structures. As was observed with the J774 cells, his-tag staining correlated with that of HO1. The cellular membranes of CPP-HO1-1,

TAT-HO1, CPP-sHO1 and, to a lesser degree, CPP-SDMHO1-treated cells also demonstrate a bubbling appearance on brightfield images (Fig. 29 A,C-E), that may represent endocytic vesicles or possibly adherent clusters of protein. These findings suggest that CPP-HO1-1, TAT-HO1, CPP-SDMHO1 and CPP-sHO1 are able to transduce HepG2 cells *in vitro*.

Only CPP-HO1-1 and CPP-HO1-2 were tested for their ability to transduce HUVEC cells, and of these two only CPP-HO1-1 treatment resulted in a strong fluorescent signal for both HO1 and the his-tag, indicative of cellular transduction (Fig. 30).

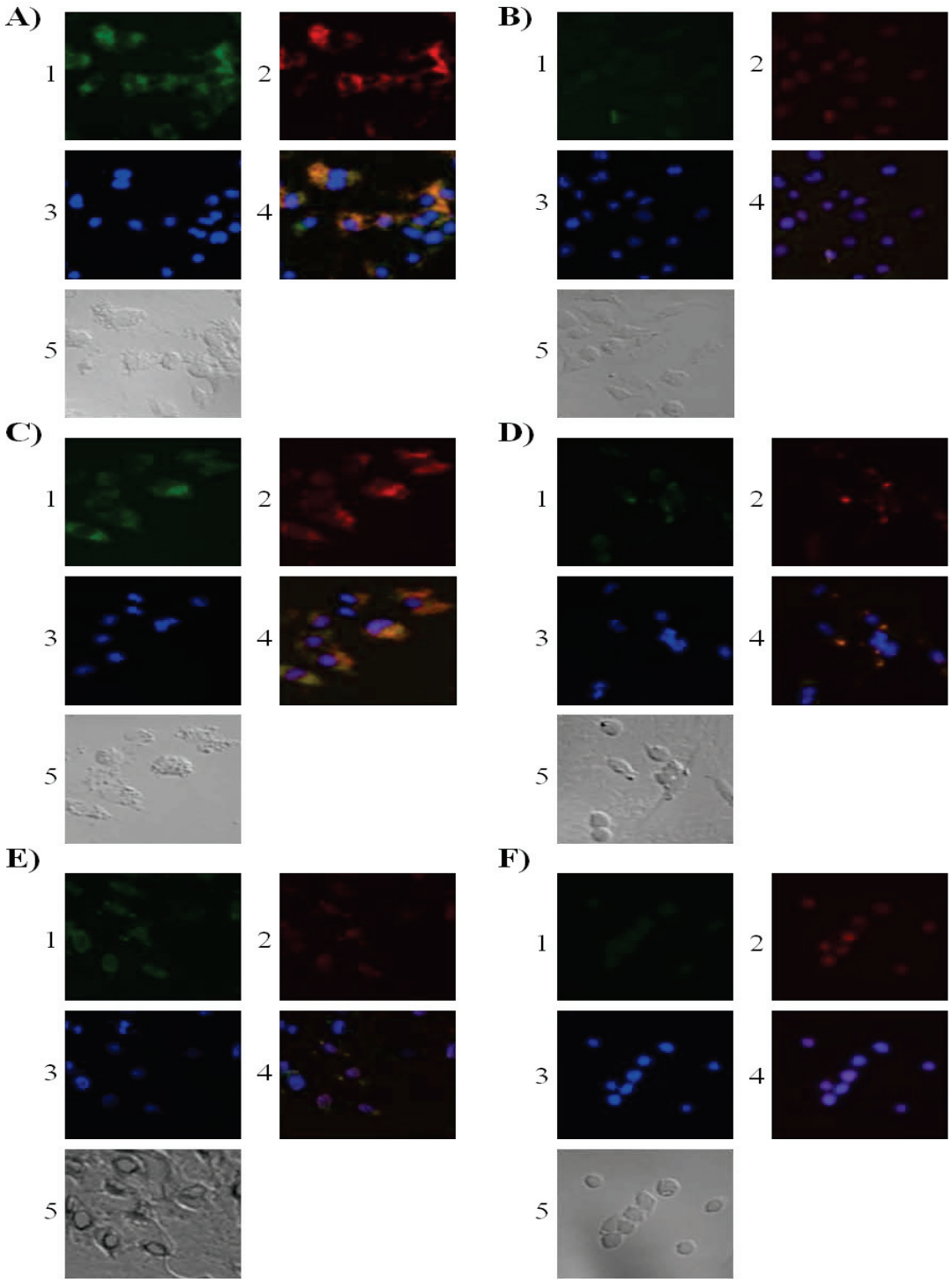

Figure 28. CPP- and TAT-HO1 proteins penetrate J774 cells. Cells were treated with 500μg of the protein of interest for 4 hours, washed, fixed, probed with primary rabbit anti-HO-1 and mouse anti-HIS, followed by anti-rabbit Cy2 (green) and anti-mouse Cy3 (red), DAPI stained (blue) and analyzed by fluorescence microscopy. **A)** J774cells treated with denatured and **B)** non-denatured CPP-HO1-1. For both panels **1:** Mouse anti-HO1 **2:** Mouse anti-his **3:** DAPI nuclear staining **4:** merge **5:** brightfield.

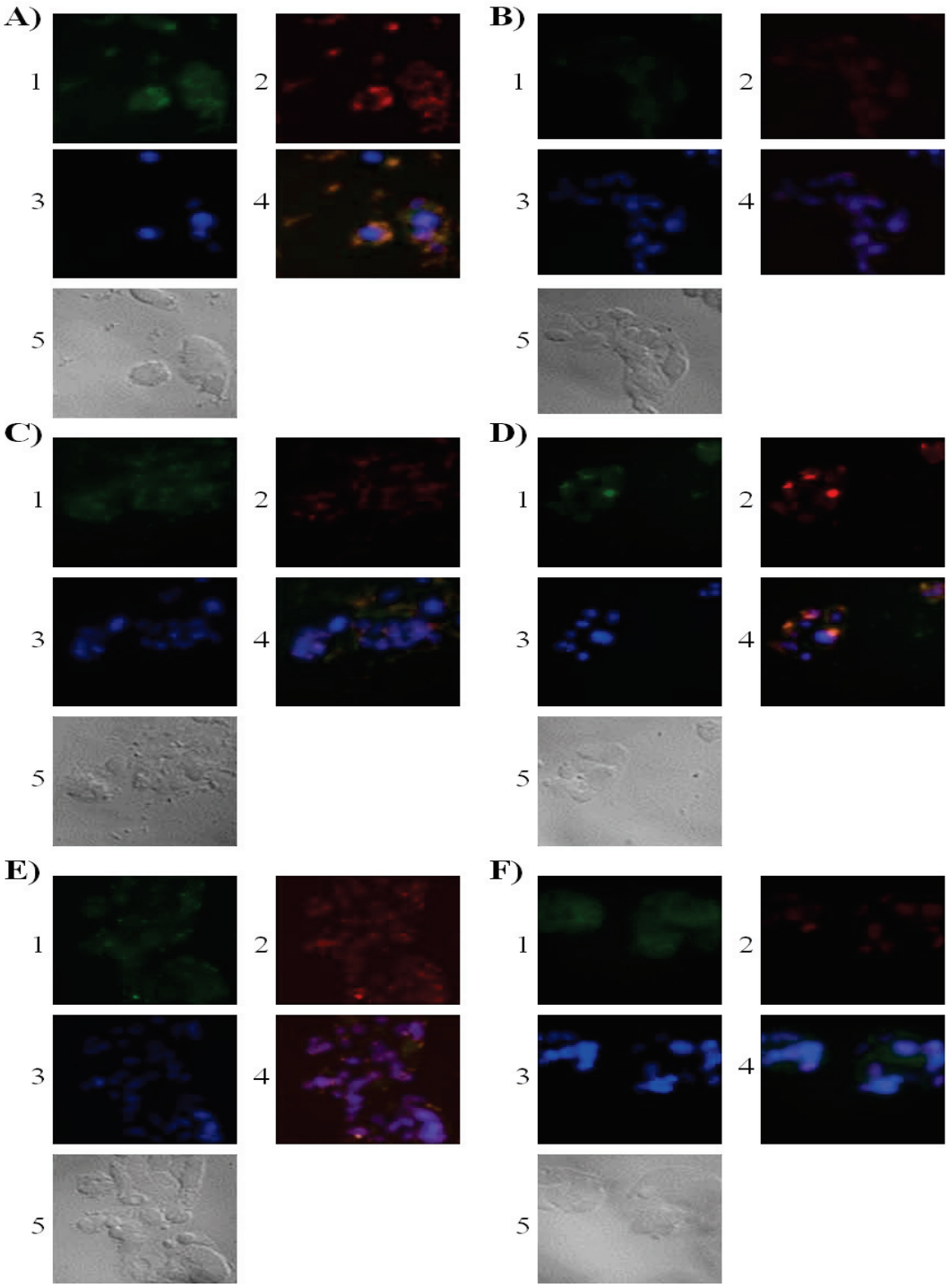

Figure 29. CPP- and TAT-HO1 proteins penetrate HepG2 cells. Cells were treated with 500µg of the protein of interest for 4 hours, washed, fixed, probed with primary rabbit anti-HO-1 and mouse anti-HIS, followed by anti-rabbit Cy2 (green) and anti-mouse Cy3 (red), DAPI stained (blue) and analyzed by fluorescence microscopy. **A)** HepG2 cells treated with denatured and **B)** non-denatured CPP-HO1-1. For both panels **1:** Mouse anti-HO1 **2:** Mouse anti-his **3:** DAPI nuclear staining **4:** merge **5:** brightfield.

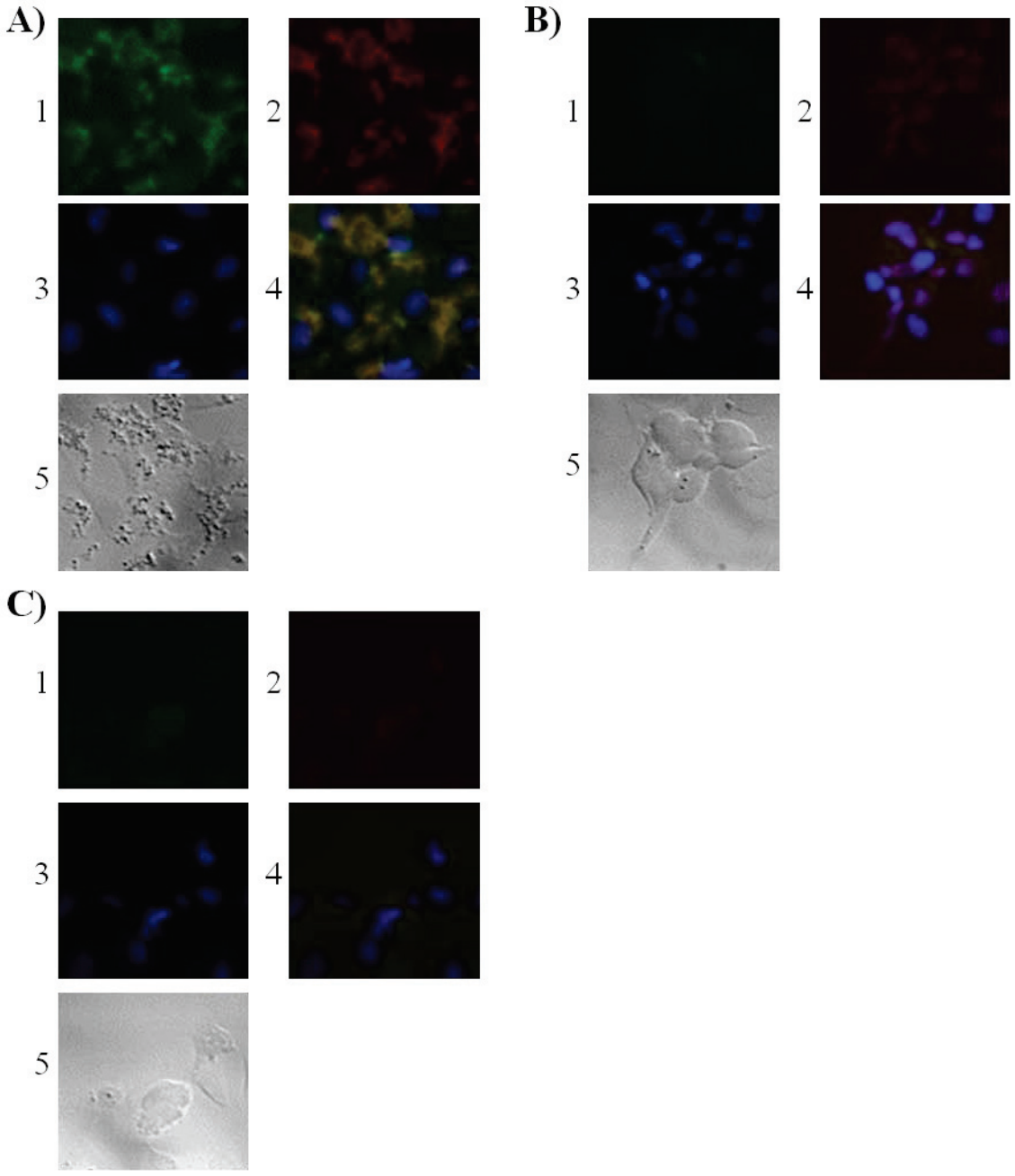

Figure 30. CPP-HO1-1 penetrates HUVEC cells. Cells were treated with 500µg of the protein of interest for 4 hours, washed, fixed, probed with primary rabbit anti-HO-1 and mouse anti-HIS, followed by anti-rabbit Cy2 (green) and anti-mouse Cy3 (red), DAPI stained (blue) and analyzed by fluorescence microscopy. **A)** CPP-HO1-1 **B)** CPP-HO1-2 **C)** Mock. For each panel **1:** Mouse anti-HO1 **2:** Mouse anti-his **3:** DAPI nuclei staining **4:** merge **5:** brightfield.

6.10 CPP-EGFP Penetrates Live Hepg2 Cells

Some investigators have observed intracellular translocation o f PTD proteins following cellular fixation but not in live cell experiments, leading to the claim that the intracellular accumulation seen in immunofluorescence experiments is due to fixation artefact rather than an ability of the PTD sequence to mediate cellular transduction [314]. To ensure that the association between the cells and the CPP- and TAT-proteins seen in the immunofluorescence experiments performed here was not a product of the fixation process, HepG2 cells were treated with CPP-EGFP and subsequently examined without fixation. CPP-EGFP purified under both denaturing and non-denaturing conditions was found to associate with HepG2 cells (Fig. 31A, B). This indicates that the CPP-sequence is able to mediate cellular penetration, and that the findings in the immunofluorescence experiments are unlikely due to fixation artifact.

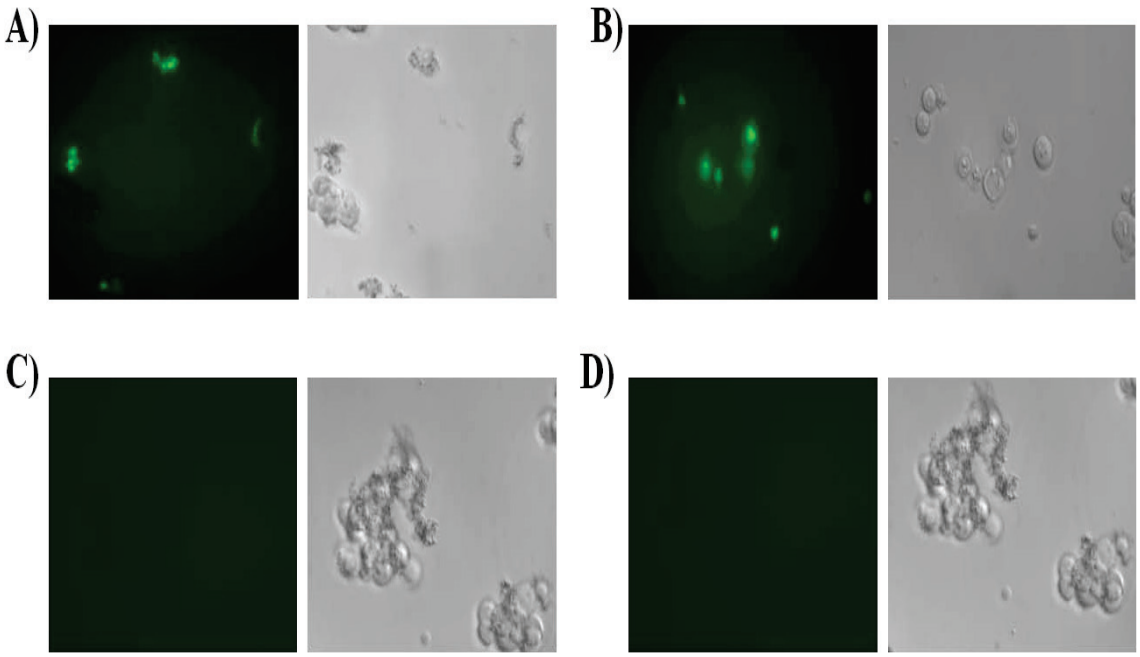

Figure 31. CPP-EGFP penetrates live HepG2 cells. CPP-EGFP was incubated with HepG2 cells at a concentration of 6.7µM. Following treatment cells were washed and plated on a chamber slide, incubated for 1 hour, then examined by fluorescence microscopy. **A)** CPP-EGFP purified under denaturing conditions **B)** CPP-EGFP purified under native conditions **C)** mock treatment control **D)** negative control. Left panels: fluorescent images, Right panels: brightfield images.

Chapter 7: Discussion

The ability to increase the resistance of steatotic livers to IRI has the potential to significantly increase the number of potential donor organs for liver transplantation, providing a lifesaving therapy for those with end-stage liver disease. Increasing HO-1 expression has been shown to reduce IRI and improve survival in animal models of transplantation; however, current methods of upregulating HO-1 all have drawbacks that may limit their clinical application. The ability to transiently deliver a fully functional HO-1 protein to the organ during the *ex vivo* phase, holds significant promise, and the use of cell-penetrating peptides appear to be an ideal way to do this. To this end the purpose of this research was the creation and testing of a cell-penetrating HO-1 protein for use in an animal model of steatotic liver transplantation. The data presented in this thesis show the cloning, protein expression, and testing of multiple forms of a recombinant human HO-1 using either the TAT or a separate (CPP) protein transduction sequence. Although the production of many of these proteins (CPP-HO1-1, TAT-HO1, CPP-SDMHO1) is not novel, the intended use for which they have been generated is. The use of a cell-penetrating HO-1 protein for the treatment steatotic livers *ex vivo* prior to transplantation is a novel application that is hypothesized to improve the resistance of these organs to IRI and may, ultimately, result in expansion of the donor pool by rendering previously unacceptable organs useable. This work also describes the novel generation and testing of a soluble form of CPP-HO1 (CPP-sHO1), that lacks the HO1 C-terminal membrane binding region, while retaining enzyme function. Two separate cell-penetrating EGFP proteins were produced. These proteins were used to evaluate the cell-penetrating ability of the TAT and CPP sequences into cells and whole organs. They will also serve as comparative controls in animal studies, helping to control against any potential effects of the CPP/TAT sequence or transduction process on hepatic IRI and survival outcomes.

7.1 Cloning

7.1.1 Choice Of Proteins For Cloning

The objective of this research is to improve the utility of steatotic livers by enhancing their resistance to I/R injury. HO-1 has been recognized in the literature as a major cellular protectant against reperfusion injury [186-190]. Upregulation of HO-1 has been shown to be protective against IRI in animal models of solid organ transplantation [191-197]. I hypothesized that the protective effect of HO-1 activity would be even more pronounced in steatotic livers, resulting in reduced graft injury, improved graft function and improved overall survival. Increasing HO-1 activity can be accomplished by increasing endogenous expression, or by delivery of the gene or gene products. In the setting of human transplantation the method of gene therapy delivery is of particular importance. Significant ethical challenges face the implementation of experimental therapies that require systemic treatment of human donors. The most logical time for treatment of donor organs that avoids many of these ethical problems is during the *ex vivo* storage period. The use of cell-penetrating peptides is an attractive method for cellular delivery of active proteins during this period. During the past 20 years a significant amount of research has been directed towards the utilization of these protein sequences for the delivery of therapeutic molecules of all kinds [297-311]. These findings led me to pursue a CPP model for the delivery of HO-1 in attempts to improve the resistance of steatotic livers to IRI.

Most of the early literature regarding cell-penetrating proteins as carrier molecules was performed using the TAT sequence; therefore I decided to use this as one of our carrier molecules. In addition, a modified sequence (CPP) has recently been shown to have 33 times the transduction efficiency of regular TAT [316] and has been used to treat hearts *ex vivo* in an animal model of transplantation [313]. The purported efficiency of this CPP led us to create clones using it as the carrier molecule for HO-1 as well. In order to determine if any beneficial effects seen were due to HO-1 activity a HO-1 mutant was created, to act as a negative control in future experiments, containing histidine to alanine

mutations at amino acids 25 and 132. Histidine 25 serves as a heme binding ligand and is necessary for HO-1 function [165,166]. In order to easily test the function of the TAT and CPP sequences, I decided to construct separate clones containing EGFP to allow for simple assessment of the ability of these sequences to mediate cellular transduction using fluorescence microscopy.

7.1.2 Expression System Selection

The most common host for protein expression is *E. coli* because of its low cost, fast expression, high yields and variety of strong promoters [315, 316]. However, the use of bacterial systems can pose some challenges when trying to express biologically active proteins for therapeutic use. Many eukaryotic protein sequences contain codons that are infrequently used in *E. coli* [316], and undergo post-translational modifications such as phosphorylation, signal sequence cleavage, proteolytic processing and glycosylation that *E. coli* does not perform [317]. Eukaryotic expression systems such as yeast, insect or mammalian cells are able to perform many of these functions, although generally with lower yields of desired protein and at much higher costs. A review of the literature suggests that HO-1 does not undergo significant post-translational modification. In addition, multiple groups have successfully produced functional HO-1 using *E. coli* as an expression host [160, 308, 313, 318].

The expression system used for these experiments consists of the pET-28b(+) vector and the bacteriophage Rosetta2(DE3)pLysS *E. coli*. The pET-28b(+) vector contains a multiple cloning site downstream from a T7*lac* promoter. The multiple cloning site contains NheI and HindIII restriction endonuclease sites, neither of which are located within the CPP-HO1 or CPP-EGFP sequences, making it ideal for easy cloning of these sequences into the plasmid. The T7*lac* promoter initiates transcription by T7 RNA polymerase, which transcribes DNA 5 times faster than bacterial RNA polymerase, under control of a *lac* operator sequence [319]. Transcription also results in expression of a downstream kanamycin resistance gene that allows for selection of positive transformants

based on growth on kanamycin containing medium. Rosetta2(DE3) *E. coli* contain a chromosomal copy of the T7 RNA polymerase gene under the control of the *lac*UV5 promoter, and a chromosomal copy of the *lac*I gene. Both the T7*lac* promoter and the *lac*UV5 promoter contain *lac* operator sequences, and that are under the control of the *lac* repressor (product of the *lac*I gene). Under normal growth conditions *lac* repressor is constitutively expressed and binds to the *lac* operator sequence on both promoters, inhibiting the expression of T7RNA polymerase and any gene cloned into the pET-28b(+) plasmid [320, 321]. When IPTG (a non-hydrolyzable lactose analog) is added to bacterial culture it binds the *lac* operator sequences, displacing the *lac* inhibitor and initiates transcription of T7 RNA polymerase. Expressed T7 RNA polymerase is then free to bind to the T7*lac* promoter on the pET-28b(+) and initiate transcription of the cloned gene of interest [316]. Despite containing a *lac* operator sequence, the *lac*UV5 promoter is known to incompletely inhibit T7 RNA polymerase expression [316]. This 'leaky' promoter can result in undesireable expression of the gene of interest located on the pET plasmid. In the case of clones containing toxic genes this can inhibit the ability to store cultures for future use. However, because pET-28b(+) contains a T7*lac* promoter, expression of target genes by basal levels of T7 RNA polymerase is inhibited by the *lac* repressor. The high efficiency, easily inducible promoter, and unique multiple cloning sequence make this and ideal recipient vector for the CPP-EGFP and CPP-HO1 sequences. In addition, the pTAT vector received from Dr. Steven Dowdy is based on the pET-28b(+) vector, allowing for expression of genes cloned into this vector using the same strain of *E. coli* and similar expression conditions.

I chose to use the *E. coli* BL21 derivative strain Rosetta2(DE3)pLyS as the host for protein expression, because of its many features that make it an optimal host for expression of HO-1 containing proteins. In addition to containing an IPTG-inducible chromosomal copy of T7 polymerase [319], BL21 and its derivatives also lack the *ompT* and *lon* proteases [316], which are responsible for the degradation of T7RNA polymerase [322] and misfolded or recombinant proteins [323] respectively. Rosetta2 strains contain the pRARE2 plasmid [324] encodes seven rare tRNA that contain sequences

complementary to ones commonly found in mRNA encoding human proteins but are rare in bacteria [316]. The pLysS contains a copy of the T7 lysozyme gene oriented in a fashion that results in the expression of low levels the enzyme [320]. T7 lysozyme is a bifunctional inhibitor of T7 RNA polymerase [325] and it cuts a bond in the peptidoglycan layer of the *E. coli* cell wall [326]. The addition of this plasmid is useful in cases where one does not want any basal T7 RNA expression, which is common with BL21 derivative strains, such as when expressing proteins that are toxic to the bacterial host. In addition, it aids in lysis of the bacterial cell wall reducing the requirements for the addition of lysozyme or detergents during protein purification.

7.1.3 Generation Of Clones

Generation of recombinant proteins required the creation of expression vectors containing the DNA sequence of interest. Creation of the vectors for CPP-HO1-1, CPP-SDMHO1 and CPP-EGFP benefited from the publication of a primer used by others that contained the sequences for a PTD and EGFP, as well as wild-type and mutant primers for human HO-1 [160]. The primers used to direct amplification of CPP-sHO1 and CPP-HO1-2, however, were self-designed. The CPP-EGFP primer was engineered to include an EcoRI cut site between the CPP and EGFP sequences. This produces vector pCPP-EGFP, which can be used to generate a CPP-tagged version of any desired protein (not containing an internal EcoRI sequence) through simple excision of the EGFP sequence and subsequent insertion of a separate gene sequence such as that of HO-1. I used PCR to amplify the CPP-EGFP sequence, and then cloned it, in frame, into pET-28b(+). I subsequently excised the EGFP sequence, and ligated in PCR-amplified HO1, HO1-2, sHO1 and SDMHO1. pTAT-HO1 and pTAT-EGFP were created by cloning the respective gene sequences, in frame, into the pTAT2.1 vector already containing the TAT sequence (generously donated by Dr. Steven Dowdy).

No significant difficulties were encountered in creating these clones, and correct insertion of gene sequences was confirmed by restriction digest analysis (Figure 6), as well as DNA sequence analysis.

7.2 Protein Expression

After successfully generating the desired clones the next step was to determine the optimal conditions for expression of the CPP- and TAT-proteins in *E. coli.* Initial attempts demonstrated the production of proteins that were identified by SDS-PAGE to be consistent with the expected sizes (Figure 7). In addition the production of the CPP-proteins resulted in a colour change in the bacterial culture (green- CPP-HO1-1, CPP-HO1-2, CPP-sHO1, TAT-HO1; yellow – CPP-EGFP, TAT-EGFP; Fig 8, 9), that proved to be a very useful indicator for rapidly assessing the success of protein expression. The green colour change can be attributed to the production of biliverdin as a consequence of HO-1 activity [160, 308]. EGFP expression is known to result in a change in colour of bacterial culture and pellets to fluorescent green when viewed under a UV light [327]. The yellow colour change is presumed to be a secondary to the production of EGFP as this colour change was not seen in uninduced cultures or induced cultures that did not contain the CPP-EGFP or pTAT-EGFP clones. The knowledge that modified forms of GFP are known to result in a change of bacterial color to yellow-green in white light, supports this conclusion [328]. Initial efforts led to poor yields upon protein purification leading to an investigation of potential methods to increase protein expression.

E. coli is the most commonly used host for production of recombinant proteins and as such many strategies have been developed in attempts to optimize protein yield. These strategies range from modification of expression vector sequences and host organisms to differences in culture conditions. Often a certain set of conditions that may result in efficient production of one protein does not translate to other proteins. As previously mentioned the T7 RNA polymerase is highly efficient at transcribing DNA to mRNA for protein production. Once the T7lac promoter is induced most of the cellular machinery is

dedicated to production of the protein under its control, to the point that it can amount to up to 50% of the total cellular protein [316].

Although initial efforts at protein expression resulted in the expression of the proteins of interest, it was found that *E. coli* cells containing pCPP-HO1 and pTAT-HO1 stored as glycerol stocks appeared to rapidly lose their ability to express protein upon induction, leading to questions about the stability of these clones. A review of the literature did not yield any information regarding instability of recombinant HO-1-containing clones. I questioned whether HO-1 was toxic to *E. coli*; however, in the setting of a T7*lac* promoter and the pLysS plasmid, basal expression of HO-1 should be negligible. Therefore it is less likely that the cause of loss of expression is due to the accumulation of HO-1 to toxic amounts in the cultures used to make the glycerol stocks. This inhibition of 'leaky' gene expression is due to *lac* repressor inhibition of T7 RNA polymerase expression and T7 lysozyme degradation of any T7 RNA polymerase that is produced [320]. The T7 lysozyme gene on the LysS plasmid is under control of a chloramphenicol acetyl transferase (CAT) promoter, which is catabolite-sensitive. When cultures reach stationary phase, glucose is depleted and cAMP levels are elevated resulting in increased expression of T7 lysozyme [320], which can increase cell lysis and lower expression of the target gene under control of the T7lac promoter. The addition of glucose to the medium and use of cultures in the exponential phase of growth for the creation of glycerol stocks should help reduce T7 lysozyme expression. However, freezing down glycerol stocks with 0.5% glucose at culture OD_{600} of 0.6, did not prolong the period of time for which a culture grown from a particular glycerol stock supported protein expression (authors' observation). The only solution identified was obtained from personal communication with Dr. L Pastori (University of Miami), who had also worked with a TAT-HO1 protein. Dr. Pastori's group had encountered similar problems and had found that once a particular glycerol stock lost expression, it could be regained by using colonies from a freshly streaked selective agar plate. When this strategy was employed it worked without fail in my hands as well. It is my theory that the loss of expression is most likely secondary to cell death from recurrent freeze-thaw cycles caused by reuse of

glycerol stocks. I do not think that the cloned plasmid, itself, is lost during glycerol stock storage, or that mutations are accumulated within the CPP-HO1 DNA sequence, because streaking the glycerol stock onto a fresh plate produced single colonies that, when cultured and induced with IPTG, resulted in a change of bacterial colour to green, indicative of HO-1 activity.

The conditions that resulted in greatest expression of CPP- and TAT-HO1 and EGFP proteins, as assessed by SDS-PAGE analysis, were similar among HO-1 clones, but differed from the optimal conditions for EGFP clones. CPP-HO1 and TAT-HO1 proteins were expressed to the greatest extent in the richer culture medium of TB. This may be due to the ability of cultures to reach greater density than accomplished when grown in LB medium. Yield was also greater at the lower temperature of 30°C. This is a common feature of proteins that fold incorrectly or form inclusion bodies at 37°C. Reducing the induction temperature results in slowing of the cellular production machinery, changes in folding kinetics and reduced protein self-association, resulting in a greater percentage of correctly folded protein [315]. In addition, there is a decrease in the degradation of proteolytically-sensitive proteins, which HO-1 is known to be [318], at lower temperatures [316]. All of these factors, combined, may explain why growth in TB medium and induction at 30°C proved to be the optimal set of conditions for expression of CPP-HO1-1, CPP-HO1-2, TAT-HO1, CPP-SDMHO1 and CPP-sHO1 (Fig. 10-14).

IPTG was used to induce protein expression by the host bacteria. It is a non-hydrolyzable lactose analogue, that binds to the *lac* operator sequence, displacing the *lac* repressor from T7*lac* promoter, resulting in activation of transcription [320]. The observation of significant protein accumulation with IPTG concentrations as low as 10μM, highlights the sensitivity of the T7*lac* promoter. Increased accumulation of CPP-EGFP and TAT-EGFP was demonstrated when transformed cells were grown in LB medium at either 30 or 37°C compared to TB medium at 30 or 37°C. This suggests that the EGFP proteins may be less toxic to host bacteria, more easily expressed, or less prone to degradation.

The similarity in expression patterns of both proteins between 30 and 37°C, as indicated by comparable intensity of CPP-EGFP and TAT-EGFP protein bands (Fig. 15A, B; 16A, B) observed using coomassie blue-stained SDS-PAGE gels, suggests that the CPP- and TAT-EGFP proteins may have less stringent folding requirements or undergo less proteolytic degradation than the CPP- and TAT-HO1 proteins expressed here.

7.3 Protein Purification

Over the past few decades there have been many innovations that have substantially simplified the process of protein purification. Traditionally, successful purification required the knowledge of many physical and biochemical characteristics of the protein of interest [329, 330]. The development of affinity choromatography has allowed the purification of many recombinant proteins using fairly standardized procedures [331]. One of the most widely-used affinity purification systems is the 6xHIS/Ni-NTA system, which takes advantage of the high-affinity interactions between the amino acid, histidine, and nickel ions. In this system high-surface area beads of agarose or sepharose are coated with nitrilo-tri-acetic acid, which tightly binds Ni^{2+} ions, immobilizing them to the beads. These ions bind proteins with adjacent histidine residues, allowing for separation of these proteins from a crude sample and allowing purification of proteins from <1% to >95% homogeneity in one step [331]. Recombinant proteins can be designed to contain a small sequence of six consecutive histidine residues (6xHIS-tag) at either terminus, to take advantage of this system. This method of protein purification has many benefits, making it one of the most widely used tools for purification of recombinant proteins. The interaction between the nickel ions and the histidine residues is independent of tertiary structure allowing for purification under both native and denaturing conditions. Because the histidine residues in the 6xHis tag are uncharged at physiologic pH, poorly immunogenic, have little to no effect on secretion and compartmentalization, and rarely affect protein structure or function, it is rarely necessary to remove the tag following purification [331, 332]. All of these characteristics, and the fact that this system had been previously used to successfully purify recombinant human HO-1 protein [160, 308] made it an ideal choice for the purposes of this work.

Because the goal of this work was to obtain a functional CPP-HO1 protein, purification of the protein in its native configuration was most desirable, thus avoiding potentially troublesome protein refolding. However, early reports using TAT-derived PTD's suggested that cellular transduction is enhanced when the protein is in a misfolded state, after it has been denatured and then rapidly desalted or dialyzed [310]. These proteins elicit biological phenotypes, indicating functionality, presumably because they are refolded by chaperones once inside the cell [310]. In contrast, other authors have successfully transduced pancreatic cells using a TAT-HO1 protein purified under non-denaturing conditions [308]; therefore I felt it prudent to compare the success of protein purification and cellular penetration under both non-denaturing and denaturing conditions.

I was able to successfully purify CPP-HO1-1 and CPP-EGFP using denaturing and non-denaturing conditions (Fig. 18, 19). It appears that denaturing conditions are not as effective for purifying CPP-HO1-1 (Fig. 19) although, most likely, that difference seen between these two methods is due to differences in cellular lysis when processing the two samples. I performed more extensive cellular lysis than that employed in the data reported in this thesis (either with multiple passes through the French press or extended sonication time), and found that yields were much higher for full length CPP- and TAT-HO1 proteins compared to that achieved with the less aggressive cellular lysis required for purifying CPP- and TAT-EGFP (authors personal observation`). This was not the case for CPP-sHO1, which did not require extensive cellular lysis to obtain high protein yield. This suggests that CPP-HO1-1 and TAT-HO1 proteins containing the C-terminal membrane binding domain associate with the bacterial membrane following production. This observation is supported by the extended sonication time reported by Ma et al., 2009 in their methods section [160]. The results in Figure 19 suggest that, when purification is performed under denaturing conditions there is an increased yield of truncated forms of CPP-HO1-1, as indicated by the presence of protein bands of slightly smaller size than predicted in the elution and desalted fractions, and visualized by Western blotting using

anti-HO-1 antibodies (Fig. 19 A). Truncated forms may lack the entirety of C-terminal binding domain and form inclusion bodies, which are purified better under denaturing conditions, or the harsher conditions may result in breakdown of HO-1, which is known to be sensitive to degradation [318]. Although denaturing conditions appeared to increase the yield of CPP-EGFP (Fig. 18 A, B), I was still able to obtain sufficient protein for cell penetration experiments using non-denaturing conditions.

The other major consideration for the purification process was whether to purify the proteins using a batch or gravity method. Batch purification involves incubation of the bacterial lysate with the Ni-NTA agarose beads prior to loading on an empty column. In gravity purification the lysate is added to a pre-equilibrated column containing packed Ni-NTA beads. The benefits of batch purification include enhanced binding of the protein when the 6xHIS tag may be poorly accessible or when the protein is present in the lysate at a low concentration [332]. I attempted a batch purification protocol because of the lack of a formal chromatography setup for protein purification and a desire to enhance protein yield. Although there was a mild increase total protein yield with the batch purification over the gravity method, the end product was less pure as indicated by the presence of multiple proteins of various sizes when analyzed using SDS-PAGE (Fig 17A vs. Fig. 19B).

Following elution of the CPP- and TAT-tagged proteins they were loaded onto a PD-10 column to remove potential contaminating molecules such as salts and imidazole, and urea when purified using denaturing conditions. PD-10 columns contain a sephadex G-25 matrix that allows for desalting based on size exclusion [333]. Molecules <5kDa are able to penetrate into the pores of the matrix, allowing a larger volume of distribution of these molecules. Proteins and molecules larger than 5kDa cannot enter the matrix and are thus the first to elute from the column [333]. Because urea, imidazole and the other salts used in the purification process are <5kDa in size they penetrate the column allowing the protein of interest to be eluted first in a relatively pure elution buffer. Because

purification using denaturing conditions results in protein unfolding removing secondary and tertiary protein structure, it is possible that there may be differences in how proteins purified under denaturing and non-denaturing conditions elute from the PD-10 column. In addition I wanted to determine when the CPP-proteins eluted from the column in order to maximize protein concentration by using the minimum amount of elution volume to obtain maximal yield of protein. To do this I collected the eluate from the PD-10 column in 2mL fractions and analyzed them using SDS-PAGE. It was found that the purification conditions did not affect how the proteins eluted from the PD-10 column, with the exception of denatured CPP-EGFP and TAT-EGFP which showed consistent protein elution in all four fractions (Fig. 20 G). The reason for this is unclear, and I believe that it is an artefact, that could be due to inadvertent mixing of samples, and would not be reproduced if the experiment were to be repeated. One other possible explanation would be that the yield was so high that it took a larger volume of HTK to completely elute all of the protein, however, if this were the case I would expect that the proteins bands observed in the first two fractions would be significantly more prominent than those in the latter two, such as was the case with CPP-sHO1 (Fig. 20E). For most proteins the majority of protein was eluted in the first 2 fractions (Fig. 20, 21). For proteins that demonstrated greater purification yield as indicated by strength of the protein band and the final protein concentration (CPP-sHO1, CPP-EGFP and TAT-EGFP (Fig. 20 E-G), significant amounts were also found in fractions 3 and 4. It is possible that the total amount of protein from these high yield runs may have overwhelmed the capacity for the desalting capacity of the PD-10, or it may be that these fractions also contain desalted protein. This could be tested by subjecting the samples to analysis for the presence of the unwanted salts. One potential method for this would be the use of mass spectroscopy. A similar pattern was observed for proteins purified under non-denaturing conditions, wherein, there was still protein observed in lanes 3 and 4 for CPP-HO1-1 and CPP-HO1-2 (Fig. 21 A, C). Interestingly, the dominant protein band in lane 3 for TAT-HO1 (Fig. 21 C) is a smaller band of ~32kDa. It is possible that this represents a truncated protein or a non-membrane bound form of the protein. Ribeiro et al., 2003 [308], described a membrane-bound form of TAT-HO1 that was 2kDa in size greater than the non-

membrane bound form on SDS-PAGE, and this may be the predominant form observed to elute in fractions 1 and 2 for TAT-HO1.

Although the findings of these experiments suggest that the generated versions of CPP-HO1, TAT-HO1, CPP-EGFP and TAT-EGFP can be purified using either denaturing or non-denaturing conditions, I feel that the potential benefits of obtaining higher purity samples of these proteins in their native/functional configurations are desirable, and favour purification using a gravity protocol under non-denaturing conditions.

7.4 Protein Function

To ensure that I had purified enzymatically active CPP-HO1, a bilirubin production assay was performed. Spectrophotometric quantification of bilirubin production is a commonly used method for the determination of HO1 activity [155, 160, 313, 318, 334-340]. In this assay purified heme oxygenase is added to a reaction mixture containing heme, NADPH and the necessary cofactors. Heme oxygeanse activity results in the production of biliverdin which, through the actions of biliverdin reductase, is converted to bilirubin. Because it has a peak absorbance in the range of 460-470nm [155], and a known extinction coefficient between 530nm and 470nm, bilirubin produced as a result of HO-1 activity can be quantified using a spectrophotometer [155, 334]. Non-denatured CPP-HO1-1 effectively catalyzed the conversion of heme to bilirubin (Fig. 22) indicating that when purified under non-denaturing conditions CPP-HO1 proteins maintained their enzymatic activity. In this work I did not assay CPP-HO1-1 purified under denaturing conditions because of a limited supply of biliverdin reductase, as well as the findings of Ma et al., 2009 [334], who demonstrated significant bilirubin production from homogenates of HEK293T cells treated with PTD-HO1 (analogous to CPP-HO1-1) purified under denaturing conditions, but not with PTD-EGFP or HTK treated cells. Their data suggests that CPP-HO1 purified under denaturing conditions undergoes refolding following cellular transduction to an enzymatically-active configuration. An ideal future test to confirm that CPP-HO1-1 treatment results in increased HO-1 activity

would be to repeat the bilirubin production assay using homogenized tissue from a transduced liver and an untransduced liver, comparing bilirubin production to determine if there is any quantitative difference in enzymatic activity following organ treatment.

7.5 Cellular Penetration

Following successful purification of CPP- and TAT- linked EGFP and HO-1 proteins, I wanted to determine if protein configuration affected cell-penetrating ability. To do this I examined the ability of the CPP-EGFP and CPP-HO1-1 proteins to penetrate HepG2 and HUVEC cells using fluorescence microscopy. CPP-EGFP and CPP-HO1 purified under non-denaturing conditions were found to transduce cells *in vitro* more effectively than when purified using denaturing conditions (Figures 23, 24). This finding was unexpected, as many groups have suggested that PTD-mediated cellular transduction is enhanced when proteins are denatured [310, 341-343]. However, one group has also demonstrated efficient cellular penetration using natively purified TAT-HO1 [308] (and personal communication by Dr. L. Pastori, University of Miami). It is possible that the inability of denatured CPP-EGFP or CPP-HO1 to penetrate HepG2 and HUVEC cells that I observed (Fig. 23, 24) is due to residual contaminants, such as urea, that were not fully removed during the desalting process, rather than an inhibition of CPP-function by purification under denaturing conditions. This is supported by the findings of Ma et al., 2009, who demonstrated efficient cellular penetration by CPP-EGFP and CPP-HO1 proteins purified using denaturing conditions [160].

The ability of the CPP- and TAT- peptide sequences to mediate cellular penetration of linked EGFP and HO-1 proteins was investigated using murine macrophages, human hepatoma cells (hepG2), and endothelial cells (HUVEC). These cell types are representative of three of the major cell types involved in hepatic IRI: macrophages/Kupffer cells, hepatocytes and sinusoidal endothelial cells [106, 113, 118]. Macrophages play a major role in IR injury, and there is evidence that HO-1-mediated IR protection is, in part, due to alterations in Kupffer cell function [206, 344, 345].

Hepatocytes are the most abundant cell type within the liver, making up 60% of the cellular mass, and are responsible for the vast majority of its biosynthetic and detoxifying functions [346]. The alteration in hepatic synthetic function and elevation of transaminases following liver IRI is secondary to hepatocyte injury and necrosis. Sinusoidal endothelial cells are the most sensitive cell type to cold IRI, and injury to these cells results in microcirculatory disturbances potentiating further organ injury [101-104]. The ability to increase HO-1 activity within these cells, with the subsequent benefits provided by BV and CO (neutralization of ROS, inhibition of apoptosis, microcirculatory relaxation), would be beneficial in reducing the degree of injury suffered by SEC`s due to IRI. Therefore I felt that it would be beneficial to know if these cell types could be transduced with CPP- and TAT-HO1.

Both the CPP and TAT peptides appear to mediate cellular penetration of J774, HepG2 cells. The CPP peptide was also shown to mediate the cellular penetration of HUVEC cells. The ability of the TAT peptide to mediate transduction of HUVEC's was not tested due to time and reagent restraints, however I believe that the TAT sequence will be able to mediate transduction of HUVEC's for two reasons: 1) TAT-peptides have been used to successfully transduce HUVEC cells in other studies [347, 348] and 2) the CPP peptide sequence is derived from the TAT sequence. Although CPP-EGFP did not appear to associate with J774 cells (Fig. 24A), it is unlikely that this is due to an inability of the CPP-peptide to mediate cellular transduction of J774 cells, as J774 cells treated with CPP-HO1-1 demonstrated strong fluorescence indicating cellular transduction by the CPP-HO1-1 protein (Fig. 28A). It is most likely that the poor cellular transduction of J774 cells by CPP-EGFP is due a low concentration of protein used to treat the cells, as different protein preparations with different concentrations were used in treating the different cell types. This effect is also seen in the case of TAT-EGFP treatment of HUVEC cells (Fig. 27B). It has been suggested that the ability of PTD's to mediate efficient cellular penetration requires the peptide to be delivered to the cell at high concentrations [268], and this assertion is supported by the results of the *in vitro* cellular penetration assays. CPP-HO1-2 and CPP-SDMHO1 treatment did not result in cellular

fluorescence, suggesting that these proteins do not transduce treated cells. However, the concentrations of these purified protein samples were much lower than those of any of the other samples (because they did not undergo extended sonication or repeated French press lysis), even though the total protein amounts were the same. Because of the large difference in protein yields (with CPP-HO1-2 and CPP-SDMHO1 being particularly low), large volumes of purified protein samples had to be added to the cells to obtain the desired treatment amount. This would have resulted in much smaller concentrations of pericellular protein (for these two proteins), with minimal membrane binding and internalization. Endosomal escape is known to be a limiting factor in the ability of cell penetrating peptides to mediate cellular transduction of proteins [349], and inefficiencies in endosomal escape may require higher treatment concentration to observe cellular penetration. In addition, it has been shown that at higher concentrations internalization also occurs via an endosomal independent process [278]. Therefore it is more likely that the inability of these proteins to penetrate J774, HepG2 and HUVEC cells is due to inadequate pericellular protein concentration. The other conclusion drawn is that full length HO-1 strongly associates with cellular membranes of *E. coli*, making it somewhat challenging to purify. CPP-sHO1, which did not contain the C-terminal membrane binding domain was more easily purified as it did not require intensive cellular lysis using extended sonication or repeated French press lysis that appears to be required for HO-1 proteins containing the C-terminal membrane binding domain. However, although this protein is more easily purified, the lack of the C-terminal membrane binding domain may affect its ability to localize properly within the transduced cell or may potentially affect its half-life. Therefore, although CPP-sHO1 warrants further investigation for its ability to confer IRI-resistance to steatotic livers I think that this should be done alongside the full length protein, CPP-HO1-1, and not in substitution for it.

Although early studies of PTD function used *in vitro* immunofluorescence, many investigators have now turned to other methods because of reports of artifactual cellular penetration secondary to protein sticking to the cell membrane [350] or nuclear relocation following fixation with methanol [314, 350]. Although these investigators suggested that

PTD peptides did not mediate cellular transduction, multiple studies since have confirmed their cellular penetrating capability [278, 287, 351, 352]. Since Leifert et al. suggested that PTDs stick to, but do not transduce, cellular membranes it has been discovered that PTDs bind cell surface heparin sulfate proteoglycans [353, 354] prior to endosomal internalization [287, 355-357], and that this binding is highly influential in the ability of these proteins to transduce cells [357]. In contrast to treating cells with purified protein, Leifert et al. transfected HeLa cells with plasmids containing the sequence for PTD-EGFP or EGFP alone and then compared cellular fluorescence conferred by internalized EGFP in live and fixed cells. They found enhanced cellular binding of the PTD-EGFP in the cells fixed with methanol but not the live cells. These findings could easily be explained by an inability of HeLa cells to export PTD-EGFP (a function which was not tested), which would result in similar observed EGFP fluorescence between the live cells transfected with pPTD-EFGP or pEGFP. Methanol treatment is known to cause cellular perrmeabilization [358], and this would result in a release of accumulated PTD-EGFP, which could then bind to the membranes of non-transfected cells prior to completion of the fixation process, accounting for the increase in cellular fluorescence seen following fixation. It is likely that live cells were never subjected to extracellular PTD-EGFP, as it would have been produced in the cell but not released until the methanol permeabilization treatment and, therefore, it is not surprising that they did not observe cellular transduction.

The other major arguement against the cell-penetrating ability of PTD`s was presented by Lundberg et al., who found nuclear relocation of the PTD herpes simplex virus VP22 following methanol fixation. However, there are fundamental differences between their methods and results and my own that lead me to conclude that my results indicate cellular transduction rather than fixation artifact. First, Lundberg et al., fixed cells using methanol which, as previously mentioned, also causes cellular permeabilization [358]. If permeabilization occurs before fixation, then unfixed VP22 could easily have relocated from the outside the cell to the nucleus. In contrast, I fixed my samples with paraformaldehyde (which does not permeabilize cells) prior to methanol

permeabilization. Second, the pattern seen in my immunofluorescence experiments is consistent with endosomal accumulation rather than nuclear localization. Wadia et al. 2004, demonstrated co-localization of a TAT-fusion protein with the endosomal marker FM4-64 (Fig. 32) [352], showing a fluorescence pattern that is strikingly similar to that seen in the cellular penetration assays in this study (especially the J774 and HUVEC cells) (Fig. 28-30). In addition, other studies have subsequently supported macropinocytosis and endosomal internalization as the primary method responsible for CPP-mediated cellular transduction [278, 287, 351].

To ensure that my findings from the immunofluorescence assays were not due to fixation artifact, I treated live HepG2 cells with CPP-EGFP and analyzed them under the fluorescence microscope without fixation. Cells treated with CPP-EGFP purified under denaturing or non-denaturing conditions demonstrated fluorescence that was not seen in control cells (Fig. 25). This finding of cellular penetration without fixation adds strength to my conclusion that the CPP-sequence is able to mediate cellular penetration of J774, HepG2 and HUVEC cells by CPP-EGFP and CPP-HO1 proteins. Further support also comes from subsequent work on this project, wherein rat livers were perfused via the portal vein with CPP-EGFP for 1 hour on ice. Treated cells demonstrate strong fluorescence that is not seen in livers perfused with HTK alone (Fig. 33). Fluorescence is observed to the greatest extent in the endothelial cells, but is also observed throughout the hepatic parenchyma indicating that the CPP-sequence is able to mediate cellular penetration of hepatocytes and endothelial cells in an intact organ as well as in cultured cells *in vitro*. The results of all of the cellular transduction experiments provide convincing evidence that the CPP-sequence effectively mediates cellular association and transduction of the CPP-HO1 and CPP-EGFP fusion proteins, and shows potential for use in the treatment of steatotic livers *ex vivo* prior to transplantation.

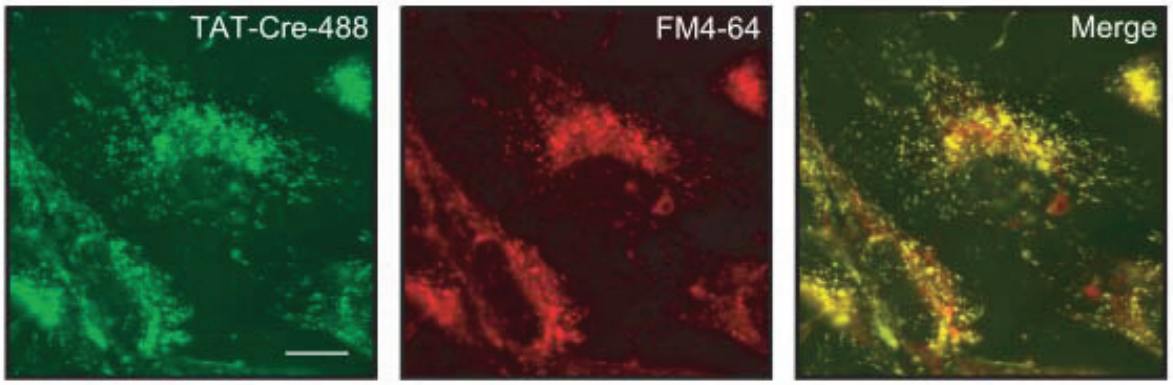

Figure 32. Endosomal entrapment and internalization of TAT-Cre-488. Fluorescently labelled TAT-Cre associates shows a similar pattern of staining as the endosomal marker FM4-64, as demonstrated by the overlapping images, staining yellow in the panel marked merge. This suggests that TAT-fusion peptides are internalized through lipid raft macropinocytosis. (Used with permission from Wadia et al, 2004 [352])

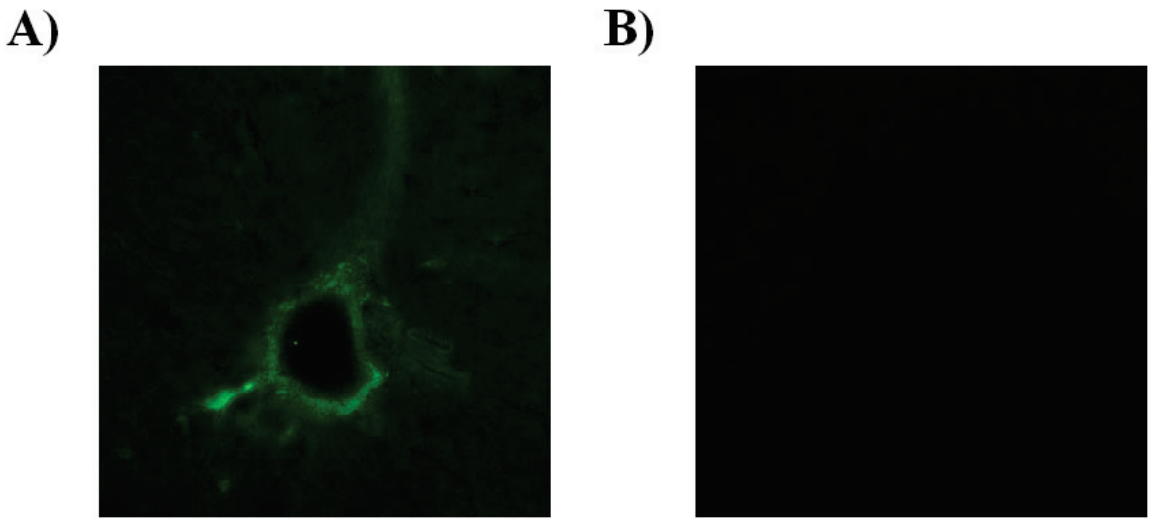

Figure 33. CPP-EGFP transduces rat livers *ex vivo.* Rat livers were removed then perfused via the portal vein with 200 micrograms CPP-EGFP in 3mL of HTK for 1 hr on ice. Livers were then sectioned and analysed by fluorescence microscopy. **A)** CPP-EGFP and **B)** HTK only perfusion. Used with permission from David Woodhall - unpublished results.

Chapter 8: Conclusions

The experiments presented in this work describe the production and purification of multiple cell-penetrating forms of CPP- and TAT- linked HO1 and EGFP. Clones were generated that encode separate membrane-binding and soluble forms of human HO-1 protein liked to a high efficiency CPP sequence. In addition, a site-directed mutant form, which appears to lack enzymatic function, has been created that should prove useful as a negative control for future experiments evaluating the ability of CPP-HO1 treatment to improve the resistance of steatotic livers to IRI. I was able to determine the optimal conditions for protein expression and subsequently purify the protein using both denaturing and non-denaturing conditions. It is likely that expressed CPP-HO1 associates strongly with the bacterial cell membrane and therefore requires aggressive cellular lysis protocols; these are not required for CPP-EGFP and CPP-sHO1 which are easily purified following simple cell lysis. In contrast to early literature suggesting that PTD's can only mediate the cellular penetration of full length proteins in the denatured state, my findings suggest that purified native CPP-EGFP and CPP-HO1 can effectively transduce cells, and that the use of denaturing agents such as urea during protein purification can be avoided. This simplifies the purification process and makes desalting simpler. Using two different assays it was shown that the CPP-sequence is able to mediate the cellular transduction of multiple cell types by HO1 and EGFP; however, it appears that this ability is concentration-dependent. Importantly, subsequent work shows that the CPP-peptide is able to mediate cellular transduction of *ex vivo* perfused livers, which is essential to its ability to be used as a therapeutic agent. Although much work has yet to be done in order to determine if CPP-HO1 can improve the resistance of steatotic livers to IRI, facilitating the transplantation of previously unuseable organs, the results of these experiments show promise that the CPP-sequence is able to confer cell-penetrating ability upon HO-1. This provides credence to the hypothesis that a cell-penetrating HO1 protein may have therapeutic potential in the field of liver transplantation.

Literature Cited

1. Starzl, T.E., et al., *Homotransplantation of the Liver in Humans.* Surg Gynecol Obstet, 1963. **117**: p. 659-76.
2. Starzl, T.E., et al., *Clinical and pathologic observations after orthotopic transplantation of the human liver.* Surg Gynecol Obstet, 1969. **128**(2): p. 327-39.
3. Jenkins, R.L., *The Boston Center for Liver Transplantation (BCLT). Initial experience of a new surgical consortium.* Arch Surg, 1986. **121**(4): p. 424-30.
4. Perera, M.T., D.F. Mirza, and E. Elias, *Liver transplantation: Issues for the next 20 years.* J Gastroenterol Hepatol, 2009. **24 Suppl 3**: p. S124-31.
5. Walia, A. and R. Schumann, *The evolution of liver transplantation practices.* Curr Opin Organ Transplant, 2008. **13**(3): p. 275-9.
6. *Canadian Organ Replacement Register Annual Report*. 2011, Canadian Institute for Health Information.
7. *2004 Annual Report of the U.S. Organ Procurement and Transplantation Network and the Scientific Registry of Transplant Recipients: Transplant Data 1994-2003*. 2004, United States Department of Health and Human Services, Health Resources and Services
8. Ahmed, A. and E.B. Keeffe, *Current indications and contraindications for liver transplantation.* Clin Liver Dis, 2007. **11**(2): p. 227-47.
9. Adam, R. and E. Hoti, *Liver transplantation: the current situation.* Semin Liver Dis, 2009. **29**(1): p. 3-18.
10. Foster, R., M. Zimmerman, and J.F. Trotter, *Expanding donor options: marginal, living, and split donors.* Clin Liver Dis, 2007. **11**(2): p. 417-29.
11. Cameron, A. and R.W. Busuttil, *AASLD/ILTS transplant course: is there an extended donor suitable for everyone?* Liver Transpl, 2005(11 Suppl 2): p. S2-5.
12. Renz, J.F., et al., *Utilization of extended donor criteria liver allografts maximizes donor use and patient access to liver transplantation.* Ann Surg, 2005. **242**(4): p. 556-63; discussion 563-5.
13. Burroughs, A.K., et al., *3-month and 12-month mortality after first liver transplant in adults in Europe: predictive models for outcome.* Lancet, 2006. **367**(9506): p. 225-32.
14. Clavien, P.A., *How far can we go with marginal donors?* J Hepatol, 2006. **45**(4): p. 483-4.
15. Ioannou, G.N., *Development and validation of a model predicting graft survival after liver transplantation.* Liver Transpl, 2006. **12**(11): p. 1594-606.
16. Abt, P.L., et al., *Survival following liver transplantation from non-heart-beating donors.* Ann Surg, 2004. **239**(1): p. 87-92.
17. Feng, S., et al., *Characteristics associated with liver graft failure: the concept of a donor risk index.* Am J Transplant, 2006. **6**(4): p. 783-90.
18. Foley, D.P., et al., *Donation after cardiac death: the University of Wisconsin experience with liver transplantation.* Ann Surg, 2005. **242**(5): p. 724-31.
19. Manzarbeitia, C.Y., et al., *Long-term outcome of controlled, non-heart-beating donor liver transplantation.* Transplantation, 2004. **78**(2): p. 211-5.
20. Briceno, J., et al., *Influence of marginal donors on liver preservation injury.* Transplantation, 2002. **74**(4): p. 522-6.
21. Piratvisuth, T., et al., *Contribution of true cold and rewarming ischemia times to factors determining outcome after orthotopic liver transplantation.* Liver Transpl Surg, 1995. **1**(5): p. 296-301.

22. Ploeg, R.J., et al., *Impact of donor factors and preservation on function and survival after liver transplantation.* Transplant Proc, 1993. **25**(6): p. 3031-3.
23. Busuttil, R.W. and K. Tanaka, *The utility of marginal donors in liver transplantation.* Liver Transpl, 2003. **9**(7): p. 651-63.
24. Gruttadauria, S., et al., *Acceptance of marginal liver donors increases the volume of liver transplant: early results of a single-center experience.* Transplant Proc, 2005. **37**(6): p. 2567-8.
25. Tisone, G., et al., *Marginal donors in liver transplantation.* Transplant Proc, 2004. **36**(3): p. 525-6.
26. Adam, R., et al., *Liver transplantation from elderly donors.* Transplant Proc, 1993. **25**(1 Pt 2): p. 1556-7.
27. Alexander, J.W. and W.K. Vaughn, *The use of "marginal" donors for organ transplantation. The influence of donor age on outcome.* Transplantation, 1991. **51**(1): p. 135-41.
28. Busquets, J., et al., *The impact of donor age on liver transplantation: influence of donor age on early liver function and on subsequent patient and graft survival.* Transplantation, 2001. **71**(12): p. 1765-71.
29. De Carlis, L., et al., *Marginal donors in liver transplantation: the role of donor age.* Transplant Proc, 1999. **31**(1-2): p. 397-400.
30. Detre, K.M., et al., *Influence of donor age on graft survival after liver transplantation--United Network for Organ Sharing Registry.* Liver Transpl Surg, 1995. **1**(5): p. 311-9.
31. Marino, I.R., et al., *Effect of donor age and sex on the outcome of liver transplantation.* Hepatology, 1995. **22**(6): p. 1754-62.
32. Strasberg, S.M., et al., *Selecting the donor liver: risk factors for poor function after orthotopic liver transplantation.* Hepatology, 1994. **20**(4 Pt 1): p. 829-38.
33. Adam, R., et al., *The outcome of steatotic grafts in liver transplantation.* Transplant Proc, 1991. **23**(1 Pt 2): p. 1538-40.
34. Briceno, J., et al., *Assignment of steatotic livers by the Mayo model for end-stage liver disease.* Transpl Int, 2005. **18**(5): p. 577-83.
35. Selzner, M. and P.A. Clavien, *Fatty liver in liver transplantation and surgery.* Semin Liver Dis, 2001. **21**(1): p. 105-13.
36. Todo, S., et al., *Primary nonfunction of hepatic allografts with preexisting fatty infiltration.* Transplantation, 1989. **47**(5): p. 903-5.
37. Totsuka, E., et al., *Analysis of clinical variables of donors and recipients with respect to short-term graft outcome in human liver transplantation.* Transplant Proc, 2004. **36**(8): p. 2215-8.
38. Verran, D., et al., *Clinical experience gained from the use of 120 steatotic donor livers for orthotopic liver transplantation.* Liver Transpl, 2003. **9**(5): p. 500-5.
39. Angelico, M., *Donor liver steatosis and graft selection for liver transplantation: a short review.* Eur Rev Med Pharmacol Sci, 2005. **9**(5): p. 295-7.
40. Vetelainen, R., et al., *Steatosis as a risk factor in liver surgery.* Ann Surg, 2007. **245**(1): p. 20-30.
41. El-Zayadi, A.R., *Hepatic steatosis: a benign disease or a silent killer.* World J Gastroenterol, 2008. **14**(26): p. 4120-6.
42. Schreuder, T.C., et al., *Nonalcoholic fatty liver disease: an overview of current insights in pathogenesis, diagnosis and treatment.* World J Gastroenterol, 2008. **14**(16): p. 2474-86.
43. Yerian, L., *Histopathological evaluation of fatty and alcoholic liver diseases.* J Dig Dis, 2011. **12**(1): p. 17-24.

44. Browning, J.D. and J.D. Horton, *Molecular mediators of hepatic steatosis and liver injury.* J Clin Invest, 2004. **114**(2): p. 147-52.
45. McCullough, A.J., *Pathophysiology of nonalcoholic steatohepatitis.* J Clin Gastroenterol, 2006. **40 Suppl 1**: p. S17-29.
46. Alkofer, B., et al., *Extended-donor criteria liver allografts.* Semin Liver Dis, 2006. **26**(3): p. 221-33.
47. Cieslak, B., et al., *Microvesicular liver graft steatosis as a risk factor of initial poor function in relation to suboptimal donor parameters.* Transplant Proc, 2009. **41**(8): p. 2985-8.
48. Yoong, K.F., et al., *Impact of donor liver microvesicular steatosis on the outcome of liver retransplantation.* Transplant Proc, 1999. **31**(1-2): p. 550-1.
49. Briceno, J., G. Solorzano, and C. Pera, *A proposal for scoring marginal liver grafts.* Transpl Int, 2000. **13 Suppl 1**: p. S249-52.
50. Fishbein, T.M., et al., *Use of livers with microvesicular fat safely expands the donor pool.* Transplantation, 1997. **64**(2): p. 248-51.
51. Rossi, M., et al., *Liver transplantation: expanding the donor pool.* Transplant Proc, 2001. **33**(1-2): p. 1307-9.
52. Urena, M.A., et al., *Assessing risk of the use of livers with macro and microsteatosis in a liver transplant program.* Transplant Proc, 1998. **30**(7): p. 3288-91.
53. Bugianesi, E., A.J. McCullough, and G. Marchesini, *Insulin resistance: a metabolic pathway to chronic liver disease.* Hepatology, 2005. **42**(5): p. 987-1000.
54. Camma, C., et al., *Insulin resistance is associated with steatosis in nondiabetic patients with genotype 1 chronic hepatitis C.* Hepatology, 2006. **43**(1): p. 64-71.
55. Choudhury, J. and A.J. Sanyal, *Insulin resistance and the pathogenesis of nonalcoholic fatty liver disease.* Clin Liver Dis, 2004. **8**(3): p. 575-94, ix.
56. Choudhury, J. and A.J. Sanyal, *Insulin resistance in NASH.* Front Biosci, 2005. **10**: p. 1520-33.
57. Diehl, A.M., J. Clarke, and F. Brancati, *Insulin resistance syndrome and nonalcoholic fatty liver disease.* Endocr Pract, 2003. **9 Suppl 2**: p. 93-6.
58. Eguchi, Y., et al., *Visceral fat accumulation and insulin resistance are important factors in nonalcoholic fatty liver disease.* J Gastroenterol, 2006. **41**(5): p. 462-9.
59. Tilg, H. and G.S. Hotamisligil, *Nonalcoholic fatty liver disease: Cytokine-adipokine interplay and regulation of insulin resistance.* Gastroenterology, 2006. **131**(3): p. 934-45.
60. Utzschneider, K.M. and S.E. Kahn, *Review: The role of insulin resistance in nonalcoholic fatty liver disease.* J Clin Endocrinol Metab, 2006. **91**(12): p. 4753-61.
61. Graham, T.E., et al., *Retinol-binding protein 4 and insulin resistance in lean, obese, and diabetic subjects.* N Engl J Med, 2006. **354**(24): p. 2552-63.
62. Kojima, M., et al., *Ghrelin is a growth-hormone-releasing acylated peptide from stomach.* Nature, 1999. **402**(6762): p. 656-60.
63. Maeda, K., et al., *cDNA cloning and expression of a novel adipose specific collagen-like factor, apM1 (AdiPose Most abundant Gene transcript 1).* Biochem Biophys Res Commun, 1996. **221**(2): p. 286-9.
64. Steppan, C.M., et al., *The hormone resistin links obesity to diabetes.* Nature, 2001. **409**(6818): p. 307-12.
65. Yang, Q., et al., *Serum retinol binding protein 4 contributes to insulin resistance in obesity and type 2 diabetes.* Nature, 2005. **436**(7049): p. 356-62.
66. Zhang, Y., et al., *Positional cloning of the mouse obese gene and its human homologue.* Nature, 1994. **372**(6505): p. 425-32.

67. Shimomura, I., et al., *Decreased IRS-2 and increased SREBP-1c lead to mixed insulin resistance and sensitivity in livers of lipodystrophic and ob/ob mice.* Mol Cell, 2000. **6**(1): p. 77-86.
68. Kantartzis, K., et al., *Environmental and genetic determinants of fatty liver in humans.* Dig Dis, 2010. **28**(1): p. 169-78.
69. Bedogni, G. and S. Bellentani, *Fatty liver: how frequent is it and why?* Ann Hepatol, 2004. **3**(2): p. 63-5.
70. Ground, K.E., *Liver pathology in aircrew.* Aviat Space Environ Med, 1982. **53**(1): p. 14-8.
71. Hilden, M., et al., *Liver histology in a 'normal' population--examinations of 503 consecutive fatal traffic casualties.* Scand J Gastroenterol, 1977. **12**(5): p. 593-7.
72. Underwood Ground, K.E., *Prevalence of fatty liver in healthy male adults accidentally killed.* Aviat Space Environ Med, 1984. **55**(1): p. 59-61.
73. McCormack, L., et al., *Liver transplantation using fatty livers: always feasible?* J Hepatol, 2011. **54**(5): p. 1055-62.
74. Bellentani, S., et al., *Prevalence of and risk factors for hepatic steatosis in Northern Italy.* Ann Intern Med, 2000. **132**(2): p. 112-7.
75. D'Alessandro, A.M., et al., *The predictive value of donor liver biopsies on the development of primary nonfunction after orthotopic liver transplantation.* Transplant Proc, 1991. **23**(1 Pt 2): p. 1536-7.
76. Garcia Urena, M.A., et al., *Hepatic steatosis in liver transplant donors: common feature of donor population?* World J Surg, 1998. **22**(8): p. 837-44.
77. Kakizoe, S., et al., *Evaluation of protocol before transplantation and after reperfusion biopsies from human orthotopic liver allografts: considerations of preservation and early immunological injury.* Hepatology, 1990. **11**(6): p. 932-41.
78. Karayalcin, K., et al., *The role of dynamic and morphological studies in the assessment of potential liver donors.* Transplantation, 1994. **57**(9): p. 1323-7.
79. Markin, R.S., et al., *Frozen section evaluation of donor livers before transplantation.* Transplantation, 1993. **56**(6): p. 1403-9.
80. Monsour, H.P., Jr., et al., *Utility of preoperative liver biopsy in live-related donor patients for liver transplantation.* Transplant Proc, 1994. **26**(1): p. 138-9.
81. Ploeg, R.J., et al., *Risk factors for primary dysfunction after liver transplantation--a multivariate analysis.* Transplantation, 1993. **55**(4): p. 807-13.
82. Portman B, W.D., *Pathology of Liver Transplantation*. Liver Transplantation, ed. C. R. 1987, Orlando, FL: Grune and Stratton. 437.
83. Kaibori, M., et al., *Liver regeneration in donors evaluated by Tc-99m-GSA scintigraphy after living donor liver transplantation.* Dig Dis Sci, 2008. **53**(3): p. 850-5.
84. Seifalian, A.M., et al., *The effect of graded steatosis on flow in the hepatic parenchymal microcirculation.* Transplantation, 1999. **68**(6): p. 780-4.
85. Theruvath, T.P., et al., *Minocycline and N-methyl-4-isoleucine cyclosporin (NIM811) mitigate storage/reperfusion injury after rat liver transplantation through suppression of the mitochondrial permeability transition.* Hepatology, 2008. **47**(1): p. 236-46.
86. Baccarani, U., et al., *Steatosis of the hepatic graft as a risk factor for post-transplant biliary complications.* Clin Transplant, 2010. **24**(5): p. 631-5.
87. McCormack, L. and P.A. Clavien, *Understanding the meaning of fat in the liver.* Liver Transpl, 2005. **11**(2): p. 137-9.
88. Nocito, A., A.M. El-Badry, and P.A. Clavien, *When is steatosis too much for transplantation?* J Hepatol, 2006. **45**(4): p. 494-9.

89. Afonso, R.C., et al., *Impact of steatotic grafts on initial function and prognosis after liver transplantation.* Transplant Proc, 2004. **36**(4): p. 909-11.
90. Angele, M.K., et al., *Effect of graft steatosis on liver function and organ survival after liver transplantation.* Am J Surg, 2008. **195**(2): p. 214-20.
91. Doyle, M.B., et al., *Short- and long-term outcomes after steatotic liver transplantation.* Arch Surg, 2010. **145**(7): p. 653-60.
92. McCormack, L., et al., *Use of severely steatotic grafts in liver transplantation: a matched case-control study.* Ann Surg, 2007. **246**(6): p. 940-6; discussion 946-8.
93. Perez-Daga, J.A., et al., *Influence of degree of hepatic steatosis on graft function and postoperative complications of liver transplantation.* Transplant Proc, 2006. **38**(8): p. 2468-70.
94. Urena, M.A., et al., *An approach to the rational use of steatotic donor livers in liver transplantation.* Hepatogastroenterology, 1999. **46**(26): p. 1164-73.
95. Spitzer, A.L., et al., *The biopsied donor liver: incorporating macrosteatosis into high-risk donor assessment.* Liver Transpl, 2010. **16**(7): p. 874-84.
96. Noujaim, H.M., et al., *Expanding postmortem donor pool using steatotic liver grafts: a new look.* Transplantation, 2009. **87**(6): p. 919-25.
97. Deroose, J.P., et al., *Hepatic steatosis is not always a contraindication for cadaveric liver transplantation.* HPB (Oxford), 2011. **13**(6): p. 417-25.
98. Soejima, Y., et al., *Use of steatotic graft in living-donor liver transplantation.* Transplantation, 2003. **76**(2): p. 344-8.
99. Montalti, R., et al., *Donor pool expansion in liver transplantation.* Transplant Proc, 2004. **36**(3): p. 520-2.
100. Canelo, R., et al., *Is a fatty liver dangerous for transplantation?* Transplant Proc, 1999. **31**(1-2): p. 414-5.
101. Chen, H., et al., *Multi-factor analysis of initial poor graft function after orthotopic liver transplantation.* Hepatobiliary Pancreat Dis Int, 2007. **6**(2): p. 141-6.
102. Selzner, M., et al., *Mechanisms of ischemic injury are different in the steatotic and normal rat liver.* Hepatology, 2000. **32**(6): p. 1280-8.
103. Selzner, N., et al., *Mouse livers with macrosteatosis are more susceptible to normothermic ischemic injury than those with microsteatosis.* J Hepatol, 2006. **44**(4): p. 694-701.
104. Tevar, A.D., et al., *The effect of hepatic ischemia reperfusion injury in a murine model of nonalcoholic steatohepatitis.* J Surg Res, 2011. **169**(1): p. e7-e14.
105. Klune, J.R. and A. Tsung, *Molecular biology of liver ischemia/reperfusion injury: established mechanisms and recent advancements.* Surg Clin North Am, 2010. **90**(4): p. 665-77.
106. de Rougemont, O., P. Dutkowski, and P.A. Clavien, *Biological modulation of liver ischemia-reperfusion injury.* Curr Opin Organ Transplant, 2010. **15**(2): p. 183-9.
107. Imamura, H., A. Brault, and P.M. Huet, *Effects of extended cold preservation and transplantation on the rat liver microcirculation.* Hepatology, 1997. **25**(3): p. 664-71.
108. Clavien, P.A., P.R. Harvey, and S.M. Strasberg, *Preservation and reperfusion injuries in liver allografts. An overview and synthesis of current studies.* Transplantation, 1992. **53**(5): p. 957-78.
109. Bigelow, D.J. and D.D. Thomas, *Rotational dynamics of lipid and the Ca-ATPase in sarcoplasmic reticulum. The molecular basis of activation by diethyl ether.* J Biol Chem, 1987. **262**(28): p. 13449-56.

110. Upadhya, G.A., et al., *Effect of cold preservation on intracellular calcium concentration and calpain activity in rat sinusoidal endothelial cells.* Hepatology, 2003. **37**(2): p. 313-23.
111. Upadhya, A.G., et al., *Evidence of a role for matrix metalloproteinases in cold preservation injury of the liver in humans and in the rat.* Hepatology, 1997. **26**(4): p. 922-8.
112. Upadhya, G.A. and S.M. Strasberg, *Platelet adherence to isolated rat hepatic sinusoidal endothelial cells after cold preservation.* Transplantation, 2002. **73**(11): p. 1764-70.
113. Siriussawakul, A., A. Zaky, and J.D. Lang, *Role of nitric oxide in hepatic ischemia-reperfusion injury.* World J Gastroenterol, 2010. **16**(48): p. 6079-86.
114. Gao, W., et al., *Apoptosis of sinusoidal endothelial cells is a critical mechanism of preservation injury in rat liver transplantation.* Hepatology, 1998. **27**(6): p. 1652-60.
115. Selzner, M., et al., *Increased ischemic injury in old mouse liver: an ATP-dependent mechanism.* Liver Transpl, 2007. **13**(3): p. 382-90.
116. Dutkowski, P., et al., *Rat liver preservation by hypothermic oscillating liver perfusion compared to simple cold storage.* Cryobiology, 1998. **36**(1): p. 61-70.
117. Jennings, R.B., et al., *Mitochondrial matrix densities in myocardial ischemia and autolysis.* Exp Mol Pathol, 1978. **29**(1): p. 55-65.
118. Abu-Amara, M., et al., *Liver ischemia/reperfusion injury: processes in inflammatory networks--a review.* Liver Transpl, 2010. **16**(9): p. 1016-32.
119. Colletti, L.M., et al., *Role of tumor necrosis factor-alpha in the pathophysiologic alterations after hepatic ischemia/reperfusion injury in the rat.* J Clin Invest, 1990. **85**(6): p. 1936-43.
120. Jaeschke, H., C.V. Smith, and J.R. Mitchell, *Reactive oxygen species during ischemia-reflow injury in isolated perfused rat liver.* J Clin Invest, 1988. **81**(4): p. 1240-6.
121. Jaeschke, H., C.V. Smith, and J.R. Mitchell, *Hypoxic damage generates reactive oxygen species in isolated perfused rat liver.* Biochem Biophys Res Commun, 1988. **150**(2): p. 568-74.
122. Jaeschke, H., et al., *Superoxide generation by Kupffer cells and priming of neutrophils during reperfusion after hepatic ischemia.* Free Radic Res Commun, 1991. **15**(5): p. 277-84.
123. Llacuna, L., et al., *Reactive oxygen species mediate liver injury through parenchymal nuclear factor-kappaB inactivation in prolonged ischemia/reperfusion.* Am J Pathol, 2009. **174**(5): p. 1776-85.
124. Wanner, G.A., et al., *Liver ischemia and reperfusion induces a systemic inflammatory response through Kupffer cell activation.* Shock, 1996. **5**(1): p. 34-40.
125. Shirasugi, N., et al., *Up-regulation of oxygen-derived free radicals by interleukin-1 in hepatic ischemia/reperfusion injury.* Transplantation, 1997. **64**(10): p. 1398-403.
126. Jaeschke, H., *Reperfusion injury after warm ischemia or cold storage of the liver: role of apoptotic cell death.* Transplant Proc, 2002. **34**(7): p. 2656-8.
127. Jaeschke, H., et al., *Mechanisms of inflammatory liver injury: adhesion molecules and cytotoxicity of neutrophils.* Toxicol Appl Pharmacol, 1996. **139**(2): p. 213-26.
128. Omar, R., et al., *Prevention of postischaemic lipid peroxidation and liver cell injury by iron chelation.* Gut, 1989. **30**(4): p. 510-4.
129. Le Moine, O., et al., *Cold liver ischemia-reperfusion injury critically depends on liver T cells and is improved by donor pretreatment with interleukin 10 in mice.* Hepatology, 2000. **31**(6): p. 1266-74.

130. Sanlioglu, S., et al., *Lipopolysaccharide induces Rac1-dependent reactive oxygen species formation and coordinates tumor necrosis factor-alpha secretion through IKK regulation of NF-kappa B.* J Biol Chem, 2001. **276**(32): p. 30188-98.
131. Hanschen, M., et al., *Reciprocal activation between CD4+ T cells and Kupffer cells during hepatic ischemia-reperfusion.* Transplantation, 2008. **86**(5): p. 710-8.
132. Colletti, L.M., et al., *The role of cytokine networks in the local liver injury following hepatic ischemia/reperfusion in the rat.* Hepatology, 1996. **23**(3): p. 506-14.
133. Kato, A., et al., *Specific role of interleukin-1 in hepatic neutrophil recruitment after ischemia/reperfusion.* Am J Pathol, 2002. **161**(5): p. 1797-803.
134. Caldwell, C.C., et al., *Divergent functions of CD4+ T lymphocytes in acute liver inflammation and injury after ischemia-reperfusion.* Am J Physiol Gastrointest Liver Physiol, 2005. **289**(5): p. G969-76.
135. Farhood, A., et al., *Intercellular adhesion molecule 1 (ICAM-1) expression and its role in neutrophil-induced ischemia-reperfusion injury in rat liver.* J Leukoc Biol, 1995. **57**(3): p. 368-74.
136. Singh, I., et al., *Role of P-selectin expression in hepatic ischemia and reperfusion injury.* Clin Transplant, 1999. **13**(1 Pt 2): p. 76-82.
137. Jaeschke, H., *Mechanisms of Liver Injury. II. Mechanisms of neutrophil-induced liver cell injury during hepatic ischemia-reperfusion and other acute inflammatory conditions.* Am J Physiol Gastrointest Liver Physiol, 2006. **290**(6): p. G1083-8.
138. Yadav, S.S., et al., *P-Selectin mediates reperfusion injury through neutrophil and platelet sequestration in the warm ischemic mouse liver.* Hepatology, 1999. **29**(5): p. 1494-502.
139. Yadav, S.S., et al., *L-selectin and ICAM-1 mediate reperfusion injury and neutrophil adhesion in the warm ischemic mouse liver.* Am J Physiol, 1998. **275**(6 Pt 1): p. G1341-52.
140. Caldwell, C.C., J. Tschoep, and A.B. Lentsch, *Lymphocyte function during hepatic ischemia/reperfusion injury.* J Leukoc Biol, 2007. **82**(3): p. 457-64.
141. Natori, S., et al., *Apoptosis of sinusoidal endothelial cells occurs during liver preservation injury by a caspase-dependent mechanism.* Transplantation, 1999. **68**(1): p. 89-96.
142. El-Badry, A.M., et al., *Prevention of reperfusion injury and microcirculatory failure in macrosteatotic mouse liver by omega-3 fatty acids.* Hepatology, 2007. **45**(4): p. 855-63.
143. Teramoto, K., et al., *A rat fatty liver transplant model.* Transplantation, 1993. **55**(4): p. 737-41.
144. Teramoto, K., et al., *Hepatic microcirculatory changes after reperfusion in fatty and normal liver transplantation in the rat.* Transplantation, 1993. **56**(5): p. 1076-82.
145. Caraceni, P., et al., *The reduced tolerance of rat fatty liver to ischemia reperfusion is associated with mitochondrial oxidative injury.* J Surg Res, 2005. **124**(2): p. 160-8.
146. Serafin, A., et al., *Ischemic preconditioning increases the tolerance of Fatty liver to hepatic ischemia-reperfusion injury in the rat.* Am J Pathol, 2002. **161**(2): p. 587-601.
147. Koneru, B., et al., *Studies of hepatic warm ischemia in the obese Zucker rat.* Transplantation, 1995. **59**(7): p. 942-6.
148. Risby, T.H., et al., *Evidence for free radical-mediated lipid peroxidation at reperfusion of human orthotopic liver transplants.* Surgery, 1994. **115**(1): p. 94-101.
149. Letteron, P., et al., *Acute and chronic hepatic steatosis lead to in vivo lipid peroxidation in mice.* J Hepatol, 1996. **24**(2): p. 200-8.
150. Ijaz, S., et al., *Impairment of hepatic microcirculation in fatty liver.* Microcirculation, 2003. **10**(6): p. 447-56.
151. Hakamada, K., et al., *Sinusoidal flow block after warm ischemia in rats with diet-induced fatty liver.* J Surg Res, 1997. **70**(1): p. 12-20.

152. Ohhara, K., *[Study of microcirculatory changes in experimental dietary fatty liver].* Hokkaido Igaku Zasshi, 1989. **64**(2): p. 177-85.
153. Teramoto, K., et al., *In vivo microscopic observation of fatty liver grafts after reperfusion.* Transplant Proc, 1994. **26**(4): p. 2391.
154. Wunder, C. and R.F. Potter, *The heme oxygenase system: its role in liver inflammation.* Curr Drug Targets Cardiovasc Haematol Disord, 2003. **3**(3): p. 199-208.
155. Tenhunen, R., H.S. Marver, and R. Schmid, *The enzymatic conversion of heme to bilirubin by microsomal heme oxygenase.* Proc Natl Acad Sci U S A, 1968. **61**(2): p. 748-55.
156. Abraham, N.G., et al., *Heme oxygenase -1 gene therapy: recent advances and therapeutic applications.* Curr Gene Ther, 2007. **7**(2): p. 89-108.
157. Farombi, E.O. and Y.J. Surh, *Heme oxygenase-1 as a potential therapeutic target for hepatoprotection.* J Biochem Mol Biol, 2006. **39**(5): p. 479-91.
158. Ryter, S.W., J. Alam, and A.M. Choi, *Heme oxygenase-1/carbon monoxide: from basic science to therapeutic applications.* Physiol Rev, 2006. **86**(2): p. 583-650.
159. Katana, E., et al., *Association between the heme oxygenase-1 promoter polymorphism and renal transplantation outcome in Greece.* Transplant Proc, 2010. **42**(7): p. 2479-85.
160. Ma, J., et al., *A cell penetrating heme oxygenase protein protects heart graft against ischemia/reperfusion injury.* Gene Ther, 2009. **16**(3): p. 320-8.
161. Lad, L., et al., *Comparison of the heme-free and -bound crystal structures of human heme oxygenase-1.* J Biol Chem, 2003. **278**(10): p. 7834-43.
162. Schuller, D.J., et al., *Crystal structure of human heme oxygenase-1.* Nat Struct Biol, 1999. **6**(9): p. 860-7.
163. Ishikawa, K., M. Sato, and T. Yoshida, *Expression of rat heme oxygenase in Escherichia coli as a catalytically active, full-length form that binds to bacterial membranes.* Eur J Biochem, 1991. **202**(1): p. 161-5.
164. McCoubrey, W.K., Jr. and M.D. Maines, *Domains of rat heme oxygenase-2: the amino terminus and histidine 151 are required for heme oxidation.* Arch Biochem Biophys, 1993. **302**(2): p. 402-8.
165. Shibahara, S., et al., *Cloning and expression of cDNA for rat heme oxygenase.* Proc Natl Acad Sci U S A, 1985. **82**(23): p. 7865-9.
166. Tenhunen, R., H.S. Marver, and R. Schmid, *Microsomal heme oxygenase. Characterization of the enzyme.* J Biol Chem, 1969. **244**(23): p. 6388-94.
167. Tenhunen, R., H.S. Marver, and R. Schmid, *The enzymatic catabolism of hemoglobin: stimulation of microsomal heme oxygenase by hemin.* J Lab Clin Med, 1970. **75**(3): p. 410-21.
168. Pimstone, N.R., et al., *Inducible heme oxygenase in the kidney: a model for the homeostatic control of hemoglobin catabolism.* J Clin Invest, 1971. **50**(10): p. 2042-50.
169. Pimstone, N.R., et al., *The enzymatic degradation of hemoglobin to bile pigments by macrophages.* J Exp Med, 1971. **133**(6): p. 1264-81.
170. Simon, T., I. Anegon, and P. Blancou, *Heme oxygenase and carbon monoxide as an immunotherapeutic approach in transplantation and cancer.* Immunotherapy, 2011. **3**(4 Suppl): p. 15-8.
171. Chauveau, C., et al., *Heme oxygenase-1 expression inhibits dendritic cell maturation and proinflammatory function but conserves IL-10 expression.* Blood, 2005. **106**(5): p. 1694-702.
172. Pae, H.O., et al., *Differential expressions of heme oxygenase-1 gene in CD25- and CD25+ subsets of human CD4+ T cells.* Biochem Biophys Res Commun, 2003. **306**(3): p. 701-5.

173. Remy, S., et al., *Carbon monoxide inhibits TLR-induced dendritic cell immunogenicity.* J Immunol, 2009. **182**(4): p. 1877-84.
174. Elbirt, K.K., et al., *Mechanism of sodium arsenite-mediated induction of heme oxygenase-1 in hepatoma cells. Role of mitogen-activated protein kinases.* J Biol Chem, 1998. **273**(15): p. 8922-31.
175. Morse, D. and A.M. Choi, *Heme oxygenase-1: the "emerging molecule" has arrived.* Am J Respir Cell Mol Biol, 2002. **27**(1): p. 8-16.
176. Li, P., et al., *Angiotensin II induces carbon monoxide production in the perfused kidney: relationship to protein kinase C activation.* Am J Physiol Renal Physiol, 2004. **287**(5): p. F914-20.
177. Numazawa, S., et al., *Atypical protein kinase C mediates activation of NF-E2-related factor 2 in response to oxidative stress.* Am J Physiol Cell Physiol, 2003. **285**(2): p. C334-42.
178. Immenschuh, S., et al., *The rat heme oxygenase-1 gene is transcriptionally induced via the protein kinase A signaling pathway in rat hepatocyte cultures.* Mol Pharmacol, 1998. **53**(3): p. 483-91.
179. Elbirt, K.K. and H.L. Bonkovsky, *Heme oxygenase: recent advances in understanding its regulation and role.* Proc Assoc Am Physicians, 1999. **111**(5): p. 438-47.
180. Immenschuh, S. and G. Ramadori, *Gene regulation of heme oxygenase-1 as a therapeutic target.* Biochem Pharmacol, 2000. **60**(8): p. 1121-8.
181. Bauer, M., et al., *Evidence for a functional link between stress response and vascular control in hepatic portal circulation.* Am J Physiol, 1996. **271**(5 Pt 1): p. G929-35.
182. Li Volti, G., et al., *Natural heme oxygenase-1 inducers in hepatobiliary function.* World J Gastroenterol, 2008. **14**(40): p. 6122-32.
183. Fujita, T., et al., *Paradoxical rescue from ischemic lung injury by inhaled carbon monoxide driven by derepression of fibrinolysis.* Nat Med, 2001. **7**(5): p. 598-604.
184. Yachie, A., et al., *Oxidative stress causes enhanced endothelial cell injury in human heme oxygenase-1 deficiency.* J Clin Invest, 1999. **103**(1): p. 129-35.
185. Lee, P.J., et al., *Regulation of heme oxygenase-1 expression in vivo and in vitro in hyperoxic lung injury.* Am J Respir Cell Mol Biol, 1996. **14**(6): p. 556-68.
186. Suttner, D.M., et al., *Protective effects of transient HO-1 overexpression on susceptibility to oxygen toxicity in lung cells.* Am J Physiol, 1999. **276**(3 Pt 1): p. L443-51.
187. Petrache, I., et al., *Heme oxygenase-1 inhibits TNF-alpha-induced apoptosis in cultured fibroblasts.* Am J Physiol Lung Cell Mol Physiol, 2000. **278**(2): p. L312-9.
188. Soares, M.P., et al., *Expression of heme oxygenase-1 can determine cardiac xenograft survival.* Nat Med, 1998. **4**(9): p. 1073-7.
189. Katori, M., et al., *Heme oxygenase-1 overexpression protects rat hearts from cold ischemia/reperfusion injury via an antiapoptotic pathway.* Transplantation, 2002. **73**(2): p. 287-92.
190. Melo, L.G., et al., *Gene therapy strategy for long-term myocardial protection using adeno-associated virus-mediated delivery of heme oxygenase gene.* Circulation, 2002. **105**(5): p. 602-7.
191. Foresti, R., et al., *Role of heme oxygenase-1 in hypoxia-reoxygenation: requirement of substrate heme to promote cardioprotection.* Am J Physiol Heart Circ Physiol, 2001. **281**(5): p. H1976-84.
192. Kacimi, R., et al., *Hypoxia differentially regulates stress proteins in cultured cardiomyocytes: role of the p38 stress-activated kinase signaling cascade, and relation to cytoprotection.* Cardiovasc Res, 2000. **46**(1): p. 139-50.

193. Sato, K., et al., *Carbon monoxide generated by heme oxygenase-1 suppresses the rejection of mouse-to-rat cardiac transplants.* J Immunol, 2001. **166**(6): p. 4185-94.
194. Raju, V.S. and M.D. Maines, *Renal ischemia/reperfusion up-regulates heme oxygenase-1 (HSP32) expression and increases cGMP in rat heart.* J Pharmacol Exp Ther, 1996. **277**(3): p. 1814-22.
195. Salahudeen, A.A., et al., *Overexpression of heme oxygenase protects renal tubular cells against cold storage injury: studies using hemin induction and HO-1 gene transfer.* Transplantation, 2001. **72**(9): p. 1498-504.
196. Yamada, N., et al., *Microsatellite polymorphism in the heme oxygenase-1 gene promoter is associated with susceptibility to emphysema.* Am J Hum Genet, 2000. **66**(1): p. 187-95.
197. Exner, M., et al., *The role of heme oxygenase-1 promoter polymorphisms in human disease.* Free Radic Biol Med, 2004. **37**(8): p. 1097-104.
198. Amersi, F., et al., *Upregulation of heme oxygenase-1 protects genetically fat Zucker rat livers from ischemia/reperfusion injury.* J Clin Invest, 1999. **104**(11): p. 1631-9.
199. Kobayashi, T., et al., *The protective role of Kupffer cells in the ischemia-reperfused rat liver.* Arch Histol Cytol, 2002. **65**(3): p. 251-61.
200. Coito, A.J., et al., *Heme oxygenase-1 gene transfer inhibits inducible nitric oxide synthase expression and protects genetically fat Zucker rat livers from ischemia-reperfusion injury.* Transplantation, 2002. **74**(1): p. 96-102.
201. Kato, H., et al., *Heme oxygenase-1 overexpression protects rat livers from ischemia/reperfusion injury with extended cold preservation.* Am J Transplant, 2001. **1**(2): p. 121-8.
202. Redaelli, C.A., et al., *Extended preservation of rat liver graft by induction of heme oxygenase-1.* Hepatology, 2002. **35**(5): p. 1082-92.
203. Wunder, C., et al., *Inhibition of haem oxygenase activity increases leukocyte accumulation in the liver following limb ischaemia-reperfusion in mice.* J Physiol, 2002. **540**(Pt 3): p. 1013-21.
204. Tsuchihashi, S., et al., *Basal rather than induced heme oxygenase-1 levels are crucial in the antioxidant cytoprotection.* J Immunol, 2006. **177**(7): p. 4749-57.
205. Ke, B., et al., *Small interfering RNA targeting heme oxygenase-1 (HO-1) reinforces liver apoptosis induced by ischemia-reperfusion injury in mice: HO-1 is necessary for cytoprotection.* Hum Gene Ther, 2009. **20**(10): p. 1133-42.
206. Zeng, Z., et al., *Heme oxygenase-1 protects donor livers from ischemia/reperfusion injury: the role of Kupffer cells.* World J Gastroenterol, 2010. **16**(10): p. 1285-92.
207. Sass, G., et al., *Heme oxygenase-1 and its reaction product, carbon monoxide, prevent inflammation-related apoptotic liver damage in mice.* Hepatology, 2003. **38**(4): p. 909-18.
208. Vallabhaneni, R., et al., *Heme oxygenase 1 protects against hepatic hypoxia and injury from hemorrhage via regulation of cellular respiration.* Shock, 2010. **33**(3): p. 274-81.
209. Wang, X.H., et al., *Heme oxygenase-1 alleviates ischemia/reperfusion injury in aged liver.* World J Gastroenterol, 2005. **11**(5): p. 690-4.
210. Ke, B., et al., *Heme oxygenase-1 gene therapy: a novel immunomodulatory approach in liver allograft recipients?* Transplant Proc, 2001. **33**(1-2): p. 581-2.
211. Mokuno, Y., et al., *Technique for expanding the donor liver pool: heat shock preconditioning in a rat fatty liver model.* Liver Transpl, 2004. **10**(2): p. 264-72.
212. Franco-Gou, R., et al., *How ischaemic preconditioning protects small liver grafts.* J Pathol, 2006. **208**(1): p. 62-73.

213. Lai, I.R., et al., *Transient limb ischemia induces remote preconditioning in liver among rats: the protective role of heme oxygenase-1.* Transplantation, 2006. **81**(9): p. 1311-7.
214. Massip-Salcedo, M., et al., *Heat shock proteins and mitogen-activated protein kinases in steatotic livers undergoing ischemia-reperfusion: some answers.* Am J Pathol, 2006. **168**(5): p. 1474-85.
215. Llesuy, S.F. and M.L. Tomaro, *Heme oxygenase and oxidative stress. Evidence of involvement of bilirubin as physiological protector against oxidative damage.* Biochim Biophys Acta, 1994. **1223**(1): p. 9-14.
216. Stocker, R. and B.N. Ames, *Potential role of conjugated bilirubin and copper in the metabolism of lipid peroxides in bile.* Proc Natl Acad Sci U S A, 1987. **84**(22): p. 8130-4.
217. Fondevila, C., et al., *Biliverdin therapy protects rat livers from ischemia and reperfusion injury.* Hepatology, 2004. **40**(6): p. 1333-41.
218. Baranano, D.E., et al., *Biliverdin reductase: a major physiologic cytoprotectant.* Proc Natl Acad Sci U S A, 2002. **99**(25): p. 16093-8.
219. Ossola, J.O., M.D. Groppa, and M.L. Tomaro, *Relationship between oxidative stress and heme oxygenase induction by copper sulfate.* Arch Biochem Biophys, 1997. **337**(2): p. 332-7.
220. Ossola, J.O. and M.L. Tomaro, *Heme oxygenase induction by UVA radiation. A response to oxidative stress in rat liver.* Int J Biochem Cell Biol, 1998. **30**(2): p. 285-92.
221. Sedlak, T.W. and S.H. Snyder, *Bilirubin benefits: cellular protection by a biliverdin reductase antioxidant cycle.* Pediatrics, 2004. **113**(6): p. 1776-82.
222. Nakao, A., et al., *Protective effect of carbon monoxide inhalation for cold-preserved small intestinal grafts.* Surgery, 2003. **134**(2): p. 285-92.
223. Amersi, F., et al., *Ex vivo exposure to carbon monoxide prevents hepatic ischemia/reperfusion injury through p38 MAP kinase pathway.* Hepatology, 2002. **35**(4): p. 815-23.
224. Ali, Y., et al., *Early graft function and carboxyhemoglobin level in liver transplanted patients.* Middle East J Anesthesiol, 2007. **19**(3): p. 513-25.
225. Brune, B. and V. Ullrich, *Inhibition of platelet aggregation by carbon monoxide is mediated by activation of guanylate cyclase.* Mol Pharmacol, 1987. **32**(4): p. 497-504.
226. Zhang, X., et al., *Carbon monoxide modulates Fas/Fas ligand, caspases, and Bcl-2 family proteins via the p38alpha mitogen-activated protein kinase pathway during ischemia-reperfusion lung injury.* J Biol Chem, 2003. **278**(24): p. 22061-70.
227. Wang, R., Z. Wang, and L. Wu, *Carbon monoxide-induced vasorelaxation and the underlying mechanisms.* Br J Pharmacol, 1997. **121**(5): p. 927-34.
228. Wang, R., *Resurgence of carbon monoxide: an endogenous gaseous vasorelaxing factor.* Can J Physiol Pharmacol, 1998. **76**(1): p. 1-15.
229. Pannen, B.H., et al., *Protective role of endogenous carbon monoxide in hepatic microcirculatory dysfunction after hemorrhagic shock in rats.* J Clin Invest, 1998. **102**(6): p. 1220-8.
230. Suematsu, M., et al., *Carbon monoxide: an endogenous modulator of sinusoidal tone in the perfused rat liver.* J Clin Invest, 1995. **96**(5): p. 2431-7.
231. Coceani, F., et al., *Carbon monoxide formation in the ductus arteriosus in the lamb: implications for the regulation of muscle tone.* Br J Pharmacol, 1997. **120**(4): p. 599-608.
232. Shinoda, Y., et al., *Carbon monoxide as a regulator of bile canalicular contractility in cultured rat hepatocytes.* Hepatology, 1998. **28**(2): p. 286-95.

233. Brouard, S., et al., *Heme oxygenase-1-derived carbon monoxide requires the activation of transcription factor NF-kappa B to protect endothelial cells from tumor necrosis factor-alpha-mediated apoptosis.* J Biol Chem, 2002. **277**(20): p. 17950-61.
234. Balla, G., et al., *Exposure of endothelial cells to free heme potentiates damage mediated by granulocytes and toxic oxygen species.* Lab Invest, 1991. **64**(5): p. 648-55.
235. Valko, M., H. Morris, and M.T. Cronin, *Metals, toxicity and oxidative stress.* Curr Med Chem, 2005. **12**(10): p. 1161-208.
236. Lloyd, R.V., P.M. Hanna, and R.P. Mason, *The origin of the hydroxyl radical oxygen in the Fenton reaction.* Free Radic Biol Med, 1997. **22**(5): p. 885-8.
237. Eisenstein, R.S., et al., *Regulation of ferritin and heme oxygenase synthesis in rat fibroblasts by different forms of iron.* Proc Natl Acad Sci U S A, 1991. **88**(3): p. 688-92.
238. Gonzales, S., et al., *Glutamine is highly effective in preventing in vivo cobalt-induced oxidative stress in rat liver.* World J Gastroenterol, 2005. **11**(23): p. 3533-8.
239. Grosser, N., et al., *Antioxidant action of L-alanine: heme oxygenase-1 and ferritin as possible mediators.* Biochem Biophys Res Commun, 2004. **314**(2): p. 351-5.
240. Ferris, C.D., et al., *Haem oxygenase-1 prevents cell death by regulating cellular iron.* Nat Cell Biol, 1999. **1**(3): p. 152-7.
241. Abraham, N.G. and A. Kappas, *Pharmacological and clinical aspects of heme oxygenase.* Pharmacol Rev, 2008. **60**(1): p. 79-127.
242. Ryter, S.W. and R.M. Tyrrell, *The heme synthesis and degradation pathways: role in oxidant sensitivity. Heme oxygenase has both pro- and antioxidant properties.* Free Radic Biol Med, 2000. **28**(2): p. 289-309.
243. Wagener, F.A., et al., *Different faces of the heme-heme oxygenase system in inflammation.* Pharmacol Rev, 2003. **55**(3): p. 551-71.
244. Takahashi, H. and K. Koshi, *Solubility and cell toxicity of cobalt, zinc and lead.* Ind Health, 1981. **19**(1): p. 47-59.
245. Evans, E.J. and I.T. Thomas, *The in vitro toxicity of cobalt-chrome-molybdenum alloy and its constituent metals.* Biomaterials, 1986. **7**(1): p. 25-9.
246. Nemery, B., C.P. Lewis, and M. Demedts, *Cobalt and possible oxidant-mediated toxicity.* Sci Total Environ, 1994. **150**(1-3): p. 57-64.
247. Simmons, S.O., et al., *NRF2 Oxidative Stress Induced by Heavy Metals is Cell Type Dependent.* Curr Chem Genomics, 2011. **5**: p. 1-12.
248. Devitt, B.M., et al., *Cobalt ions induce chemokine secretion in a variety of systemic cell lines.* Acta Orthop, 2010. **81**(6): p. 756-64.
249. Harris, R.M., et al., *Reactive oxygen species and oxidative DNA damage mediate the cytotoxicity of tungsten-nickel-cobalt alloys in vitro.* Toxicol Appl Pharmacol, 2011. **250**(1): p. 19-28.
250. Walsh, K.B., et al., *Inflammatory mediators of liver ischemia-reperfusion injury.* Exp Clin Transplant, 2009. **7**(2): p. 78-93.
251. Gurusamy, K.S., et al., *Ischaemic preconditioning for liver transplantation.* Cochrane Database Syst Rev, 2008(1): p. CD006315.
252. Ferrandiz, M.L. and I. Devesa, *Inducers of heme oxygenase-1.* Curr Pharm Des, 2008. **14**(5): p. 473-86.
253. Sun, J., et al., *Identification of histidine 25 as the heme ligand in human liver heme oxygenase.* Biochemistry, 1994. **33**(46): p. 13734-40.
254. Seiler, M.P., V. Cerullo, and B. Lee, *Immune response to helper dependent adenoviral mediated liver gene therapy: challenges and prospects.* Curr Gene Ther, 2007. **7**(5): p. 297-305.

255. Douglas, J.T., *Adenoviral vectors for gene therapy.* Mol Biotechnol, 2007. **36**(1): p. 71-80.
256. Volpers, C. and S. Kochanek, *Adenoviral vectors for gene transfer and therapy.* J Gene Med, 2004. **6 Suppl 1**: p. S164-71.
257. Busserolles, J., et al., *Heme oxygenase-1 inhibits apoptosis in Caco-2 cells via activation of Akt pathway.* Int J Biochem Cell Biol, 2006. **38**(9): p. 1510-7.
258. Hirai, K., et al., *Inhibition of heme oxygenase-1 by zinc protoporphyrin IX reduces tumor growth of LL/2 lung cancer in C57BL mice.* Int J Cancer, 2007. **120**(3): p. 500-5.
259. Jozkowicz, A., H. Was, and J. Dulak, *Heme oxygenase-1 in tumors: is it a false friend?* Antioxid Redox Signal, 2007. **9**(12): p. 2099-117.
260. Kocanova, S., et al., *Induction of heme-oxygenase 1 requires the p38MAPK and PI3K pathways and suppresses apoptotic cell death following hypericin-mediated photodynamic therapy.* Apoptosis, 2007. **12**(4): p. 731-41.
261. Tanaka, S., et al., *Antiapoptotic effect of haem oxygenase-1 induced by nitric oxide in experimental solid tumour.* Br J Cancer, 2003. **88**(6): p. 902-9.
262. Tsui, T.Y., et al., *Heme oxygenase-1-derived carbon monoxide stimulates adenosine triphosphate generation in human hepatocyte.* Biochem Biophys Res Commun, 2005. **336**(3): p. 898-902.
263. Ryser, H.J. and R. Hancock, *Histones and basic polyamino acids stimulate the uptake of albumin by tumor cells in culture.* Science, 1965. **150**(3695): p. 501-3.
264. Frankel, A.D. and C.O. Pabo, *Cellular uptake of the tat protein from human immunodeficiency virus.* Cell, 1988. **55**(6): p. 1189-93.
265. Joliot, A., et al., *Antennapedia homeobox peptide regulates neural morphogenesis.* Proc Natl Acad Sci U S A, 1991. **88**(5): p. 1864-8.
266. Derossi, D., et al., *The third helix of the Antennapedia homeodomain translocates through biological membranes.* J Biol Chem, 1994. **269**(14): p. 10444-50.
267. Vives, E., P. Brodin, and B. Lebleu, *A truncated HIV-1 Tat protein basic domain rapidly translocates through the plasma membrane and accumulates in the cell nucleus.* J Biol Chem, 1997. **272**(25): p. 16010-7.
268. Noguchi, H., et al., *Recent advances in protein transduction technology.* Cell Transplant, 2010. **19**(6): p. 649-54.
269. Jarver, P. and U. Langel, *The use of cell-penetrating peptides as a tool for gene regulation.* Drug Discov Today, 2004. **9**(9): p. 395-402.
270. Joliot, A., *Transduction peptides within naturally occurring proteins.* Sci STKE, 2005. **2005**(313): p. pe54.
271. Moschos, S.A., et al., *Lung delivery studies using siRNA conjugated to TAT(48-60) and penetratin reveal peptide induced reduction in gene expression and induction of innate immunity.* Bioconjug Chem, 2007. **18**(5): p. 1450-9.
272. Lindgren, M. and U. Langel, *Classes and prediction of cell-penetrating peptides.* Methods Mol Biol, 2011. **683**: p. 3-19.
273. Schwarze, S.R., et al., *In vivo protein transduction: delivery of a biologically active protein into the mouse.* Science, 1999. **285**(5433): p. 1569-72.
274. Chugh, A., F. Eudes, and Y.S. Shim, *Cell-penetrating peptides: Nanocarrier for macromolecule delivery in living cells.* IUBMB Life, 2010. **62**(3): p. 183-93.
275. Johnson, R.M., S.D. Harrison, and D. Maclean, *Therapeutic applications of cell-penetrating peptides.* Methods Mol Biol, 2011. **683**: p. 535-51.
276. Heitz, F., M.C. Morris, and G. Divita, *Twenty years of cell-penetrating peptides: from molecular mechanisms to therapeutics.* Br J Pharmacol, 2009. **157**(2): p. 195-206.

277. Holm, T., S.E. Andaloussi, and U. Langel, *Comparison of CPP uptake methods.* Methods Mol Biol, 2011. **683**: p. 207-17.
278. Duchardt, F., et al., *A comprehensive model for the cellular uptake of cationic cell-penetrating peptides.* Traffic, 2007. **8**(7): p. 848-66.
279. Deshayes, S., et al., *Delivery of proteins and nucleic acids using a non-covalent peptide-based strategy.* Adv Drug Deliv Rev, 2008. **60**(4-5): p. 537-47.
280. Ter-Avetisyan, G., et al., *Cell entry of arginine-rich peptides is independent of endocytosis.* J Biol Chem, 2009. **284**(6): p. 3370-8.
281. Wender, P.A., et al., *The design of guanidinium-rich transporters and their internalization mechanisms.* Adv Drug Deliv Rev, 2008. **60**(4-5): p. 452-72.
282. Wender, P.A., et al., *The design, synthesis, and evaluation of molecules that enable or enhance cellular uptake: peptoid molecular transporters.* Proc Natl Acad Sci U S A, 2000. **97**(24): p. 13003-8.
283. Gump, J.M. and S.F. Dowdy, *TAT transduction: the molecular mechanism and therapeutic prospects.* Trends Mol Med, 2007. **13**(10): p. 443-8.
284. Richard, J.P., et al., *Cellular uptake of unconjugated TAT peptide involves clathrin-dependent endocytosis and heparan sulfate receptors.* J Biol Chem, 2005. **280**(15): p. 15300-6.
285. Potocky, T.B., A.K. Menon, and S.H. Gellman, *Cytoplasmic and nuclear delivery of a TAT-derived peptide and a beta-peptide after endocytic uptake into HeLa cells.* J Biol Chem, 2003. **278**(50): p. 50188-94.
286. Fittipaldi, A., et al., *Cell membrane lipid rafts mediate caveolar endocytosis of HIV-1 Tat fusion proteins.* J Biol Chem, 2003. **278**(36): p. 34141-9.
287. Console, S., et al., *Antennapedia and HIV transactivator of transcription (TAT) "protein transduction domains" promote endocytosis of high molecular weight cargo upon binding to cell surface glycosaminoglycans.* J Biol Chem, 2003. **278**(37): p. 35109-14.
288. Fischer, R., et al., *Break on through to the other side-biophysics and cell biology shed light on cell-penetrating peptides.* Chembiochem, 2005. **6**(12): p. 2126-42.
289. Mai, J.C., et al., *Efficiency of protein transduction is cell type-dependent and is enhanced by dextran sulfate.* J Biol Chem, 2002. **277**(33): p. 30208-18.
290. El-Andaloussi, S., et al., *Cargo-dependent cytotoxicity and delivery efficacy of cell-penetrating peptides: a comparative study.* Biochem J, 2007. **407**(2): p. 285-92.
291. Tunnemann, G., et al., *Cargo-dependent mode of uptake and bioavailability of TAT-containing proteins and peptides in living cells.* FASEB J, 2006. **20**(11): p. 1775-84.
292. Silhol, M., et al., *Different mechanisms for cellular internalization of the HIV-1 Tat-derived cell penetrating peptide and recombinant proteins fused to Tat.* Eur J Biochem, 2002. **269**(2): p. 494-501.
293. Bright, R., et al., *Protein kinase C delta mediates cerebral reperfusion injury in vivo.* J Neurosci, 2004. **24**(31): p. 6880-8.
294. Asoh, S., et al., *Protection against ischemic brain injury by protein therapeutics.* Proc Natl Acad Sci U S A, 2002. **99**(26): p. 17107-12.
295. Mochly-Rosen, D., *Localization of protein kinases by anchoring proteins: a theme in signal transduction.* Science, 1995. **268**(5208): p. 247-51.
296. Hirt, L., et al., *D-JNKI1, a cell-penetrating c-Jun-N-terminal kinase inhibitor, protects against cell death in severe cerebral ischemia.* Stroke, 2004. **35**(7): p. 1738-43.
297. Bian, J., et al., *Effect of cell-based intercellular delivery of transcription factor GATA4 on ischemic cardiomyopathy.* Circ Res, 2007. **100**(11): p. 1626-33.

298. Inagaki, K., et al., *Inhibition of delta-protein kinase C protects against reperfusion injury of the ischemic heart in vivo.* Circulation, 2003. **108**(19): p. 2304-7.
299. Inagaki, K., et al., *Additive protection of the ischemic heart ex vivo by combined treatment with delta-protein kinase C inhibitor and epsilon-protein kinase C activator.* Circulation, 2003. **108**(7): p. 869-75.
300. Sivaraman, V., et al., *The divergent roles of protein kinase C epsilon and delta in simulated ischaemia-reperfusion injury in human myocardium.* J Mol Cell Cardiol, 2009. **46**(5): p. 758-64.
301. Liu, X.J., et al., *Treatment of inflammatory and neuropathic pain by uncoupling Src from the NMDA receptor complex.* Nat Med, 2008. **14**(12): p. 1325-32.
302. Kim, J., et al., *Centrosomal PKCbetaII and pericentrin are critical for human prostate cancer growth and angiogenesis.* Cancer Res, 2008. **68**(16): p. 6831-9.
303. Meyer-Losic, F., et al., *DTS-108, a novel peptidic prodrug of SN38: in vivo efficacy and toxicokinetic studies.* Clin Cancer Res, 2008. **14**(7): p. 2145-53.
304. Meyer-Losic, F., et al., *Improved therapeutic efficacy of doxorubicin through conjugation with a novel peptide drug delivery technology (Vectocell).* J Med Chem, 2006. **49**(23): p. 6908-16.
305. Michiue, H., et al., *Ubiquitination-resistant p53 protein transduction therapy facilitates anti-cancer effect on the growth of human malignant glioma cells.* FEBS Lett, 2005. **579**(18): p. 3965-9.
306. Snyder, E.L., et al., *Treatment of terminal peritoneal carcinomatosis by a transducible p53-activating peptide.* PLoS Biol, 2004. **2**(2): p. E36.
307. Yoshiji, H., et al., *Protein kinase C lies on the signaling pathway for vascular endothelial growth factor-mediated tumor development and angiogenesis.* Cancer Res, 1999. **59**(17): p. 4413-8.
308. Ribeiro, M.M., et al., *Heme oxygenase-1 fused to a TAT peptide transduces and protects pancreatic beta-cells.* Biochem Biophys Res Commun, 2003. **305**(4): p. 876-81.
309. Srivastava, K.K., et al., *Molecular basis for heme-dependent induction of heme oxygenase in primary cultures of chick embryo hepatocytes. Demonstration of acquired refractoriness to heme.* Eur J Biochem, 1993. **213**(3): p. 909-17.
310. Vocero-Akbani, A., N.A. Lissy, and S.F. Dowdy, *Transduction of full-length Tat fusion proteins directly into mammalian cells: analysis of T cell receptor activation-induced cell death.* Methods Enzymol, 2000. **322**: p. 508-21.
311. Schwarze, S.R., K.A. Hruska, and S.F. Dowdy, *Protein transduction: unrestricted delivery into all cells?* Trends Cell Biol, 2000. **10**(7): p. 290-5.
312. Ho, A., et al., *Synthetic protein transduction domains: enhanced transduction potential in vitro and in vivo.* Cancer Res, 2001. **61**(2): p. 474-7.
313. Wilks, A. and P.R. Ortiz de Montellano, *Rat liver heme oxygenase. High level expression of a truncated soluble form and nature of the meso-hydroxylating species.* J Biol Chem, 1993. **268**(30): p. 22357-62.
314. Lundberg, M. and M. Johansson, *Positively charged DNA-binding proteins cause apparent cell membrane translocation.* Biochem Biophys Res Commun, 2002. **291**(2): p. 367-71.
315. Georgiou, G. and P. Valax, *Expression of correctly folded proteins in Escherichia coli.* Curr Opin Biotechnol, 1996. **7**(2): p. 190-7.
316. Francis, D.M. and R. Page, *Strategies to optimize protein expression in E. coli.* Curr Protoc Protein Sci, 2010. **Chapter 5**: p. Unit 5 24 1-29.

317. John J. Trill, R.K., Allan R. Shatzman, Alice Marcy, *Eukaryotic Expression*, in *Molecular Biology Problem Solver: A Laboratory Guide*, A.S. Gerstein, Editor. 2001, Wiley-Liss Inc. p. 491-542.
318. Huber, W.J., 3rd and W.L. Backes, *Expression and characterization of full-length human heme oxygenase-1: the presence of intact membrane-binding region leads to increased binding affinity for NADPH cytochrome P450 reductase.* Biochemistry, 2007. **46**(43): p. 12212-9.
319. Studier, F.W., et al., *Use of T7 RNA polymerase to direct expression of cloned genes.* Methods Enzymol, 1990. **185**: p. 60-89.
320. *User Protoco TB055 Rev. C 0611JN - pET System Manual 11th Edition*, Novagen, Editor. 2011, EMD Chemicals: Darmstadt, Germany. p. 31-32.
321. *pET System Manual 11th Edition*, Novagen, Editor. 2011. p. 45-47.
322. Grodberg, J. and J.J. Dunn, *ompT encodes the Escherichia coli outer membrane protease that cleaves T7 RNA polymerase during purification.* J Bacteriol, 1988. **170**(3): p. 1245-53.
323. Phillips, T.A., R.A. VanBogelen, and F.C. Neidhardt, *lon gene product of Escherichia coli is a heat-shock protein.* J Bacteriol, 1984. **159**(1): p. 283-7.
324. *User Protocol TB009 Rev: H 0211JN - Competent Cells*, Novagen, Editor. 2011, EMD Chemicals: Darmstadt, Germany. p. 4.
325. Moffatt, B.A. and F.W. Studier, *T7 lysozyme inhibits transcription by T7 RNA polymerase.* Cell, 1987. **49**(2): p. 221-7.
326. Inouye, M., N. Arnheim, and R. Sternglanz, *Bacteriophage T7 lysozyme is an N-acetylmuramyl-L-alanine amidase.* J Biol Chem, 1973. **248**(20): p. 7247-52.
327. Chalfie, M., et al., *Green fluorescent protein as a marker for gene expression.* Science, 1994. **263**(5148): p. 802-5.
328. Soots, B.C., Linda, *Biotechnology in the Classroom* in *Bacterial Transformation: Green Fluorescent protein*. 2009, University of California Davis. p. 4.
329. Scopes, R.K., *Overview of protein purification and characterization.* Curr Protoc Protein Sci, 2001. **Chapter 1**: p. Unit 1 1.
330. Linn, S., *Strategies and considerations for protein purifications.* Methods Enzymol, 2009. **463**: p. 9-19.
331. Crowe, J., et al., *6xHis-Ni-NTA chromatography as a superior technique in recombinant protein expression/purification.* Methods Mol Biol, 1994. **31**: p. 371-87.
332. *The QIAexpressionist*, Qiagen, Editor. 2003, Qiagen Worldwide: Hilden, Germany. p. 1-128.
333. Healthcare, G., *PD-10 Desalting Columns Instructions 52-1308-00 BB*. 2007, General Electric Company. p. 1-12.
334. Carraway, M.S., et al., *Induction of ferritin and heme oxygenase-1 by endotoxin in the lung.* Am J Physiol, 1998. **275**(3 Pt 1): p. L583-92.
335. Demirogullari, B., et al., *A comparative study of the effects of hemin and bilirubin on bilateral renal ischemia reperfusion injury.* Nephron Exp Nephrol, 2006. **103**(1): p. e1-5.
336. Huber, W.J., 3rd, et al., *Measurement of membrane-bound human heme oxygenase-1 activity using a chemically defined assay system.* Drug Metab Dispos, 2009. **37**(4): p. 857-64.
337. Maines, M.D. and A. Kappas, *Cobalt induction of hepatic heme oxygenase; with evidence that cytochrome P-450 is not essential for this enzyme activity.* Proc Natl Acad Sci U S A, 1974. **71**(11): p. 4293-7.

338. Schacter, B.A., et al., *Immunochemical evidence for an association of heme oxygenase with the microsomal electron transport system.* J Biol Chem, 1972. **247**(11): p. 3601-7.
339. Yoshida, T. and G. Kikuchi, *Purification and properties of heme oxygenase from pig spleen microsomes.* J Biol Chem, 1978. **253**(12): p. 4224-9.
340. Yoshida, T. and G. Kikuchi, *Purification and properties of heme oxygenase from rat liver microsomes.* J Biol Chem, 1979. **254**(11): p. 4487-91.
341. Chauhan, A., et al., *The taming of the cell penetrating domain of the HIV Tat: myths and realities.* J Control Release, 2007. **117**(2): p. 148-62.
342. Wadia, J.S. and S.F. Dowdy, *Protein transduction technology.* Curr Opin Biotechnol, 2002. **13**(1): p. 52-6.
343. Schwarze, S.R. and S.F. Dowdy, *In vivo protein transduction: intracellular delivery of biologically active proteins, compounds and DNA.* Trends Pharmacol Sci, 2000. **21**(2): p. 45-8.
344. Mandal, P., et al., *Adiponectin and heme oxygenase-1 suppress TLR4/MyD88-independent signaling in rat Kupffer cells and in mice after chronic ethanol exposure.* J Immunol, 2010. **185**(8): p. 4928-37.
345. Devey, L., et al., *Tissue-resident macrophages protect the liver from ischemia reperfusion injury via a heme oxygenase-1-dependent mechanism.* Mol Ther, 2009. **17**(1): p. 65-72.
346. Sabiston, D.C. and C.M. Townsend, *Sabiston textbook of surgery : the biological basis of modern surgical practice*. 18th ed. 2008, Philadelphia, PA: Saunders/Elsevier. xxv, 2353 p.
347. Farina, H.G., et al., *CIGB-300, a proapoptotic peptide, inhibits angiogenesis in vitro and in vivo.* Exp Cell Res, 2011. **317**(12): p. 1677-88.
348. Eguchi, A. and S.F. Dowdy, *siRNA delivery using peptide transduction domains.* Trends Pharmacol Sci, 2009. **30**(7): p. 341-5.
349. El-Sayed, A., S. Futaki, and H. Harashima, *Delivery of macromolecules using arginine-rich cell-penetrating peptides: ways to overcome endosomal entrapment.* AAPS J, 2009. **11**(1): p. 13-22.
350. Leifert, J.A., S. Harkins, and J.L. Whitton, *Full-length proteins attached to the HIV tat protein transduction domain are neither transduced between cells, nor exhibit enhanced immunogenicity.* Gene Ther, 2002. **9**(21): p. 1422-8.
351. Saalik, P., et al., *Protein cargo delivery properties of cell-penetrating peptides. A comparative study.* Bioconjug Chem, 2004. **15**(6): p. 1246-53.
352. Wadia, J.S., R.V. Stan, and S.F. Dowdy, *Transducible TAT-HA fusogenic peptide enhances escape of TAT-fusion proteins after lipid raft macropinocytosis.* Nat Med, 2004. **10**(3): p. 310-5.
353. Hakansson, S., A. Jacobs, and M. Caffrey, *Heparin binding by the HIV-1 tat protein transduction domain.* Protein Sci, 2001. **10**(10): p. 2138-9.
354. Yanagishita, M. and V.C. Hascall, *Cell surface heparan sulfate proteoglycans.* J Biol Chem, 1992. **267**(14): p. 9451-4.
355. Marty, C., et al., *Enhanced heparan sulfate proteoglycan-mediated uptake of cell-penetrating peptide-modified liposomes.* Cell Mol Life Sci, 2004. **61**(14): p. 1785-94.
356. Sandgren, S., F. Cheng, and M. Belting, *Nuclear targeting of macromolecular polyanions by an HIV-Tat derived peptide. Role for cell-surface proteoglycans.* J Biol Chem, 2002. **277**(41): p. 38877-83.
357. Ziegler, A., et al., *The cationic cell-penetrating peptide CPP(TAT) derived from the HIV-1 protein TAT is rapidly transported into living fibroblasts: optical, biophysical, and metabolic evidence.* Biochemistry, 2005. **44**(1): p. 138-48.

358. Jamur, M.C. and C. Oliver, *Permeabilization of cell membranes.* Methods Mol Biol, 2010. **588**: p. 63-6.

Appendix A: Copyright Agreement Letters

JOHN WILEY AND SONS LICENSE TERMS AND CONDITIONS

Mar 26, 2012

This is a License Agreement between Scott M Livingstone ("You") and John Wiley and Sons ("John Wiley and Sons") provided by Copyright Clearance Center ("CCC"). The license consists of your order details, the terms and conditions provided by John Wiley and Sons, and the payment terms and conditions.

All payments must be made in full to CCC. For payment instructions, please see information listed at the bottom of this form.

License Number	2750380184619
License date	Sep 15, 2011
Licensed content publisher	John Wiley and Sons
Licensed content publication	Journal of Digestive Diseases
Licensed content title	Histopathological evaluation of fatty and alcoholic liver diseases
Licensed content author	Lisa YERIAN
Licensed content date	Feb 1, 2011
Start page	17
End page	24
Type of use	Dissertation/Thesis
Requestor type	University/Academic
Format	Print and electronic
Portion	Figure/table
Number of figures/tables	2
Number of extracts	
Original Wiley figure/table number(s)	figure 1, figure 2
Will you be translating?	No
Order reference number	
Total	0.00 USD
Terms and Conditions	

TERMS AND CONDITIONS

This copyrighted material is owned by or exclusively licensed to John Wiley & Sons, Inc. or one of its group companies (each a "Wiley Company") or a society for whom a Wiley Company has exclusive publishing rights in relation to a particular journal (collectively WILEY"). By clicking "accept" in connection with completing this licensing transaction, you agree that the following terms and conditions apply to this transaction (along with the billing and payment terms and conditions established by the Copyright Clearance Center Inc., ("CCC's Billing and Payment terms and conditions"), at the time that you opened your Rightslink account (these are available at any time at http://myaccount.copyright.com)

Terms and Conditions

1. The materials you have requested permission to reproduce (the "Materials") are protected by copyright.

2. You are hereby granted a personal, non-exclusive, non-sublicensable, non-transferable, worldwide, limited license to reproduce the Materials for the purpose specified in the licensing process. This license is for a one-time use only with a maximum distribution equal to the number that you identified in the licensing process. Any form of republication granted by this licence must be completed within two years of the date of the grant of this licence (although copies prepared before may be distributed thereafter). The Materials shall not be used in any other manner or for any other purpose. Permission is granted subject to an appropriate acknowledgement given to the author, title of the material/book/journal and the publisher. You shall also duplicate the copyright notice that appears in the Wiley publication in your use of the Material. Permission is also granted on the understanding that nowhere in the text is a previously published source acknowledged for all or part of this Material. Any third party material is expressly excluded from this permission.

3. With respect to the Materials, all rights are reserved. Except as expressly granted by the terms of the license, no part of the Materials may be copied, modified, adapted (except for minor reformatting required by the new Publication), translated, reproduced, transferred or distributed, in any form or by any means, and no derivative works may be made based on the Materials without the prior permission of the respective copyright owner. You may not alter, remove or suppress in any manner any copyright, trademark or other notices displayed by the Materials. You may not license, rent, sell, loan, lease, pledge, offer as security, transfer or assign the Materials, or any of the rights granted to you hereunder to any other person.

4. The Materials and all of the intellectual property rights therein shall at all times remain the exclusive property of John Wiley & Sons Inc or one of its related companies (WILEY) or their respective licensors, and your interest therein is only that of having possession of and the right to reproduce the Materials pursuant to Section 2 herein during the continuance of this Agreement. You agree that you own no right, title or interest in or to the Materials or any of the intellectual property rights therein. You shall have no rights hereunder other than the license as provided for above in Section 2. No right, license or interest to any trademark, trade name, service mark or other branding ("Marks") of WILEY or its licensors is granted hereunder, and you agree that you shall not assert any such right, license or interest with respect thereto.

5. NEITHER WILEY NOR ITS LICENSORS MAKES ANY WARRANTY OR REPRESENTATION OF ANY KIND TO YOU OR ANY THIRD PARTY, EXPRESS, IMPLIED OR STATUTORY, WITH RESPECT TO THE MATERIALS OR THE ACCURACY OF ANY INFORMATION CONTAINED IN THE MATERIALS, INCLUDING, WITHOUT LIMITATION, ANY IMPLIED WARRANTY OF MERCHANTABILITY, ACCURACY, SATISFACTORY QUALITY, FITNESS FOR A PARTICULAR PURPOSE, USABILITY, INTEGRATION OR NON-INFRINGEMENT AND ALL SUCH WARRANTIES ARE HEREBY EXCLUDED BY WILEY AND ITS LICENSORS AND WAIVED BY YOU.

6. WILEY shall have the right to terminate this Agreement immediately upon breach of this Agreement by you.

7. You shall indemnify, defend and hold harmless WILEY, its Licensors and their respective directors, officers, agents and employees, from and against any actual or threatened claims, demands, causes of action or proceedings arising from any breach of this Agreement by you.

8. IN NO EVENT SHALL WILEY OR ITS LICENSORS BE LIABLE TO YOU OR ANY OTHER PARTY OR ANY OTHER PERSON OR ENTITY FOR ANY SPECIAL, CONSEQUENTIAL, INCIDENTAL, INDIRECT, EXEMPLARY OR PUNITIVE DAMAGES, HOWEVER CAUSED, ARISING OUT OF OR IN CONNECTION WITH THE DOWNLOADING, PROVISIONING, VIEWING OR USE OF THE MATERIALS REGARDLESS OF THE FORM OF ACTION, WHETHER FOR BREACH OF CONTRACT, BREACH OF WARRANTY, TORT, NEGLIGENCE, INFRINGEMENT OR OTHERWISE (INCLUDING, WITHOUT LIMITATION, DAMAGES BASED ON LOSS OF PROFITS, DATA, FILES, USE, BUSINESS OPPORTUNITY OR CLAIMS OF THIRD PARTIES), AND WHETHER OR NOT THE PARTY HAS BEEN ADVISED OF THE POSSIBILITY OF SUCH DAMAGES. THIS LIMITATION SHALL APPLY NOTWITHSTANDING ANY

FAILURE OF ESSENTIAL PURPOSE OF ANY LIMITED REMEDY PROVIDED HEREIN.

9. Should any provision of this Agreement be held by a court of competent jurisdiction to be illegal, invalid, or unenforceable, that provision shall be deemed amended to achieve as nearly as possible the same economic effect as the original provision, and the legality, validity and enforceability of the remaining provisions of this Agreement shall not be affected or impaired thereby.

10. The failure of either party to enforce any term or condition of this Agreement shall not constitute a waiver of either party's right to enforce each and every term and condition of this Agreement. No breach under this agreement shall be deemed waived or excused by either party unless such waiver or consent is in writing signed by the party granting such waiver or consent. The waiver by or consent of a party to a breach of any provision of this Agreement shall not operate or be construed as a waiver of or consent to any other or subsequent breach by such other party.

11. This Agreement may not be assigned (including by operation of law or otherwise) by you without WILEY's prior written consent.

12. Any fee required for this permission shall be non-refundable after thirty (30) days from receipt.

13. These terms and conditions together with CCC's Billing and Payment terms and conditions (which are incorporated herein) form the entire agreement between you and WILEY concerning this licensing transaction and (in the absence of fraud) supersedes all prior agreements and representations of the parties, oral or written. This Agreement may not be amended except in writing signed by both parties. This Agreement shall be binding upon and inure to the benefit of the parties' successors, legal representatives, and authorized assigns.

14. In the event of any conflict between your obligations established by these terms and conditions and those established by CCC's Billing and Payment terms and conditions, these terms and conditions shall prevail.

15. WILEY expressly reserves all rights not specifically granted in the combination of (i) the license details provided by you and accepted in the course of this licensing transaction, (ii) these terms and conditions and (iii) CCC's Billing and Payment terms and conditions.

16. This Agreement will be void if the Type of Use, Format, Circulation, or Requestor Type was misrepresented during the licensing process.

17. This Agreement shall be governed by and construed in accordance with the laws of the State of New York, USA, without regards to such state's conflict of law rules. Any legal action, suit or proceeding arising out of or relating to these Terms and Conditions or the breach thereof shall be instituted in a court of competent jurisdiction in New York County in the State of New York in the United States of America and each party hereby consents and submits to the personal jurisdiction of such court, waives any objection to venue in such court and consents to service of process by registered or certified mail, return receipt requested, at the last known address of such party.

Wiley Open Access Terms and Conditions

All research articles published in Wiley Open Access journals are fully open access: immediately freely available to read, download and share. Articles are published under the terms of the Creative Commons Attribution Non Commercial License. which permits use, distribution and reproduction in any medium, provided the original work is properly cited and is not used for commercial purposes. The license is subject to the Wiley Open Access terms and conditions: Wiley Open Access articles are protected by copyright and are posted to repositories and websites in accordance with the terms of the Creative Commons Attribution Non Commercial License. At the time of deposit, Wiley Open Access articles include all changes made during peer review, copyediting, and publishing. Repositories and websites that host the article are responsible for incorporating any publisher-supplied amendments or retractions issued subsequently.

Wiley Open Access articles are also available without charge on Wiley's publishing platform, **Wiley Online Library** or any successor sites.

Use by non-commercial users

For non-commercial and non-promotional purposes individual users may access, download, copy, display and redistribute to colleagues Wiley Open Access articles, as well as adapt, translate, text- and data-mine the content subject to the following conditions:

- The authors' moral rights are not compromised. These rights include the right of "paternity" (also known as "attribution" - the right for the author to be identified as such) and "integrity" (the right for the author not to have the work altered in such a way that the author's reputation or integrity may be impugned).
- Where content in the article is identified as belonging to a third party, it is the obligation of the user to ensure that any reuse complies with the copyright policies of the owner of that content.
- If article content is copied, downloaded or otherwise reused for non-commercial research and education purposes, a link to the appropriate bibliographic citation (authors, journal, article title, volume, issue, page numbers, DOI and the link to the definitive published version on Wiley Online Library) should be maintained. Copyright notices and disclaimers must not be deleted.
- Any translations, for which a prior translation agreement with Wiley has not been agreed, must prominently display the statement: "This is an unofficial translation of an article that appeared in a Wiley publication. The publisher has not endorsed this translation."

Use by commercial "for-profit" organisations

Use of Wiley Open Access articles for commercial, promotional, or marketing purposes requires further explicit permission from Wiley and will be subject to a fee. Commercial purposes include:

- Copying or downloading of articles, or linking to such articles for further redistribution, sale or licensing;
- Copying, downloading or posting by a site or service that incorporates advertising with such content;
- The inclusion or incorporation of article content in other works or services (other than normal quotations with an appropriate citation) that is then available for sale or licensing, for a fee (for example, a compilation produced for marketing purposes, inclusion in a sales pack)
- Use of article content (other than normal quotations with appropriate citation) by for-profit organisations for promotional purposes
- Linking to article content in e-mails redistributed for promotional, marketing or educational purposes;
- Use for the purposes of monetary reward by means of sale, resale, licence, loan, transfer or other form of commercial exploitation such as marketing products
- Print reprints of Wiley Open Access articles can be purchased from: corporatesales@wiley.com

Other Terms and Conditions:

BY CLICKING ON THE "I AGREE..." BOX, YOU ACKNOWLEDGE THAT YOU HAVE READ AND FULLY UNDERSTAND EACH OF THE SECTIONS OF AND PROVISIONS SET FORTH IN THIS AGREEMENT AND THAT YOU ARE IN AGREEMENT WITH AND ARE WILLING TO ACCEPT ALL OF YOUR OBLIGATIONS AS SET FORTH IN THIS AGREEMENT.

v1.7

If you would like to pay for this license now, please remit this license along with your payment made payable to "COPYRIGHT CLEARANCE CENTER" otherwise you will be invoiced within 48 hours of the license date. Payment should be in the form of a check or money order referencing your account number and this invoice number RLNK11056068.
Once you receive your invoice for this order, you may pay your invoice by credit card. Please follow instructions provided at that time.

Make Payment To:
Copyright Clearance Center
Dept 001
P.O. Box 843006
Boston, MA 02284-3006

For suggestions or comments regarding this order, contact RightsLink Customer Support: customercare@copyright.com or +1-877-622-5543 (toll free in the US) or +1-978-646-2777.

Gratis licenses (referencing $0 in the Total field) are free. Please retain this printable license for your reference. No payment is required.

JOHN WILEY AND SONS LICENSE TERMS AND CONDITIONS

Mar 26, 2012

This is a License Agreement between Scott M Livingstone ("You") and John Wiley and Sons ("John Wiley and Sons") provided by Copyright Clearance Center ("CCC"). The license consists of your order details, the terms and conditions provided by John Wiley and Sons, and the payment terms and conditions.

All payments must be made in full to CCC. For payment instructions, please see information listed at the bottom of this form.

License Number	2876551203171
License date	Mar 26, 2012
Licensed content publisher	John Wiley and Sons
Licensed content publication	Liver Transplantation
Licensed content title	Liver ischemia/reperfusion injury: Processes in inflammatory networks—A review
Licensed content author	Mahmoud Abu-Amara,Shi Yu Yang,Niteen Tapuria,Barry Fuller,Brian Davidson,Alexander Seifalian
Licensed content date	Sep 1, 2010
Start page	1016
End page	1032
Type of use	Dissertation/Thesis
Requestor type	University/Academic
Format	Electronic
Portion	Figure/table
Number of figures/tables	1
Number of extracts	
Original Wiley figure/table number(s)	figure 2
Will you be translating?	No
Order reference number	
Total	0.00 USD

Terms and Conditions

TERMS AND CONDITIONS

This copyrighted material is owned by or exclusively licensed to John Wiley & Sons, Inc. or one of its group companies (each a "Wiley Company") or a society for whom a Wiley Company has exclusive publishing rights in relation to a particular journal (collectively WILEY"). By clicking "accept" in connection with completing this licensing transaction, you agree that the following terms and conditions apply to this transaction (along with the billing and payment terms and conditions established by the Copyright Clearance Center Inc., ("CCC's Billing and Payment terms

and conditions"), at the time that you opened your Rightslink account (these are available at any time at http://myaccount.copyright.com)

Terms and Conditions

1. The materials you have requested permission to reproduce (the "Materials") are protected by copyright.

2. You are hereby granted a personal, non-exclusive, non-sublicensable, non-transferable, worldwide, limited license to reproduce the Materials for the purpose specified in the licensing process. This license is for a one-time use only with a maximum distribution equal to the number that you identified in the licensing process. Any form of republication granted by this licence must be completed within two years of the date of the grant of this licence (although copies prepared before may be distributed thereafter). The Materials shall not be used in any other manner or for any other purpose. Permission is granted subject to an appropriate acknowledgement given to the author, title of the material/book/journal and the publisher. You shall also duplicate the copyright notice that appears in the Wiley publication in your use of the Material. Permission is also granted on the understanding that nowhere in the text is a previously published source acknowledged for all or part of this Material. Any third party material is expressly excluded from this permission.

3. With respect to the Materials, all rights are reserved. Except as expressly granted by the terms of the license, no part of the Materials may be copied, modified, adapted (except for minor reformatting required by the new Publication), translated, reproduced, transferred or distributed, in any form or by any means, and no derivative works may be made based on the Materials without the prior permission of the respective copyright owner. You may not alter, remove or suppress in any manner any copyright, trademark or other notices displayed by the Materials. You may not license, rent, sell, loan, lease, pledge, offer as security, transfer or assign the Materials, or any of the rights granted to you hereunder to any other person.

4. The Materials and all of the intellectual property rights therein shall at all times remain the exclusive property of John Wiley & Sons Inc or one of its related companies (WILEY) or their respective licensors, and your interest therein is only that of having possession of and the right to reproduce the Materials pursuant to Section 2 herein during the continuance of this Agreement. You agree that you own no right, title or interest in or to the Materials or any of the intellectual property rights therein. You shall have no rights hereunder other than the license as provided for above in Section 2. No right, license or interest to any trademark, trade name, service mark or other branding ("Marks") of WILEY or its licensors is granted hereunder, and you agree that you shall not assert any such right, license or interest with respect thereto.

5. NEITHER WILEY NOR ITS LICENSORS MAKES ANY WARRANTY OR REPRESENTATION OF ANY KIND TO YOU OR ANY THIRD PARTY, EXPRESS, IMPLIED OR STATUTORY, WITH RESPECT TO THE MATERIALS OR THE ACCURACY OF ANY INFORMATION CONTAINED IN THE MATERIALS, INCLUDING, WITHOUT LIMITATION, ANY IMPLIED WARRANTY OF MERCHANTABILITY, ACCURACY, SATISFACTORY QUALITY, FITNESS FOR A PARTICULAR PURPOSE, USABILITY, INTEGRATION OR NON-INFRINGEMENT AND ALL SUCH WARRANTIES ARE HEREBY EXCLUDED BY WILEY AND ITS LICENSORS AND WAIVED BY YOU.

6. WILEY shall have the right to terminate this Agreement immediately upon breach of this Agreement by you.

7. You shall indemnify, defend and hold harmless WILEY, its Licensors and their respective directors, officers, agents and employees, from and against any actual or threatened claims, demands, causes of action or proceedings arising from any breach of this Agreement by you.

8. IN NO EVENT SHALL WILEY OR ITS LICENSORS BE LIABLE TO YOU OR ANY OTHER PARTY OR ANY OTHER PERSON OR ENTITY FOR ANY SPECIAL, CONSEQUENTIAL, INCIDENTAL, INDIRECT, EXEMPLARY OR PUNITIVE DAMAGES, HOWEVER CAUSED, ARISING OUT OF OR IN CONNECTION WITH THE DOWNLOADING, PROVISIONING, VIEWING OR USE OF THE MATERIALS REGARDLESS OF THE FORM OF ACTION, WHETHER FOR BREACH OF CONTRACT, BREACH OF WARRANTY, TORT, NEGLIGENCE, INFRINGEMENT OR OTHERWISE (INCLUDING, WITHOUT LIMITATION,

DAMAGES BASED ON LOSS OF PROFITS, DATA, FILES, USE, BUSINESS OPPORTUNITY OR CLAIMS OF THIRD PARTIES), AND WHETHER OR NOT THE PARTY HAS BEEN ADVISED OF THE POSSIBILITY OF SUCH DAMAGES. THIS LIMITATION SHALL APPLY NOTWITHSTANDING ANY FAILURE OF ESSENTIAL PURPOSE OF ANY LIMITED REMEDY PROVIDED HEREIN.

9. Should any provision of this Agreement be held by a court of competent jurisdiction to be illegal, invalid, or unenforceable, that provision shall be deemed amended to achieve as nearly as possible the same economic effect as the original provision, and the legality, validity and enforceability of the remaining provisions of this Agreement shall not be affected or impaired thereby.

10. The failure of either party to enforce any term or condition of this Agreement shall not constitute a waiver of either party's right to enforce each and every term and condition of this Agreement. No breach under this agreement shall be deemed waived or excused by either party unless such waiver or consent is in writing signed by the party granting such waiver or consent. The waiver by or consent of a party to a breach of any provision of this Agreement shall not operate or be construed as a waiver of or consent to any other or subsequent breach by such other party.

11. This Agreement may not be assigned (including by operation of law or otherwise) by you without WILEY's prior written consent.

12. Any fee required for this permission shall be non-refundable after thirty (30) days from receipt.

13. These terms and conditions together with CCC's Billing and Payment terms and conditions (which are incorporated herein) form the entire agreement between you and WILEY concerning this licensing transaction and (in the absence of fraud) supersedes all prior agreements and representations of the parties, oral or written. This Agreement may not be amended except in writing signed by both parties. This Agreement shall be binding upon and inure to the benefit of the parties' successors, legal representatives, and authorized assigns.

14. In the event of any conflict between your obligations established by these terms and conditions and those established by CCC's Billing and Payment terms and conditions, these terms and conditions shall prevail.

15. WILEY expressly reserves all rights not specifically granted in the combination of (i) the license details provided by you and accepted in the course of this licensing transaction, (ii) these terms and conditions and (iii) CCC's Billing and Payment terms and conditions.

16. This Agreement will be void if the Type of Use, Format, Circulation, or Requestor Type was misrepresented during the licensing process.

17. This Agreement shall be governed by and construed in accordance with the laws of the State of New York, USA, without regards to such state's conflict of law rules. Any legal action, suit or proceeding arising out of or relating to these Terms and Conditions or the breach thereof shall be instituted in a court of competent jurisdiction in New York County in the State of New York in the United States of America and each party hereby consents and submits to the personal jurisdiction of such court, waives any objection to venue in such court and consents to service of process by registered or certified mail, return receipt requested, at the last known address of such party.

Wiley Open Access Terms and Conditions

All research articles published in Wiley Open Access journals are fully open access: immediately freely available to read, download and share. Articles are published under the terms of the Creative Commons Attribution Non Commercial License. which permits use, distribution and reproduction in any medium, provided the original work is properly cited and is not used for commercial purposes. The license is subject to the Wiley Open Access terms and conditions: Wiley Open Access articles are protected by copyright and are posted to repositories and websites in accordance with the terms of the Creative Commons Attribution Non Commercial License. At

the time of deposit, Wiley Open Access articles include all changes made during peer review, copyediting, and publishing. Repositories and websites that host the article are responsible for incorporating any publisher-supplied amendments or retractions issued subsequently.
Wiley Open Access articles are also available without charge on Wiley's publishing platform, **Wiley Online Library** or any successor sites.

Use by non-commercial users

For non-commercial and non-promotional purposes individual users may access, download, copy, display and redistribute to colleagues Wiley Open Access articles, as well as adapt, translate, text- and data-mine the content subject to the following conditions:

- The authors' moral rights are not compromised. These rights include the right of "paternity" (also known as "attribution" - the right for the author to be identified as such) and "integrity" (the right for the author not to have the work altered in such a way that the author's reputation or integrity may be impugned).
- Where content in the article is identified as belonging to a third party, it is the obligation of the user to ensure that any reuse complies with the copyright policies of the owner of that content.
- If article content is copied, downloaded or otherwise reused for non-commercial research and education purposes, a link to the appropriate bibliographic citation (authors, journal, article title, volume, issue, page numbers, DOI and the link to the definitive published version on Wiley Online Library) should be maintained. Copyright notices and disclaimers must not be deleted.
- Any translations, for which a prior translation agreement with Wiley has not been agreed, must prominently display the statement: "This is an unofficial translation of an article that appeared in a Wiley publication. The publisher has not endorsed this translation."

Use by commercial "for-profit" organisations

Use of Wiley Open Access articles for commercial, promotional, or marketing purposes requires further explicit permission from Wiley and will be subject to a fee. Commercial purposes include:

- Copying or downloading of articles, or linking to such articles for further redistribution, sale or licensing;
- Copying, downloading or posting by a site or service that incorporates advertising with such content;
- The inclusion or incorporation of article content in other works or services (other than normal quotations with an appropriate citation) that is then available for sale or licensing, for a fee (for example, a compilation produced for marketing purposes, inclusion in a sales pack)
- Use of article content (other than normal quotations with appropriate citation) by for-profit organisations for promotional purposes
- Linking to article content in e-mails redistributed for promotional, marketing or educational purposes;
- Use for the purposes of monetary reward by means of sale, resale, licence, loan, transfer or other form of commercial exploitation such as marketing products

• Print reprints of Wiley Open Access articles can be purchased from:
corporatesales@wiley.com

Other Terms and Conditions:

BY CLICKING ON THE "I AGREE..." BOX, YOU ACKNOWLEDGE THAT YOU HAVE READ AND FULLY UNDERSTAND EACH OF THE SECTIONS OF AND PROVISIONS SET FORTH IN THIS AGREEMENT AND THAT YOU ARE IN AGREEMENT WITH AND ARE WILLING TO ACCEPT ALL OF YOUR OBLIGATIONS AS SET FORTH IN THIS AGREEMENT.

v1.7

If you would like to pay for this license now, please remit this license along with your payment made payable to "COPYRIGHT CLEARANCE CENTER" otherwise you will be invoiced within 48 hours of the license date. Payment should be in the form of a check or money order referencing your account number and this invoice number RLNK500747269.
Once you receive your invoice for this order, you may pay your invoice by credit card. Please follow instructions provided at that time.

Make Payment To:
Copyright Clearance Center
Dept 001
P.O. Box 843006
Boston, MA 02284-3006

For suggestions or comments regarding this order, contact RightsLink Customer Support: customercare@copyright.com or +1-877-622-5543 (toll free in the US) or +1-978-646-2777.

Gratis licenses (referencing $0 in the Total field) are free. Please retain this printable license for your reference. No payment is required.

NATURE PUBLISHING GROUP LICENSE TERMS AND CONDITIONS

Mar 26, 2012

This is a License Agreement between Scott M Livingstone ("You") and Nature Publishing Group ("Nature Publishing Group") provided by Copyright Clearance Center ("CCC"). The license consists of your order details, the terms and conditions provided by Nature Publishing Group, and the payment terms and conditions.

All payments must be made in full to CCC. For payment instructions, please see information listed at the bottom of this form.

License Number	2806111127650
License date	Dec 11, 2011
Licensed content publisher	Nature Publishing Group
Licensed content publication	Nature Medicine
Licensed content title	Transducible TAT-HA fusogenic peptide enhances escape of TAT-fusion proteins after lipid raft macropinocytosis
Licensed content author	Jehangir S Wadia, Radu V Stan, Steven F Dowdy
Licensed content date	Feb 8, 2004
Type of Use	reuse in a thesis/dissertation
Requestor type	academic/educational
Format	electronic
Portion	figures/tables/illustrations
Number of figures/tables /illustrations	1
High-res required	no
Figures	figure 2
Author of this NPG article	no
Your reference number	
Title of your thesis / dissertation	A cell penetrating heme oxygenase to improve the resistance of steatotic livers to reperfusion injury following transplantation
Expected completion date	Jan 2012
Estimated size (number of pages)	115
Total	0.00 USD
Terms and Conditions	

Terms and Conditions for Permissions

Nature Publishing Group hereby grants you a non-exclusive license to reproduce this material for this purpose, and for no other use, subject to the conditions below:

1. NPG warrants that it has, to the best of its knowledge, the rights to license reuse of this material. However, you should ensure that the material you are requesting is original to Nature Publishing Group and does not carry the copyright of another entity (as credited in the published version). If the credit line on any part of the material you have requested indicates that it was reprinted or adapted by NPG with permission from another source, then you should also seek permission from that source to reuse the material.

2. Permission granted free of charge for material in print is also usually granted for any electronic version of that work, provided that the material is incidental to the work as a whole and that the electronic version is essentially equivalent to, or substitutes for, the print version. Where print permission has been granted for a fee, separate permission must be obtained for any additional, electronic re-use (unless, as in the case of a full paper, this has already been accounted for during your initial request in the calculation of a print run). NB: In all cases, web-based use of full-text articles must be authorized separately through the 'Use on a Web Site' option when requesting permission.

3. Permission granted for a first edition does not apply to second and subsequent editions and for editions in other languages (except for signatories to the STM Permissions Guidelines, or where the first edition permission was granted for free).

4. Nature Publishing Group's permission must be acknowledged next to the figure, table or abstract in print. In electronic form, this acknowledgement must be visible at the same time as the figure/table/abstract, and must be hyperlinked to the journal's homepage.

5. The credit line should read:
   Reprinted by permission from Macmillan Publishers Ltd: [JOURNAL NAME] (reference citation), copyright (year of publication)
   For AOP papers, the credit line should read:
   Reprinted by permission from Macmillan Publishers Ltd: [JOURNAL NAME], advance online publication, day month year (doi: 10.1038/sj.[JOURNAL ACRONYM].XXXXX)

   Note: For republication from the *British Journal of Cancer*, the following credit lines apply.
   Reprinted by permission from Macmillan Publishers Ltd on behalf of Cancer Research UK: [JOURNAL NAME] (reference citation), copyright (year of publication) For AOP papers, the credit line should read:
   Reprinted by permission from Macmillan Publishers Ltd on behalf of Cancer Research UK: [JOURNAL NAME], advance online publication, day month year (doi: 10.1038/sj.[JOURNAL ACRONYM].XXXXX)

6. Adaptations of single figures do not require NPG approval. However, the adaptation should be credited as follows:

   Adapted by permission from Macmillan Publishers Ltd: [JOURNAL NAME] (reference citation), copyright (year of publication)

   Note: For adaptation from the *British Journal of Cancer*, the following credit line applies.
   Adapted by permission from Macmillan Publishers Ltd on behalf of Cancer Research UK: [JOURNAL NAME] (reference citation), copyright (year of publication)

7. Translations of 401 words up to a whole article require NPG approval. Please visit http://www.macmillanmedicalcommunications.com for more information.
   Translations of up to a 400 words do not require NPG approval. The translation should be credited as follows:

   Translated by permission from Macmillan Publishers Ltd: [JOURNAL NAME] (reference citation), copyright (year of publication).

   Note: For translation from the *British Journal of Cancer*, the following credit line applies.
   Translated by permission from Macmillan Publishers Ltd on behalf of Cancer Research UK: [JOURNAL NAME] (reference citation), copyright (year of publication)

We are certain that all parties will benefit from this agreement and wish you the best in the use of this material. Thank you.

Special Terms:

v1.1

If you would like to pay for this license now, please remit this license along with your payment made payable to "COPYRIGHT CLEARANCE CENTER" otherwise you will be invoiced within 48 hours of the license date. Payment should be in the form of a check or money order referencing your account number and this invoice number RLNK500681697.
Once you receive your invoice for this order, you may pay your invoice by credit card. Please follow instructions provided at that time.

Make Payment To:
Copyright Clearance Center
Dept 001
P.O. Box 843006
Boston, MA 02284-3006

For suggestions or comments regarding this order, contact RightsLink Customer Support: customercare@copyright.com or +1-877-622-5543 (toll free in the US) or +1-978-646-2777.

Gratis licenses (referencing $0 in the Total field) are free. Please retain this printable license for your reference. No payment is required.